TWO-STAGE STOCHASTIC AGGREGATE PRODUCTION PLANNING MODELS WITH RENEWABLE ENERGY PROSUMERS CONSIDERING MULTIPLE FACILITIES AND HOURLY TIME OF USE

by

Sayed Rezwanul Islam

A thesis submitted to the Graduate Council of
Texas State University in partial fulfillment
of the requirements for the degree of
Master of Science
with a Major in Engineering
August 2021

Committee Members:

Clara Novoa, Chair

Tongdan Jin

Dincer Konur

FAIR USE AND AUTHOR'S PERMISSION STATEMENT

DEDICATION

I express my sincere gratitude to my family for providing their support, and encouragement throughout my time of study. This accomplishment would not have been possible without them.

ACKNOWLEDGMENTS

I would like to express my sincere gratitude to my advisor Dr. Clara Novoa for providing me the great opportunity to work with her supervision. Besides making me a hardworking student, Dr. Clara Novoa has provided me her continuous support and encouragement, patience during my thesis that would lead me a good researcher in the future.

I would also like to express my gratitude to Dr. Tongdan Jin for his constructive criticisms, moral support and great motivation to perform my research in a more productive way.

I would like to express special thanks to Dr. Vishu Viswanathan, Graduate Advisor at the Ingram School of Engineering, for all his valuable guidance throughout the MS program.

I am very thankful to my parents, my beloved wife and friends for their continuous encouragement and moral support in my life.

I also thank the National Science Foundation for partially funding this thesis project under NSF CBET ME-GREEN Project (award #1704933).

TABLE OF CONTENTS

Page

ACKNOWLEDGEMENTS v

LIST OF TABLES xi

LIST OF FIGURES xiv

LIST OF ABBREVIATIONS xvii

ABSTRACT xx

CHAPTER

1. INTRODUCTION AND LITERATURE REVIEW 1

1.1 Renewable energy projects in the industrial sector 2

1.2 Literature review 5

1.2.1 PP considering conventional energy 5
1.2.2 APP considering conventional energy 8
1.2.3 PP considering renewable energy 11
1.2.4 APP without renewable energy 15
1.2.5 RE models considering energy prosumers 19

1.3 Estimation of a WT capacity factor 25

1.4 Estimation of a solar PV capacity factor 26

1.5 Thesis goal and contributions 30

1.6 Document organization 32

2. APP CONSIDERING DAILY ENERGY REQUIREMENTS 33
2.1 Problem statement 34
2.1.1 Research questions 36
2.2 Methodology 36
2.2.1 APP modeled as a two-stage stochastic program 37
2.3 Stochastic APP models 39
2.3.1 Island microgrid with BS 43
2.3.2 Prosumer model 48
2.3.3 Models' assumptions 52
2.4 Estimation of uncertain parameters in the models 53
2.4.1 Estimation of product demands 53
2.4.2 Estimation of machine hours capacity 54
2.4.3 Estimation of labor hours capacity 54
2.4.4 Estimation of WT capacity factor 55
2.4.5 Estimation of solar PV capacity factor 57
2.5 Numerical experiments single factory and single warehouse . . 60
2.5.1 Values for input parameters 60
2.6 Computational results - base case 61
2.6.1 Levelized cost of energy (LCOE) 63
2.6.2 Energy production comparison 64
2.6.3 Technology installation at factory 64
2.6.4 Technology installation at warehouse 66
2.6.5 Cost comparison 66
2.7 Sensitivity analysis using DOE 68
2.7.1 Total cost comparison 70
2.7.2 WT and PV installation at factory 71

2.7.3 WT and PV installation at warehouse 72
2.7.4 Battery storage installation at factory 73
2.7.5 Battery storage installation at warehouse 73
2.7.6 Amount of energy bought at factory 74
2.7.7 Energy selling amount from factory 75
2.7.8 Energy buying amount at warehouse 76
2.7.9 Energy selling amount from warehouse 76

3. APP CONSIDERING HOURLY ENERGY REQUIREMENTS . . . 79

3.1 Problem statement and research questions 80

3.2 Two stage stochastic APP models 81

3.2.1 Decision variables of the APP models 82
3.2.2 Constraints of the APP models 82
3.2.3 Island microgrid with BS 83
3.2.4 Prosumer without TOU 86
3.2.5 Model assumptions 89

3.3 Estimation of uncertain parameters 90

3.3.1 Estimation of product demands 90
3.3.2 Estimation of machine hours capacity 90
3.3.3 Estimation of labor hours capacity 91
3.3.4 Estimation of Austin WT capacity factor 91
3.3.5 Estimation of Boston WT capacity factor 92
3.3.6 Estimation of Dallas WT capacity factor 93
3.3.7 Estimation of New York WT capacity factor 94
3.3.8 Estimation of Austin solar PV capacity factor 95
3.3.9 Estimation of Boston solar PV capacity factor 96
3.3.10 Estimation of Dallas solar PV capacity factor 98
3.3.11 Estimation of New York solar PV capacity factor . . . 99

3.4 Computational results - base case 101
3.4.1 Levelized cost of energy (LCOE) 104
3.4.2 Energy production comparison 105
3.4.3 Cost comparison 106
3.4.4 Technology installation at factory 107
3.4.5 Technology installation at warehouse 108
3.4.6 BS installation at Factory 109
3.4.7 BS installation at warehouse 110

4. APP CONSIDERING HOURLY TOU 111

4.1 Prosumer model with BS and TOU - hourly granularity 113

4.2 Computational results - base case 117
4.2.1 Levelized cost of energy (LCOE) 118
4.2.2 Energy production, buy and sell comparison 118
4.2.3 Technology installation at factory 119
4.2.4 Technology installation at warehouse 120
4.2.5 Cost comparison 121

4.3 Sensitivity analysis using DOE 122
4.3.1 Total cost comparison 123
4.3.2 WT and PV installation at Austin 124
4.3.3 WT and PV installation at Boston 125
4.3.4 WT and PV installation at Dallas 126
4.3.5 WT and PV installation at New York 127
4.3.6 Energy buying amount at factory and warehouse 128
4.3.7 BS installation at factory and warehouse 129
4.3.8 Energy selling amount at factory and warehouse 129

4.4 VSS for the hourly prosumer microgrid models 130

4.5 Analysis of the design of experiments 132

4.6 Hourly vs. daily models' comparison and analysis 136
4.6.1 Total cost comparison 137
4.6.2 Energy cost comparison 138
4.6.3 Total energy produced and bought 140
4.6.4 Microgrid sizing of San Francisco 140
4.6.5 Microgrid sizing of Austin 142
4.6.6 Microgrid sizing of Boston 143
4.6.7 Microgrid sizing of Phoenix 144
4.6.8 Microgrid sizing of Dallas 145
4.6.9 Microgrid sizing of New York 147
4.6.10 LCOE comparison 148
4.6.11 Computational time comparison 149

5. CONCLUSIONS AND FUTURE WORK 152

APPENDIX SECTION 156

REFERENCES 178

LIST OF TABLES

Page

1.1 Comparison of several key previous works and the proposed research . . 24
2.1 Sets . . . 40
2.2 Decision variables . . . 40
2.3 Parameters . . . 41
2.4 Parameters continuation . . . 42
2.5 Probability distributions for generating the product demands . . . 53
2.6 Probability distributions for generating the machine hours capacity . . . 54
2.7 Discrete uniform distribution for generating labor hours capacity . . . 55
2.8 San Francisco wind turbine capacity factor analysis . . . 56
2.9 Phoenix WT capacity factor analysis . . . 57
2.10 San Francisco PV capacity factor analysis . . . 58
2.11 Phoenix PV capacity factor analysis . . . 59
2.12 Computational time comparison . . . 61
2.13 Comparison of decision variables and constraints . . . 62
2.14 Levelized cost of energy . . . 63
2.15 Energy production . . . 65
2.16 Technology installation at factory . . . 65
2.17 Technology installation at warehouse . . . 66
2.18 Annual cost breakdown . . . 67
3.1 Decision variables . . . 82
3.2 Parameters . . . 82
3.3 Distribution of product demands for different factories . . . 90

3.4 Distribution of machine hours capacity for different factories 90
3.5 Distribution of machine hours capacity for different factories 91
3.6 Austin WT capacity factor analysis 91
3.7 Boston WT capacity factor analysis 93
3.8 Dallas WT capacity factor analysis 94
3.9 New York WT capacity factor analysis 95
3.10 Austin solar PV capacity factor analysis 96
3.11 Boston solar PV capacity factor analysis 97
3.12 Dallas solar PV capacity factor analysis 98
3.13 New York solar PV capacity factor analysis 100
3.14 Average capacity factor of WT and PV of six US cities 101
3.15 Median and standard deviation of WT and PV CF of six US cities . . . 101
3.16 Comparison of decision variables and constraints 103
3.17 Levelized cost of energy 104
3.18 Energy production 105
3.19 Annual cost breakdown 106
3.20 Technology installation at factory 107
3.21 Technology installation at warehouse 108
3.22 BS installation at factory 109
3.23 BS installation at warehouse 110
4.1 Parameters 113
4.2 Comparison of decision variables and constraints 117
4.3 Energy production, buy and sell 118
4.4 Technology installation at factory 119

4.5 Technology installation at warehouse 120
4.6 Annual cost breakdown 121
4.7 VSS comparison for prosumer models - hourly granularity 131
4.8 Analysis of variance for transformed response 134
4.9 Coefficients for transformed response 134
4.10 Model summary for transformed response 135
4.11 Total cost comparison 137
4.12 Energy cost comparison 139
4.13 Energy produced, bought and sold comparison 140
4.14 Microgrid sizing of San Francisco 141
4.15 Microgrid sizing of Austin 142
4.16 Microgrid sizing of Boston 143
4.17 Microgrid sizing of Phoenix 144
4.18 Microgrid sizing of Dallas 146
4.19 Microgrid sizing of New York 147
4.20 LCOE comparison 148
4.21 Computational time comparison (CPU seconds) 150

LIST OF FIGURES

Page

1.1 A wind turbine power curve . . . 25

2.1 Onsite microgrid install at factory and warehouse . . . 34

2.2 Scenario tree for two-stage stochastic programming model . . . 38

2.3 San Francisco average daily WT capacity factor . . . 56

2.4 Phoenix average daily WT capacity factor . . . 57

2.5 San Francisco average daily PV capacity factor . . . 58

2.6 Phoenix average daily PV capacity factor . . . 59

2.7 Comparison of decision variables and constraints . . . 62

2.8 Comparison of levelized cost of energy . . . 64

2.9 Energy production comparison . . . 65

2.10 Technology installation at factory . . . 66

2.11 Technology installation at warehouse . . . 67

2.12 Energy cost and total cost comparison . . . 68

2.13 Total cost comparison . . . 70

2.14 WT and PV installation at factory . . . 71

2.15 WT and PV installation at warehouse . . . 72

2.16 BS installation at factory . . . 73

2.17 BS installation at warehouse . . . 74

2.18 Energy buying amount at factory . . . 74

2.19 Energy selling amount from factory . . . 75

2.20 Energy buying amount at warehouse . . . 76

2.21 Energy selling amount from warehouse . . . 77

3.1 Onsite microgrid install at multiple factories and warehouses 80
3.2 Austin average daily WT capacity factor 92
3.3 Boston average daily WT capacity factor 93
3.4 Dallas average daily WT capacity factor 94
3.5 New York average daily WT capacity factor 95
3.6 Austin average daily PV capacity factor 97
3.7 Boston average daily PV capacity factor 98
3.8 Dallas average daily PV capacity factor 99
3.9 New York average daily PV capacity factor 100
3.10 Decision variables and constraints 103
3.11 Levelized cost of energy 104
3.12 Energy production comparison 105
3.13 Energy cost and total cost comparison 106
3.14 Technology installation at factory 107
3.15 Technology installation at warehouse 109
4.1 Energy produced, bought and sold 119
4.2 Technology installation at factory 120
4.3 Technology installation at warehouse 121
4.4 Total cost comparison 124
4.5 WT and PV installation at Austin 125
4.6 WT and PV installation at Boston 126
4.7 WT and PV installation at Dallas 126
4.8 WT and PV installation at New York 127
4.9 Energy buying amount at factory and warehouse 128

4.10 BS installation at factory and warehouse 129

4.11 Energy selling amount at factory and warehouse 130

4.12 Normal probability plot 135

4.13 Residuals vs. Fits graph 136

4.14 Total cost comparison 137

4.15 Energy cost comparison 139

4.16 Microgrid sizing of San Francisco 141

4.17 Microgrid sizing of Austin 142

4.18 Microgrid sizing of Boston 143

4.19 Microgrid sizing of Phoenix 145

4.20 Microgrid sizing of Dallas 146

4.21 Microgrid sizing of New York 147

4.22 LCOE comparison 148

LIST OF ABBREVIATIONS

Abbreviation	**Description**
AHP	Analytic hierarchy process
AMPL	A mathematical programming language
AOD	Appliance operation delay
APP	Aggregate production planning
B&BC	Branch and Benders cut
BD	Benders decomposition
BS	Battery storage
CES	Community energy storage
CF	Capacity factors
CCP	Chance constrained programming
CHP	Combined heat and power
CNSM	Cost of not using the stochastic model
COT	Coil outlet temperature
CPPS	Capacitated production planning and scheduling
CVaR	Conditional value at risk
DC	Direct current
DCC	Digital command control
DER	Distributed energy resources
DM	Decision manager
DG	Distributed generation
DOE	Design of experiments
DSO	Distribution system operator
ESS	Energy storage system
EPA	United States environmental protection agency
EPA	Energy prosumer approach
EV	Electric vehicle
FMS	Flexible manufacturing system
FBGA	Fuzzy based genetic algorithm
F&O	Fix and optimize

FUR	Flexibility usage rate
GA	Genetic algorithm
GAMS	General algebraic modeling system
GEC	Green energy coefficient
GR	Grid revenue
HES	Household energy storage
HRESs	Hybrid renewable energy systems
IEEE	Institute of electrical and electronic engineers
IM	Island microgrid
JS	Job shop
LCOE	Levelized cost of energy
LS	Lot sizing
MILP	Mixed-integer linear programming
MINLP	Mixed-integer non-linear programming
MIP	Mixed integer programming
MOOM	Multi-objective optimization model
MOOP	Multi-objective optimization problem
NSP	Nonlinear non-smooth problems
PAR	Peak-to-average ratio
PCB	Prosumer cost-benefit
PDR	Peak demand reduction
PDAP	Production-distribution aggregate planning
PEC	Prosumer energy cost
PES	Prosumer energy surplus
PP	Production planning
PSO	Particle swarm optimization
PV	Solar phtovoltaic
RE	Renewable energy
RESs	Renewable energy sources
RIA	Renewable integration analytics
RMILP	Robust mixed integer linear programming
SEEPP	Smart energy efficient production planning

SEEPP	Smart energy efficient production planning
SG	Smart grid
SLA	Service level agreement
SLR	Self load satisfaction rate
SMIP	Stochastic mixed integer programming
SSR	Self sufficiency rate
TSS	Thermal storage system
TOU	Time of use
VMS	Value of multistage stochastic programming
VSS	Value of the stochastic solution
VPPAs	Virtual power purchase agreements
WEPs	Wind energy prosumers
WT	Wind turbine

ABSTRACT

This thesis work presents a two-stage stochastic aggregate production planning model to determine the optimum renewable energy capacity, production plan, machine and workforce levels that minimize the operational cost of a production system consisting of multiple facilities operating in different geographic locations. The model considers uncertainty on the demand of products, machine and labor capacities, and on the renewable energy supply under a horizon of twelve months. The goal of this work is to evaluate the feasibility of decarbonizing the manufacturing, transportation and warehouse operations by adopting wind turbine and solar photovoltaics coupled with battery storage (BS) assuming the facilities are energy prosumers. In the model, the first-stage decisions are the sitting and sizing of the renewable generation technologies, the capacity of the BS, amount of product to produce, hours of labor to keep, hire or layoff, and regular, overtime, and idle machine hours to use for the entire planning horizon. Second-stage recourse actions include storing product in inventory, subcontracting or backorder it, buying energy, selling renewable energy to the main grid, and using BS to respond to variations in wind profile and weather conditions. Climate analytics performed in six U.S. cities permits to estimate the capacity factors of the renewables and test their feasibility of adoption. Numerical experiments performed on three model instances: island microgrid (IM), energy prosumer with and without time-of-use (TOU) tariffs, show favorable levelized costs of energy in \$50-\$100 per MWh. The instances are relevant to manufacturing companies and the society since they replace the usage of fossil fuels and accelerate eco-friendly operations to achieve net-zero carbon manufacturing operations.

1. INTRODUCTION AND LITERATURE REVIEW

The global energy market consists of industrial, transportation, residential, and commercial sectors. The industrial and transportation sectors consumed 80% of the energy globally whereas the consumption of the industrial sector is as high as 54.9% (Carlton, 2018). Hence, these huge energy consumption make industrial and transportation sectors an important target for a switch to renewable energy (RE). The unprecedented growth in RE purchasing, development and commitments occurring in 2018 made evident the clean energy revolution happening across the country. U.S. corporations have stimulated a global movement towards purchasing RE over the last decade (Kaldjian and Barua, 2019). Companies in the United States purchased a record 6.43 GW of renewable power, which is more than double the previous record of 3.22 GW in 2015. Now, a growing number of large buyers are committing to source 100% of their electricity from renewables.

Roberts (2018) performed a survey which showed that in 2018 there were 53 Fortune 500 companies with 100% RE goals and in January 2017 there were only 23 companies with the same target. In 2018, more than 300 U.S. cities, towns or counties have made commitments to 100% RE, up from just 50 cities in 2017. Roberts (2018) also shows that six U.S. cities (Greensburg, KS; Georgetown, TX; Aspen, CO; Burlington, VT; Kodiak Island, AK; and Rockport, MO) have already met their 100% RE goals through a variety of approaches, including on-site renewables installations, off-site purchases from grid renewables, etc. Roberts (2018) shows that renewables provide only 17% of total electricity generation. Thus, fossil fuels are still the dominant energy source in the United States. It is projected that renewables (wind, solar, and energy storage systems) will shift approximately 80% conventional energy that is used to run manufacturing process by 2050. Intel, Apple, Honda, Tesla, Nike, Walmart, and Vestas are successful examples of large RE projects pioneered by the industrial sector. The two-stage stochastic aggregate production planning (APP) model presented in this thesis work aims to help more industries in the transition from conventional energy to RE use.

The remainder of this introductory chapter is organized as follows. Section 1.1 provides details about large RE projects undertaken by manufacturing and service industries and a couple of examples related to recent research in wind and solar energy technology. Subsections 1.2.1 and 1.2.2 present a literature review on considering conventional energy in production planning (PP) and APP, respectively. Subsection 1.2.3 review works incorporating RE in production planning. Subsection 1.2.4 review contributions in aggregate production planning that do not incorporate RE because at the best of the thesis author's knowledge there are no previous contributions of this kind. Subsection 1.2.5 reviews literature on RE models considering energy prosumers. Sections 1.3 and 1.4 review previous work on estimation of wind turbine (WT) and solar photovoltaic (PV) capacity factors (CF) or utilization because they are the theoretical base for the computation of CF input to the APP models developed in this thesis. Section 1.5 provides the goals and contributions of this thesis. Section 1.6 goes over the organization of the remainder of this thesis document.

1.1 Renewable energy projects in the industrial sector

Intel′s 360-acre Leixlip campus is home to one of the world′s most advanced manufacturing processes (John, 2017). It makes Intel one of the largest voluntaries, private purchasers of RE in Ireland. It also helps Intel reduce its impact on the environment and keep its commitment as a global energy sustainability champion. Simultaneously, Intel has also greened its energy supply in over a dozen major European facilities to 100%. According to EPA data, in the United States Intel also has been the largest voluntary green power purchaser for the past nine years. Intel′s decision to go green will help to stimulate the RE market further and encourage other businesses to follow suit. More participation in the green power market will ultimately further help the environment and lower costs.

Apple is committed to leaving the world better than it found it. The company announced that its global facilities are powered with 100% clean energy (Apple, 2018). Apple will keep pushing the boundaries of what is possible with the materials in their products, the way they recycle them, their facilities, and their work with suppliers to establish new creative and forward-looking RE sources because they know the future depends on it. Their achievement includes clean energy in retail stores, offices, data centers, and co-located facilities in 43 countries, including the United States, the United Kingdom, China, and India.

Honda has entered into long-term virtual power purchase agreements (VPPAs) for renewable wind and solar power to slash CO_2 emissions from its North American manufacturing operations (Honda, 2019). In Fall 2021, from a 200 MW Texas solar power facility, Honda secured an additional 482,000 MWh/year. These agreements help Honda cover more than 60% of the electricity it uses in North America and enable the company to fully offset the remaining carbon-intensive grid-supplied electricity used in its Ohio, Indiana, and Alabama automobile manufacturing operations. Because of the deal, Honda is one of the top automakers globally in the adoption of RE to power its operations.

Tesla currently makes battery packs and electric motors for their products in Sparks, Nevada, and will eventually have the world's largest rooftop solar array (Tesla, 2019). It will consist of 200,000 solar panels. Tesla will be the first large-scale battery factory to run on 100% RE. The company redesigned its manufacturing processes to adopt RE, avoid fossil fuels, and maximize energy efficiency. Tesla created the net-zero initiative for the entire facility and the gigafactory could be a blueprint for more sustainable industries.

Nike opens a new distribution center that runs on 100% clean energy sourced from five local sources: wind, solar, geothermal, hydroelectric, and biomass (Forde, 2019). It can recycle 95% of the waste generated on-site. The company also aims to achieve zero carbon operations by 2025 and eliminate waste from its supply chain.

Walmart has taken some business strategies which will drive the biggest, fastest, and most sustainable acceleration of new RE projects globally (Walmart, 2020). Walmart drives new RE projects through onsite generation such as solar, wind, and fuel cells. Large projects off-take agreements such as wind farms, wholesale energy purchases in deregulated markets coupled with RE supplies, and utility green power purchases. Pivoting from fossil fuels to RE is the wave of the future (Northwester, 2020). Thus, RE is part of the future of the manufacturing and service industry.

Vestas has taken initiatives to increase its sustainability performance to become a carbon-neutral company by no later than 2030 (Vestas, 2020). The company stated that it would reduce its global carbon footprint through a 55% CO_2 by 2025, reaching 100% by 2030. The company already took some step by transitioning to electric vehicles and replacing its global service vehicle fleet with renewable fuel vehicles. Vesta's factories and offices are powered by 100% renewable electricity since 2013. The company also aims to reduce the CO_2 emissions from its supply chain by 45% per MWh generated by 2030. The successful application of RE by world′s leading manufacturing and service organizations makes it possible to switch from conventional energy to RE. It will reduce companies' reliance on fossil fuels, produce green quality products, and help to keep a greener environment.

The Northwester 2 offshore wind farm located in Belgium is a 219 MW project comprised of 23 MHI Vestas 164-9.5 MW turbines. These are the most powerful turbines to enter commercial operation to date. The wind farm that started producing green energy to the Belgian grid was expected to become fully operational before the summer, 2020. RE Researchers also investigate on improving solar to electricity conversion efficiency (Geisz et al., 2020). The authors stated that single-junction, flat-plate terrestrial solar cells are fundamentally limited to about 30% solar-to-electricity conversion efficiency. Geisz et al. (2020) used a monolithic, series-connected, six-junction inverted metamorphic structure operated under the direct spectrum at 143 suns concentration which demonstrates 47.1% solar conversion efficiency. The authors also concluded that over 50% efficiency is highly achievable. However, 100% efficiency is not possible due to the fundamental limits imposed by thermodynamics. Meanwhile, authors are also working on reducing the cost of III-V solar cells, which enables new markets for these highly efficient devices.

1.2 Literature review

1.2.1 PP considering conventional energy

Choi and Xirouchakis (2015) proposed a deterministic and linear production planning (PP) model that minimizes the weighted sum of energy consumption, backorder cost, and inventory holding cost on a flexible manufacturing system (FMS) considering multiple processing plans. Relative weights in the objective function for energy consumption, backorder cost and inventory holding cost are 0.01, 500, and 500, respectively. The authors proposed a methodology to estimate energy consumption from material flows of multiple process plans for each part type in a product family. They considered the consumption of energy from machining, chip and tool transportation, and material handling. The authors tested the proposed model using an industrial case study. Experimental result shows that the proposed model requires minimum energy consumption for satisfying the customer demands. Furthermore, environmental effects, such as volume of chips removal and cutting fluid consumption, can also be estimated from the proposed model. Future works include capacity planning for diverse production system configurations characterized by random changes in demand. Authors address that stochastic programming would be an option to deal with the randomness of the demand of different part families. Furthermore, authors mention that another future extension would be an integrated production planning and scheduling model to minimize energy consumption.

Zhao et al. (2016) presented a multi-period mixed-integer nonlinear programming (MINLP) model to attain the scheduling of parallel furnaces and the energy distribution of an ethylene plant. The authors investigated coke formation and product yields as a function of varying coil outlet temperature to enhance the profitability of the ethylene plant. They formulated an MINLP model with a discrete-time expression for the short-term production planning by considering the scheduling of parallel cracking furnaces. The objective is to maximize the overall profit of an ethylene plant by incorporating energy utilization in the process operation. The authors investigated an industrial ethylene plant with 15 parallel cracking furnaces, 2 cooling towers, 6 turbines, 6 compressors, and one burning boiler. Experimental results show that the proposed method obtained 13.86% improvement compared with traditional optimization. The proposed approach also provides a better balance between production and energy utilization leading to more steam generation and less fuel consumption than the original optimization approach. The experimental analysis shows that better profit with higher product yields results by considering energy consumption and optimizing operating conditions. The authors concluded that the impact of feed property on energy consumption and generation was not negligible in the parallel furnaces scheduling. Furthermore, the authors indicated that future extensions would be an integration of the long-term planning involving the cleaning operation and shutdown for the furnace and the development of a more detailed kinetic model.

Su et al. (2017) presented an integrated approach that combines carbon footprint analysis and production planning. The objective of this research is to reduce carbon emissions at the enterprise level. The authors addressed that majority of the works in the literature focus on the macro or micro levels, and only a few studies emphasize carbon footprint analysis and carbon emissions reduction at the enterprise level. They constructed carbon emission analysis models to capture the relationship between emissions and production plans. The authors then developed a production planning model based on energy consumption to minimize carbon emissions. They concluded that the proposed approach for production planning and carbon footprint analysis applies to the entire company′s operational process. The authors developed a hybrid discrete particle swarm optimization (PSO) algorithm to determine the optimal solution and investigated an actual pharmaceutical enterprise to test the effectiveness of the algorithm. The numerical analysis demonstrates that the proposed approach reduces carbon emission by 6.77% or 610.2 tons per year at the enterprise level. The authors did not consider production costs and concluded that there must be an important trade-off made between emissions reduction and production costs. As further research, the authors indicated that energy-oriented production planning can be modeled as a multi-objective optimization problem with conflicting objectives and that consideration of uncertain demand and supply risks would make the proposed model more realistic.

Liang et al. (2019) presented a mixed-integer linear programming (MILP) model of a capacitated production planning and scheduling problem considering differences in processes energy consumption and sequence-dependent setup time. The goal is to minimize the total costs, including inventory, backlog, changeover costs, and energy costs in production. The authors address that most of the existing papers investigated a similar problem without considering energy costs. In contrast, the authors mainly focus on energy efficiency and propose a fix and optimize (F&O) heuristic approach to the large-scale problem. Furthermore, the authors also extend the energy-oriented research into integrated production planning and scheduling models. The authors presented a case study of tea drink production lines in digital command control (DCC) Beijing to demonstrate the application of the model and the proposed algorithm. The computational analysis shows that as the problem size grows, the F&O algorithm tends to have better performance and the feasibility to solve the model also improves. Also, the authors found that the proposed model significantly reduces the total cost by an average of 34.74%, while energy costs reduce by 55.52%. They conclude that the proposed model balances 3 goals: production planning, scheduling, and energy saving. The model provides a better solution that dominates any other decentralized solution considering only one or two of these goals. The authors apply the proposed model to single-machine continuous production problems. It could be extended to multi-stage production lines. In addition, authors also suggest extending this research to a production line with uncertain parameters, such as uncertain processing times.

1.2.2 APP considering conventional energy

Aggregate production planning (APP) looks to determine optimum production and workforce levels for each period over a planning horizon to satisfy usually varying customers demands while minimizing costs (Cheraghalikhani et al., 2019). APP is worked as the baseline for further formulating the master production scheduling and planning for other production resources, such as capacity, raw material, etc. An efficient and successful APP can maintain the target lead times in a supply chain. A large amount of contributions in APP have been published in the last four decades mostly focusing on APP where the input parameters, such as product demands, are assumed deterministic. Some literature review works in APP such as the ones in (Lai and Hwang, 1992), (Nam and Logendran, 1992), (Cheraghalikhani et al., 2019) mention that main problems with applying stochastic models are lack of computational efficiency and inflexible probabilistic doctrines which might not be able to model the real scenarios. Importantly, Cheraghalikhani et al. (2019) mentions that attention to stochastic models have recently increased and that no paper have considered multi-objective stochastic APP model.

Chaturvedi and Bandyopadhyay (2015) proposed a methodology that is applicable to both aggregate planning of input material and APP. The authors also calculated the production levels that gave the least variations among different periods while satisfying the demands. The methodology proposed is a graphical methodology based on the principles of Pinch Analysis for energy supply chain planning to manage a production strategy considering supply and demand. This methodology is very effective in identifying production bottlenecks, and it provides an in-depth understanding of the overall APP problem. The authors also demonstrated the applicability of the methodology to supply chains considering energy through illustrative examples. They mathematically demonstrated that the graphical representation of the proposed APP problem is equivalent to the Euclidean shortest path problem in computational geometry.

Modarres and Izadpanahi (2016) considered that in energy-intensive manufacturing plants, energy savings would be an essential element to consider in the production planning. After reviewing the literature in APP, the authors found that energy savings have not been integrated into production planning models. This research paper presented a multi-product, multi-period APP model considering energy planning, demand, and production capacity simultaneously. The authors stated three objective functions, which minimize operational cost, energy cost and carbon emission. Then the multi-objective model was transformed into a single-objective model by applying a goal attainment technique. The authors applied robust optimization to deal with uncertainties such as demand, production cost, inventory cost, backorder cost, and energy specifications. Experimental results show that when the level of uncertainty is 30%, the service level of the robust optimization model is 96%, whereas in the deterministic model is 81%. Besides, the standard deviation of the robust optimization model is 105,681, whereas in the deterministic model it is 252,767. In the numerical analysis, the robust optimization model always performs better than the deterministic model. The authors also addressed the limitations of using robust optimization by saying that it is very conservative and can lead to the worst results in some cases. They mentioned that stochastic optimization would be an alternative for dealing with the uncertainty in this APP model.

Nour et al. (2017) presented an energy-based APP model for a porcelain tableware manufacturing. They developed a MILP model to maximize the profit while explicitly including energy cost as one of the cost elements. They presented a case study of a manufacturer that exports most of its production from Egypt to other countries. The factory has four production lines depending on the forming operations, but authors only consider the press production line for experimental analysis as 30% of the production comes from it. Experimental analysis shows that the proposed model outperforms the cost and demand fulfillment of current management planning practices. The total costs reduced by 23.2%, and demand fulfillment improved by 96.2%. The authors also found that energy cost was high, as it constitutes 17% of the total production cost. The authors apply the proposed model to a single-product problem. The model can be extended to a multi-product environment. Further research mentioned in this paper includes considering the uncertainty of demand, including RE technologies, such as solar PV , WT, and energy storage system (ESS).

1.2.3 PP considering renewable energy

Jin et al. (2015) developed a deterministic multi-plant, production-inventory model by directly injecting onsite and grid RE into the manufacturing facilities to achieve low-carbon operations. The authors addressed that this work takes an early step down the path to achieve low-carbon production through integrating onsite and grid RE. They measured the manufacturing sustainability performance by introducing the green energy coefficient (GEC). This research paper aims to minimize the total manufacturing cost, including energy, by optimizing the production, inventory, backorders, and energy consumption, and achieving the GEC target in each period. Numerical experiments look to verify and validate the proposed planning model at a moderate renewables penetration level. Numerical experiments show that achieving a desirable level of GEC is feasible if the manufacturer can mix onsite generation with grid renewable energy. The authors also conclude that equipment cost and power intermittency are the main obstacles that constraint the broader implementation of eco-friendly energy technology. Future work includes extending the deterministic model to a stochastic programming framework that accommodates uncertainties ranging from power intermittency, product demand, yield variation, real-time electricity pricing, and machine failures.

Golari et al. (2017) developed a multi-period, multistage stochastic production-inventory planning model in a multi-plant manufacturing system powered with onsite and grid RE. The model aims to minimize the production cost, including energy, while determining the production quantity, inventory level, and RE supply in each period. The authors' methodology consisted of three steps. First, they developed a deterministic planning model to attain the desired green energy penetration level. Then they extended the deterministic model to a multistage stochastic optimization model that considered RE uncertainty.The last step used a modified Benders Decomposition algorithm to search for the optimal production schedule using a scenario tree. The authors classified the electric power into onsite renewable energy, grid renewable energy, and grid conventional energy based on the generation sources. The first stage decisions are production quality, inventory level. and backorders and they occur before realizing RE scenarios. The authors considered three recourse decisions on the remaining stages of the problem. They are the consumption of onsite RE, grid RE or grid conventional energy. First stage decisions and recourse decisions are found considering the realizations for onsite RE, grid RE, and grid conventional energy. The authors also assessed the value of the multistage stochastic programming (VMS) model solved. Experimental results show that when the number of stages increased, the VMS also increased. The VMS for the multiple plant problem with 3, 4, and 5 stages is 3,762, 10,324, and 35,490, respectively. Experimental results also show that computational time significantly reduced when authors applied the Benders decomposition algorithm instead of solving the extensive formulation. Further work is on developing a model considering uncertainty of wind and solar energy and ESS availability. Because the model in this research did not consider ESS these factors need to be jointly investigated.

Golpîra et al. (2018) introduced Smart Energy-Efficient Production-Planning (SEEPP) for a job shop manufacturing system in the presence of grid-connected microgrid powered with wind power generation. The authors developed a novel risk-based Robust Mixed Integer Linear Programming (RMILP) model to deal with the unpredictability of wind speed and the uncertainties of demands. The scenario-based conditional value at risk (CVaR) approach is employed to deal with wind speed fluctuations as the main driver of uncertain power generation. The authors addressed a more comprehensive range of RE characteristics such as main grid, WT, combined heat and power (CHP) generator, thermal storage system

(TSS), ESS, boiler, setup costs, processing costs, holding costs, uncertain demand, and decision manager's (DM) risk aversion level. They integrate the SG energy generation-distribution management system into a multi-item, multi-period, multi-resource, lot-sizing (LS) and scheduling problem in a manufacturing system with job shop (JS) configuration. The authors also analyzed the performance of the proposed SEEPP concept in terms of robustness, accuracy, and computational efficiency. Numerical experiments show that the proposed SEEPP framework reduces costs to at least 0.55% compared to the conventional method. Furthermore, the DM's risk aversion level significantly improves the model's performance in terms of accuracy, robustness, and computational efficiency. Authors suggest extending the single-objective problem to multi-objective or multi-level programming to provide a decentralized framework. In the proposed framework, it is assumed that the demand for the products should be completely met and, therefore, any lost sale or backorder costs are not considered in the model formulation. The authors suggested that including other RE technologies such as fuel cell, PV, and microturbine could improve the model's accuracy and robustness.

Pham et al. (2019) developed an optimization framework consisting of two stages for determining the optimal production scheduling and microgrid sizing in a multi-facility production-logistics system considering variation in energy supply over the time horizon. In the first stage, the authors solved a model to minimize the total non-energy costs associated with production, backorders, and inventory in each period. In the second stage, the authors developed a model that decarbonizes the manufacturing, transportation, and warehousing operations by considering onsite wind and solar energy. This model tests the economic feasibility of achieving net-zero energy operations. Capacity factors, defined as the ratio of power generated by a generation technology over its nominal power, are input to account for the daily variations of energy supply at the factory and warehouses. The authors performed extensive climate data analytics to compute capacity factors for wind and solar generation at multiple regions in the world. Experimental results show that net-zero energy operation is cost-effective in geographical areas where WT capacity factor is above 0.25 or the PV capacity factor above 0.45, respectively. Sensitivity analyses show that net-zero energy operation is not competitive in high wind profile areas if the battery cost is high (0.1 to 0.5M/MWh). In this situation, PV coupled with battery system is always preferable. Results also show that an island microgrid yields a higher levelized cost of energy (LCOE) than a grid-connected microgrid with net metering. Future work is developing a multistage stochastic program to simultaneously find the optimal production plan and the size of the generation technologies considering uncertainties in product demand and energy supply.

Yu et al. (2019) presented a stochastic optimization approach for designing and operating hybrid renewable energy systems (HRESs). They addressed that HRESs have been introduced globally with the increasing emphasis on sustainable energy and the environment. However, the main challenge to implement HRESs is the inherent uncertainty in energy supply and demand. ESS can be a promising alternative to minimize the difference between varying supply and demand. The authors mentioned that a deterministic approach for designing the ESS is limited because it captures a fixed snapshot of the varying system. They also said that the ESS should be designed and operated based on the explicit consideration of uncertainty. Alternatively, a stochastic approach is used for designing the HRESs. The objective of the authors' proposed model is to compute the optimal size of the ESS and the detailed hourly operation plan to minimize the expected daily cost. The authors first developed a two-stage stochastic programming model to design and plan the HRESs. Then they transformed the stochastic model into a deterministic MILP. The authors compared the stochastic and deterministic approaches. They found that the deterministic approach was more expensive than the stochastic one. Experimental results showed that the HRESs design and operation cost for the stochastic model (\$ 6981/day) was at least 9.1% more economical than the one for the deterministic model (\$ 7680/day).

1.2.4 APP without renewable energy

Leung et al. (2006) proposed a two-stage stochastic programming approach for the multi-site APP problem with uncertain final product demand. The approach lets to determine optimal medium-term production and workforce plans. The authors considered production plant preference selection as an additional constraint. Leung et al. (2006) also included the shortage costs associated with the loss of goodwill from unsatisfied orders as a penalty cost. The probability distribution of the product demand and the impact of unit shortage costs on the total cost are analyzed. First stage decision variables are regular and overtime production, subcontracting quantity, required workforce level, workers hiring, and layoff level. Decision variables for the second stage of the problem are inventory and backorder quantities. The model's parameters are regular time production cost, overtime production cost, subcontracting cost, backorder cost, and sales volume. The authors considered three months of projected data for experimenting with the proposed model. Leung et al. (2006) considered four possible scenarios− boom, good, fair, and poor with associated probabilities of 0.40, 0.25, 0.20 and 0.15, respectively. Numerical analysis used a set of data from a multinational lingerie company in Hong Kong to demonstrate the robustness and effectiveness of the proposed model. The authors addressed that the selection of probability distribution of economic scenarios could be further investigated. It is an issue the author of this thesis also wants to analyze using design of experiments (DOE). The authors of the reviewed work also concluded that sensitivity analysis on the cost parameters needs further study. The authors did not present the value of the stochastic solution (VSS) to assess the benefits of the proposed stochastic model. The paper presents the extensive formulation of the two-stage stochastic program and does not research any decomposition algorithm for the solution approach. Leung et al. (2006) also did not consider RE. Nowadays, the adoption of WT, PV, and BS is happening in manufacturing setting. Thus the simultaneous integration of these RE technologies needs to be further investigated.

Aliev et al. (2007) mentioned that on developing APP models, practitioners usually face uncertain market demands and capacities, imprecise process times, and other factors introducing inherent difficulty to find the optimal solution. The authors said that some researchers used fuzzy models to deal with the drawbacks of deterministic models. However, they said that most of the existing fuzzy models deal with separate APP without considering the interrelated nature of production and distribution systems, possibly leading to inaccurate results. In their paper, the authors developed a fuzzy integrated multi-period and multi-product production and distribution model for a supply chain considering the interrelation between production and distribution systems. The model developed had the production units connected to the distribution centers and the distribution centers connected to the customer zones. The authors considered fuzzy production, fuzzy capacity constraints and fuzzy forecasted demand. Computational experiments compared the proposed fuzzy integrated production-distribution aggregate planning (PDAP) and the disintegrated approaches. The computational experiments show that the proposed fuzzy integrated PDAP model gives a profit higher by 5% to 10%) when the actual demand declines from the forecasted values or the capacities decrease over the planning horizon. The experimental result also shows that the average profit would increase by 9% to 11% if the decision-makers use fuzzy integrated PDAP rather than a disintegrated PDAP model, where the production and distribution processes are described as separate models with separate objective functions. The authors also mentioned that the traditional methods are heavy on the computational aspects and need more time to find the optimal solution. Finally, the authors used an evolutionary optimization technique named fuzzy genetic approach for solving the model. The experimental results show that there would be significant risk of large profit losses if demand and capacity change. The author of this thesis thinks that a stochastic programming model could consider a large number of scenarios for the uncertain parameters effectively and be compared to the methods used in Aliev et al. (2007).

Chakrabortty et al. (2015) proposed a possibilistic environment-based particle swarm optimization (PE-PSO) for APP. They used the linear reduction of inertia weight. It is an important PSO parameter that permits modification of the velocity and movement of the particles. Chakrabortty et al. (2015) considered a large number of decision variables, such as regular time production, overtime production, subcontracting level, backorder level, inventory, workforce hiring, and layoff level. The authors also considered escalating factors in each of the cost categories over the planning horizon. The authors addressed that the availability of raw materials and other production planning parameters are uncertain because of their inherent impreciseness. A fuzzy triangular probability distribution function copes with the uncertainties in operating costs, demands, and capacity data. A case study is performed to demonstrate the applicability of PE-PSO for solving APP problems. In the computational study, the performance of PE-PSO is contrasted to the one of a standard genetic algorithm (GA) and a fuzzy based genetic algorithm (FBGA). Computational results showed that PE-PSO performs well in the comparison. The proposed linear reduction of inertia weight approach PSO under a possibilistic environment shows better results than the traditional PSO, standard GA and fuzzy based GA. Moreover, the authors also addressed that if the objective function is linear, then the linear programming approach would be better than the GA, FBGA, and PE-PSO.

Gholamian et al. (2016) presented a fuzzy multi-objective APP model for a supply chain. Authors proposed an APP model for this situation considering uncertain cost parameters and product demands. The proposed APP model is a multi-objective, mixed-integer, nonlinear program with three conflicting objective functions. The first one minimizes total costs, including those related to production, purchased raw material, raw material inventory, labor, training, hiring, firing, final inventory, shortages, and transportation. The second one considers customer satisfaction by minimizing the sum of the maximum shortages among the customers in all periods. This objective function is nonlinear, and authors linearize it with the help of an auxiliary variable. The third one is to minimize the rate of changes in human resources. The authors carried out a case study for testing the effectiveness and validity of the presented model and used GAMS software to obtain the results. Future works include the integration of strategic decisions and tactical or operational decisions in the APP model. Furthermore, minimizing greenhouse gas emissions and industrial waste would be another relevant objective function in the multi-objective APP problem.

Djordjevic et al. (2019) proposed a fuzzy APP model considering the cycle time of different production and warehousing operations as primary indicators of performance. They considered uncertain parameters such as customer demand, production output, production time, time safety stock stays in the warehouse, and time spent preparing orders to deliver to the customers. The authors introduced fuzzy sets using historical data recorded by the supplier and the experience of a logistics management team. They found that most of the previous models minimize operational costs in manufacturing, dealing with production, inventory, or delivery costs. The authors addressed that some of the vital factors have been assumed or theoretically defined and that most APP models have been validated theoretically without testing them in realistic environments. The authors stated that the existing APP models do not consider the material flow time and that in some industrial sectors, it has a substantial impact on manufacturer performance. They estimated customer demand could be 10% higher or lower than the forecasted demand, based on the subjective supplier′s management team experience. They used a fuzzy triangular distribution for the total time required for production. They carried out several experiments using real-world data collected by the supplier to analyze the impact of uncertainty on APP. The novelty of this work is the introduction of a fuzzy-based APP model to deal with the uncertainty in material flow time. The authors also found that the developed fuzzy APP model can shorten the time required to perform the production and warehouse operations and improve the supplier's performance.

The literature review presented in this sub-section showed that to deal with the uncertainty in the parameters of APP problems one author developed a two-stage stochastic programming model (Leung et al., 2006). The other authors develop fuzzy models that in some occasions were solved heuristically. Though there are many APP studies, there is still a research gap on addressing APP models with RE and energy prosumers using stochastic programming. Factories can install onsite RE to meet their energy demands and sell the surplus energy to main grid. Then, a factory can act as a prosumer instead of just a consumer. A two-stage APP model also can help the decision-maker to evaluate the supply chain more effectively. Furthermore, considering re-manufacturing, emission of CO2, waste management, and other environment-friendly factors can help to build a green APP model.

1.2.5 RE models considering energy prosumers

An energy prosumer is someone who can produce and consume energy. Nowadays, prosumers are growing in the energy market as more people and organizations generate their power from distributed energy resources. The rise of prosumers helps preserve the natural environment, drive economic development, and sustain net-zero carbon manufacturing operations where all energy consumed or demanded over the year offsets the RE generated. Zero-carbon manufacturing spans a plethora of issues ranging from material and energy inputs, to the efficiency of manufacturing facilities and supply chains (Ball et al., 2009).

Azar et al. (2018) presented a scalable framework to coordinate the net load scheduling, sharing, and matching in a neighborhood of residential prosumers connected to the grid. The authors addressed that prosumers and aggregator's objectives conflict with each other and that they need to be optimized simultaneously. The aggregator intends to maximize the profit and minimize the grid purchase while prosumers' objective is to maximize the comfort level and minimize the electricity cost. The authors model an efficient negotiation approach in which the aggregator and the prosumers objectives are satisfied. They proposed a framework for prosumers and the aggregator, which encompasses two separate multi-objective mixed-integer optimization models. They employed GA to generate a set of feasible non-dominated solutions to the optimization problem of each prosumer and the aggregator. The authors addressed that the integration of RE sources (RESs), such as PV and BS systems, to the smart grid would lead to efficient and optimal management of peak demand reduction of the power grid. They concluded that integrating RE to the smart grid would benefit prosumers by achieving flexible utilization and electricity bill reduction. The authors presented an automated negotiation approach embedded in the framework, enabling negotiators to reactively transact on concurrent power and price using private utility functions and preferences. To assess the performance of the framework, authors define the following metrics: peak demand reduction (PDR), peak-to-average ratio (PAR), average appliance operation delay (AOD), average flexibility usage rate (FUR), average prosumer cost-benefit (PCB), average self-load-satisfaction rate (SLR), and average self-sufficiency rate (SSR). The authors evaluated the framework's effectiveness by collecting economic and environmental assessment metrics through various numerical simulations. Future work will focus on incorporating industrial and commercial prosumers, and adding a negotiation level between various aggregators.

Cui et al. (2018) proposed a two-stage energy sharing framework for a prosumers microgrid by considering RE generation, load shifting, and multiple storage units. In the first sage, to overcome the impact of uncertainties of market prices and RE and consider the worst-case scenarios, the authors developed a robust bilevel energy sharing model to get a robust energy sharing schedule for prosumers and the retailer. They addressed that the bilevel optimization structure introduces difficulties such as nonconvexity and disconnectedness. The robust optimization model turned out to be surprisingly difficult to handle mathematically, Then it was transformed into a single-level mixed-integer linear programming problem by using proper linearization techniques. In the second stage, the authors developed an online optimization model to optimize the hourly energy schedule. Simulation results showed that the proposed mixed-integer linear programming model solves quickly to implement it in real life. The authors also mentioned that stochastic optimization would be an alternative method for dealing with uncertainties rather than robust optimization.

Van Der Stelt et al. (2018) contributes to the topic of assessing the impact of energy prosumers. The authors compared the technical and economic feasibility of Household Energy Storage (HES) and Community Energy Storage (CES) from the perspective of the end-consumer because they are two promising storage scenarios for residential electricity prosumers. They addressed that the LCOE is used globally as an index of battery systems' economic performance and assumed that the feed-in pricing tariff will disappear in the long run. They developed mathematical optimization models for both scenarios (HES and CES) that schedule the allocation of energy from the PV system, battery, and main grid to satisfy the demands of the households and minimize the amount of power taken from the grid over time. Then authors formulated the proposed problem as a mixed-integer linear program (MILP) to minimize the costs of power received from the grid. Numerical analysis was performed by using real demand data and PV generation profiles of 39 households in a pilot project initiated by the Distribution System Operator (DSO) Enexis in Breda, Netherland. Numerical analysis showed that implementation of different ESS reduces annual costs by 22% to 30% and increases the self-consumption of PV power by 23% to 29%. The authors also performed sensitivity analysis which shows how investment costs of ESS per kWh play an essential role in determining the economic feasibility of HES and CES. They concluded that CES units might perform better than HES on environmental indicators such as material usage and CO2 production. Furthermore, CES systems are more reliable than HES systems if considering the safety issues related to lithium-ion batteries.

Iria et al. (2018) addressed the issues of an inflexible strategy of an aggregator of small prosumers participating in the energy market. To overcome the limitations of inflexible strategy, the authors developed two optimization models. The first one is a two-stage stochastic optimization model that minimizes aggregator's net cost of buying and selling energy at day-ahead and real-time market stages. Furthermore, the authors also used scenario-based stochastic programming to deal with the uncertainty of electricity demand, renewable generation, outdoor temperature, and end-user behavior. Subsequently, the second optimization model addresses a predictive control method to set the operation of flexible loads in real-time. The authors performed a case study of 1000 small prosumers from the Iberian market. They compared four day-ahead bidding strategies, two real-time control strategies, and combined day-ahead and real-time strategies. Numerical analysis showed that the proposed strategies reduce the aggregator's net cost by 14% compared to the inflexible strategy. The authors also compare the smart strategy adopted by the stochastic optimization model to a deterministic one. Numerical results show that the deterministic strategy places higher demand and supply bids than the smart strategy almost all days. In a nutshell, under uncertainty conditions, the smart strategy outperforms all other strategies, such as deterministic, flexible, and inflexible strategies.

Hussain et al. (2019) proposed a stochastic wind energy management model with bi-directional energy flows between smart grid and wind energy prosumers (WEPs). Furthermore, the authors also employed a non-linear stochastic price model to tackle market price uncertainty by using effective service level agreement (SLA). The authors also used wind energy estimation model within energy district for prosumer energy generation. The model consists of several sub-models that maximize the smart grid revenue (GR), prosumers energy surplus (PES) and minimize the prosumers energy costs (PEC). The sub-models tackle the uncertainties faced by fluctuations on the market price and the wind profile. To test the effectiveness of the model authors performed a case study in Capano Bay, Texas. The model is dealt with hourly parameters and solved by using two heuristic algorithms: GA and PSO. In all three aspects: GR, PES and PEC GA performed better than PSO. In this paper, the authors incorporated a wind estimation model and a probabilistic price model into their non-linear stochastic optimization model. This model is more versatile for modeling stochastic energy for the smart grid and the wind energy district prosumers than prior works. The authors also suggested investigating solar, biogas and hydel based WEPs in the near future. Finally, this research work paves the way for developing an optimization model considering hydel based WEPs in the broad area of smart grid (SG).

Based on the energy prosumers literature review, most of the existing research papers model RE projects for multiple residential customers. None of these papers optimizes the production and the siting and sizing of the RE systems in manufacturing facilities that become energy prosumers. This thesis looks for an effective way to solve such optimization problem.

Table 1.1: Comparison of several key previous works and the proposed research

Problem & author	RE	BS	Energy prosumers	Source of uncertainty	Model type	Solution method
APP in Leung et al. (2006)	N	N	N	Product demand	Two stage stochastic program	Exact solution of the LP extensive formulation
PP in Golari et al. (2017)	Y	N	N	RE supply from WT and PV	Multistage stochastic program	Modified Benders decomposition
Lot-sizing & scheduling PP in Golpîra et al. (2018)	Y	Y	N	Product demand and wind profile	Robust mixed-integer linear program (RMILP)	Exact solution of the RMILP
APP in this thesis work	Y	Y	Y	Product demand, machine and labor hours capacity, and RE supply from WT and PV with varying CF	Two stage stochastic program	Exact solution of the LP extensive formulation

Table 1.1 contrasts the previous works most closely related to this thesis

considering the relevant aspects this research work contributes (i.e., problem type, RE technologies studied, battery, energy prosumers, source of uncertainty modeled, model type, and solution method). The abbreviations PP and APP are used for production planning and aggregate production planning problems, respectively.

1.3 Estimation of a WT capacity factor

Typically, automated surface observing systems are installed at a height $h_g = 10m$ above the ground. Using equation 1.1 below, the estimated wind speed at any height h, notated as v_h, can be computed as a function of the observed wind speed (v_g), the height (h), the typical height of the observing system (h_g), and the Hellman exponent (k), which considers seaside location, air stability and terrain shape (Bañuelos-Ruedas et al., 2011). The range for this exponent is between 0.27-0.34 as stated by (Blackadar and Tennekes, 1968).

$$v_h = v_g \Big(\frac{h}{h_g}\Big)^k, \qquad h \geq h_g \tag{1.1}$$

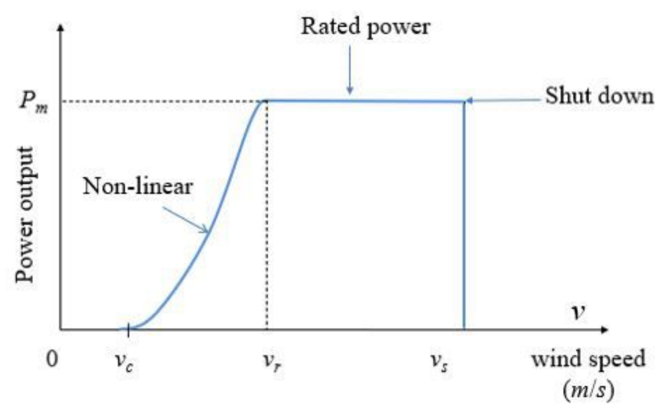

Figure 1.1: A wind turbine power curve

The wind turbine (WT) power curve shown in Figure 1.1 shows the relation between the wind speed, v, and the WT power output, P (Thiringer and Linders, 1993). The turbine power curve has four phases. The first one is the standby phase.

In this phase the power is not generated because the wind speed is below the minimum needed to operate the turbine ($v < v_c$). The next phase is the nonlinear production phase where ($v_c \leq v \leq v_r$). In this phase, power is directly proportional to the rated power, P_m, and the cube of the wind speed, and inversely proportional to the cube of the rated wind speed. In the rated power phase ($v_r \leq v \leq v_s$), the power output is equal to the rated power. In the cut-off phase ($v > v_s$), no power is generated since the turbine needs to be shut down for protection purposes.
Equation 1.2 presents a cubic model used to determine a WT electric power $P_w(v)$ as a function of the wind speed.

$$P_w(v) = \begin{cases} 0, & \text{if } v < v_c, v > v_s \\ P_m(\frac{v}{v_r})^3, & \text{if } v_c \leq v \leq v_r \\ P_m, & \text{if } v_r \leq v \leq v_s \end{cases} \tag{1.2}$$

The capacity factor (CF) of a WT, notated as λ, is the ratio of the power generated by the WT and the rated peak power P_m. The CF assesses the utilization of the WT. It is a fraction between zero and one that can be estimated using equation 1.3 when the wind speed is in the range $v_c \leq v \leq v_r$. If the wind speed is less than v_c, the capacity factor will be 0, and if the wind speed is higher than v_r, the capacity factor will be 1.

$$\lambda = \frac{P_m(\frac{v}{v_r})^3}{P_m} \tag{1.3}$$

1.4 Estimation of a solar PV capacity factor

The output energy of a PV system is a direct-current (DC) power. Under a clear sky condition, the PV output in W/m^2 can be precisely predicted using

Hottel's equation (Hottel, 1976). This equation uses multiple factors for DC power output estimation, including panel orientation, tilt angle, date and local hour, latitude, and weather conditions. According to Hottel's equation, the total solar irradiance at time t, denoted as $I_{total}(t)$, reaching the Earth's surface comprises three components as follows,

$$I_{total}(t) = I_d(t) + I_f(t) + I_r(t) \tag{1.4}$$

In equation 1.4, $I_d(t)$ represents the direct beam from the sun at time t and is also the primary energy source, $I_f(t)$ is the solar energy that is collected through diffusion, and $I_r(t)$ is the reflected solar energy. Experiments show that $I_f(t)$ is about 10% of $I_d(t)$ while $I_r(t)$ can be ignored due to its small contribution to PV generation. Thus equation 1.4 can be simplified as

$$I_{total}(t) \cong I_d(t) + 0.1I_d(t) = 1.1I_d(t) \tag{1.5}$$

The following procedure four-step procedure can be used to compute PV capacity factors. The procedure is based on the studies in Tao et al. (2010),Taboada et al. (2012), and Villarreal et al. (2012). The details of each step are described below and the notation used is presented in Table 5.1 in Appendix A.

Step 1: Compute the daily sunrise ω_{rise} and sunset hour ω_{set} perceived by the PV panel as follows,

$$cos(-\omega_{rise}) = cos(\omega_{set}) = -tan(\phi - \beta)tan\delta \tag{1.6}$$

$$\delta = 0.40928sin\left(\frac{2\pi(d + 284)}{365}\right), \quad d = 1, 2, ..., 365 \tag{1.7}$$

Note that ϕ and β are input parameters that represent the latitude and the PV tilt angle, respectively. The solar declination angle for day d ($d \in \{1, 2, ..., 365\}$), notated as δ, results from using equation 1.7.

Step 2: Compute the amount of solar irradiance incident on the PV surface. Under the clear sky condition, the direct solar beam incident on the ground at time t in day d can be estimated as follows,

$$I_d(t) = 1370 \times \left(0.7^{(cos\gamma)-0.678}\right)\left(1 + 0.034cos\left(\frac{2\pi(d-4)}{365}\right)\right) \tag{1.8}$$

where

$$cos\gamma = cos\delta(cos\phi \times cos\omega) + sin\delta sin\phi \tag{1.9}$$

Here γ represents the solar zenith angle. It depends on the solar declination angle δ, the latitude ϕ, and solar hour ω. Since the PV tilt angle may not be equal to the latitude, the actual solar irradiance incident on PV at time t in day d, denoted as $I_{pv}(t)$, is given as

$$I_{pv}(t) = I_d(t) \times \left(cos\theta + 0.1 \times \left(1 - \frac{\beta}{\phi}\right)\right) \tag{1.10}$$

where,

$$cos\theta = sin\delta sin(\phi - \beta) + cos\delta cos(\phi - \beta)cos\omega \tag{1.11}$$

Note that θ is the PV incident angle that is dependent on δ, ϕ, β, α (i.e., surface azimuth angle), and ω. Equation 1.11 has a term that depends on α dropped because energy yield is maximum if this term becomes equal to zero. In the Northern Hemisphere energy yield is maximum for a PV strictly oriented towards the South.

Step 3: Due to the weather uncertainty, the actual output of a PV system, denoted as $P_{pv}(t)$ at time t in day d is given as follows

$$P_{pv}(t) = W_t \eta A I_{pv}(t) \left[1 - 0.005(T_0 - 25)\right] \tag{1.12}$$

Where,

W_t= random variable varying between zero and one representing the stochastic weather at time t in day d. Thus, a snowy day has values for W_t equal to zero while a clear sky day has W_t equal to 1.

η = PV efficiency.

A= PV size or area (m^2).

T_0= PV operating temperature (°C)

Step 4: Compute the capacity factor using the following formula:

$$\lambda_{PV} = \frac{1}{P_{pv}^{Max} T} \sum_{t=1}^{T} P_{pv}(t) \tag{1.13}$$

where P_{pv}^{Max} and T are the rated or nominal PV system capacity and the total number of generation hours, respectively. Equation 1.12 shows that it is preferable to operate a PV at a low temperature because it can generate more power than at any higher temperature given the same weather and solar irradiance. The four-step procedure to compute the PV capacity factor presented above assumes that the PV is located in the Northern hemisphere. The model is also applicable to the Southern Hemisphere by replacing the latitude ϕ with $-\phi$ in all corresponding equations 1.6, 1.9, 1.10 and 1.11.

1.5 Thesis goal and contributions

Onsite generation, which is also known as distributed generation (DG), produces electricity by locally installing distributed energy resources (DER), such as wind turbine (WT), solar photovoltaics (PV), diesel generator, biogas fuel cell, combined heat and power, and battery storage system (BSS). A microgrid is a type of DG system. It typically consists of WT, PV, fuel cells, micro-turbines, and diesel engines (Jin et al., 2015). Onsite wind and solar generation reduce carbon emissions by providing partial or full power to a factory or a warehouse for their daily operations. Currently, large manufacturers are focused on developing onsite RE generation to produce their own power and achieve net-zero carbon manufacturing operations. Such trend soon will grow to include also medium-size manufacturers. However, the literature review in (Cheraghalikhani et al., 2019) mentioned relevant issues that research in APP has included but didn't mention about using energy from RE sources, a current critical issue manufacturing companies need to address due to climate change.

The goal of this thesis is to solve a multi-period aggregate production planning (APP) problem having four stochastic (i.e., uncertain) parameters: product demand, labor and machine hours capacity, and RE supply, and demonstrate that is is cost efficient to decarbonize manufacture, transportation and warehouse operations. The problem setting consists of an industry developing its yearly APP and considering the installation of microgrids coupled with wind turbines(WT), and photovoltaics (PV), and battery systems (BS) for its manufacturing and warehouse facilities. These facilities also can connect to the main grid as energy prosumers (i.e. buyers of energy and sellers of RE) and sign in time-varying tariffs schemes, such as time of use (TOU). The methodology researched in this thesis is two-stage stochastic programming, which also involves the use of probability and statistics for estimating the model parameters and analysing the model results. The two-stage stochastic APP models developed determine the optimum RE portfolio, generation capacity, production plan, and machine and workforce levels that minimize the company total expected operational cost. It is assumed that the company strives to become a net-zero carbon manufacturing production facility. The APP models consider uncertainty on the RE supply due to the intermittent wind and uncertain weather conditions under the yearly horizon and balance the energy requirements under two types of time granularity: daily and hourly.

Bakir and Byrne (1998) mentioned that uncertainty is one of the main characteristics of discrete manufacturing systems. They indicated that most of the uncertainties arise mainly from four factors: demand, processing times, workstations failures and maintenance times, and cost. Consequently, considering those uncertainties can make the APP models more realistic, whereas integrating the RE aspect would accelerate the use of RE in manufacturing systems looking to achieve net-zero carbon manufacturing operations.

This thesis work contributes to the relatively scarce literature on using stochastic programming to solve APP problems by: (1) incorporating two sources of RE (WT, PV), (2) considering battery systems (BS), energy prosumers, and time of use (TOU) tariffs (3) demonstrating that two-stage stochastic programming is suitable to solve large-scale APP problems, (4) exemplifying the use of big-data analytics to determine values for the model parameters that reflect the actual hour-to-hour variability on weather conditions at the cities studied, (5) assessing the expected cost differences between solving deterministic vs stochastic models and (6) measuring the benefit of modeling energy requirements under hourly time granularity vs daily time granularity. Thus, this research work extends the ones in Leung et al. (2006), Jin et al. (2015), Modarres and Izadpanahi (2016), Golari et al. (2017), Golpîra et al. (2018), Pham et al. (2019) and Yu et al. (2019).

1.6 Document organization

The remaining chapters in this thesis are organized as follows. Chapter 2 presents the two-stage stochastic APP model under daily granularity and the numerical experimentation. Chapter 3 provides the model for the two-stage stochastic APP model under hourly granularity and the numerical experimentation. Chapter 4 presents a further extension of the developed two-stage APP model to consider energy prosumers, time-of-use (TOU) energy tariffs, and hourly time granularity. Chapter 5 contains the preliminary conclusions about this research, and it mentions possible future work.

2. APP CONSIDERING DAILY ENERGY REQUIREMENTS

Over the years researchers have increased the study of the effects of using renewable energy (RE) sources, such as solar and wind power in manufacturing industries. RE generation is more volatile than conventional sources because of its dependence on weather. Active participation of energy prosumers adopting an optimal portfolio of distributed energy resources in their microgrids can reduce the volatility of RE generation and more importantly it guaranties that distributed generation based on renewables is sustainable and mitigates energy shortage, climate change, and poverty.

This chapter is organized as follows. Section 2.1 presents the aggregate production planning (APP) problem researched and the research questions. Section 2.2 gives a background on the two-stage stochastic programming with recourse method applied in this thesis work. Section 2.3 provides the mathematical formulations for two APP model instances developed in this chapter. The model instances are: (1) Island microgrid (IM) adopting battery storage (BS) and (2) Prosumer microgrid adopting BS. The mathematical formulation presented for each instance is the extensive formulation of the two-stage stochastic program with recourse. Section 2.4 describes how uncertain product demand, labor hours capacity, and machine hours capacity are represented in the models and it elaborates on the procedures to compute the capacity factors (CF) for wind turbines (WT) and solar photovoltaics (PV). Section 2.5 describes the numerical experiments. Sections 2.6 and 2.7 provide the computational results and the sensitivity analysis, respectively.

2.1 Problem statement

The system researched resembles the one in Figure 2.1. The pictures in the center of the figure show a manufacturing system consisting of a factory and a warehouse. The factory use resources, such as raw materials, machines, labor, and energy to produce different types of products. The finished goods are shipped from factory to warehouse using electric vehicles (EV). The factory and the warehouse will adopt onsite renewable energy (RE) through installing microgrids consisting of wind turbines (WT) and solar photovoltaics (PV) to meet the energy demands and become zero-carbon manufacturing facilities. Battery storage (BS) will be used for

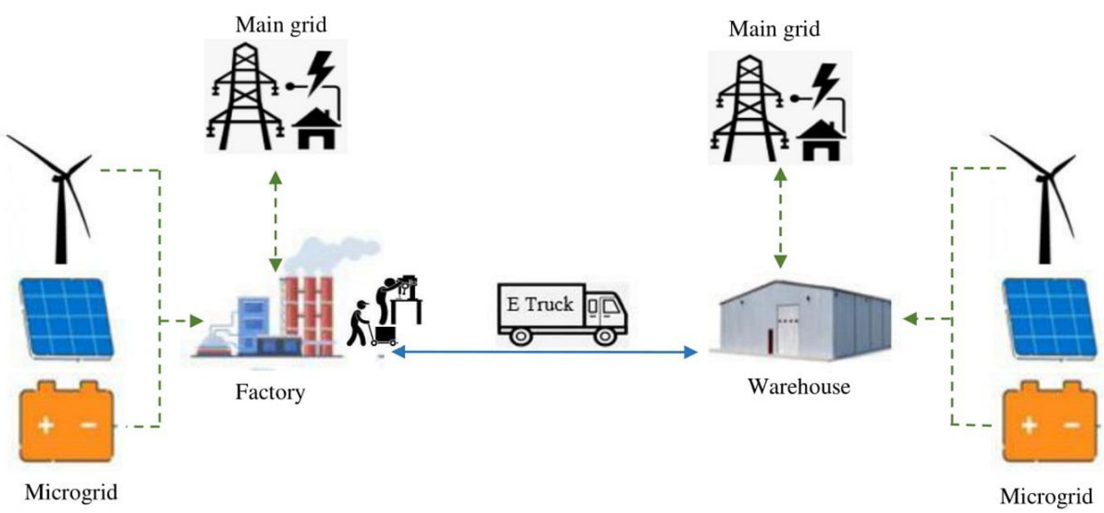

Figure 2.1: Onsite microgrid install at factory and warehouse

storing RE on those days in which the total energy generated by the WT and PV is greater than the needed one. The energy stored in BS can be used on days when the onsite generation is insufficient for meeting the energy demand. Factories and warehouses can be disconnected from the main grid (i.e., island) or connected to the grid as energy prosumers able to buy energy or sell RE. The manufacturing system could become net-zero carbon by having all energy consumed or demanded by the facilities over the year offset with the RE generated.

The problem this research work aims to solve is to simultaneously determine: (1) the optimal sitting and sizing of the renewables, and (2) the minimum cost production, machine and workforce schedules in the factory over multiple production periods considering renewables volatility and the following parameters or inputs as stochastic: final product demands, machine hours capacity, and labor hours capacity. Because the manufacturing system also generates inventory, places products in backorder, subcontracts, and transports product to the warehouse the problem's objective is to minimize the total cost incurred, which is comprised of the following costs: energy, materials, regular time labor, labor hiring, labor layoff, inventory, subcontracting, backorder, defective items, rectifying items, and transportation costs. The product demands become stochastic due to changes in economic conditions, customer preferences, innovation and competition among others. The machine hours capacity in each period may be stochastic due to machine breakdowns that lead to unplanned downtime. Machine failures halt manufacturing operations and waste time, as well as money, due to a failure in production (Radford, 2017). The labor hours capacity may vary due to learning curve effect, labor skill, absenteeism, training, physical fatigue, disruption of work rhythm etc.

This research work enhances the traditional scope of APP, which is mainly concerned with finding optimum production and workforce levels to satisfy known product demands without considering energy resources. Besides, this thesis work mainly focuses on energy-intensive and labor-intensive manufacturing industries (e.g., food, pulp and paper, iron and steel, nonmetallic minerals, nonferrous metals, semiconductor, and garment industries).

2.1.1 Research questions

The problem researched in this chapter assumes that the facilities balance the energy required to operate or sell to the main grid with RE produced or stored and energy purchased to the main grid on a daily basis. Keeping this assumption, the research in this chapter aims to solve the following two questions:

- Is it possible to decarbonize the manufacturing operations and warehouse facilities with RE integration?
- Is it feasible to integrate RE into manufacturing and warehouse operations with affordable levelized cost of energy (LCOE)?

2.2 Methodology

The two-stage stochastic programming methodology is used to model APP problem presented in the previous section. A stochastic program is a mathematical program in which some of the parameters or input data are random, and this uncertainty is explicitly included in the program through scenarios (Birge and Louveaux, 2011; Gupta and Grossmann, 2011; Rardin, 1998). Thus, exact values for some of the input data are unknown, but their probability distributions are known. The inclusion of the probability distributions helps to choose the best values for the decision variables in the mathematical program. Stochastic programs with recourse model situations where decisions occur at the beginning of the planning horizon, uncertain parameters reveal over time, and corrective actions happen as the parameters' uncertainty reveals. The pattern: decision, outcome, and corrective action fits in the APP decision problem presented in the previous section. In practice, most problems have some uncertain parameters at the time of decision making. Tran and Smith (2019) mentioned that the uncertainty in energy loads and power generation from renewable energy sources heavily affects the operating cost.

2.2.1 APP modeled as a two-stage stochastic program

Figure 2.2 exemplifies in a graphical way the two-stage stochastic programming approach for the APP problem researched in this thesis. The planning horizon consists of 12 production periods (i.e., 12 months), and the first-stage decisions occur before the first production period. These decisions include the size of the WT, solar PV, and BS to install. Other first-stage decisions taken for the entire period (i.e., 12 months) are the amount of product i to produce, subcontract, have as defective, and get rectified. Also, the labor and machine hours required and the hiring and layoff hours for the entire period are first-stage decision variables.

Figure 2.2 illustrates the manufacture of 2 products with random monthly demands, low (L) or high (H), in each production period. The machine and labor hours capacity in each production period are also stochastic and their outcomes may be at any of 3 different settings, low (L), medium (M) and high (H). Besides, the annual wind speed and weather conditions, given under a pre-specified time granularity, vary and are represented through 3 different sets of data, labeled as 1, 2, 3. Each set has associated values for the WT and PV capacity factors. Thus the exemplified problem has 5 stochastic parameters for each production period (i.e., month): demand of product 1, demand of product 2, machine hour capacity, labor hour capacity, and vectors of WT and PV capacity factors. Once the first-stage decisions are taken, outcomes for the 5 stochastic inputs will occur over the 12 months. In Figure 2.2, the possible outcomes defining a scenario are represented by the vectors depicted above the arrows. For instance, $(HHHH1)_1$, $(HHHH1)_2$, $(HHHH1)_3$, ..., $(HHHH1)_{12}$ represents the case in which the monthly demands for both products are high over the 12 production periods, machine and labor hours capacity are also high, and the WT and PV capacity factors correspond to the first set of computed values. Similarly, $(LLLL3)_1$, $(LLLL3)_2$, $(LLLL3)_3$, ..., $(LLLL3)_{12}$

represents the case in which monthly demands for both products are low over the 12 production periods, machine and labor hours capacity are also low, and the WT and PV capacity factors correspond to the third set of computed values. It is assumed that the way the outcomes realize for a particular production period replicates exactly over the remaining periods. Thus, the exemplified APP has $(2 \times 2 \times 3 \times 3 \times 3) = 108$ scenarios. If assuming the outcomes replicate in a different way, the number of scenarios would be extremely large, $(2 \times 2 \times 3 \times 3 \times 3)^{12} = 2.52{\times}10^{24}$.

The second-stage starts as soon as a recourse action occurs. A recourse action would be based only on the realized uncertainty. However, the final recourse action occurs after the uncertainty of the last period (i.e., period twelve) is realized. In Figure 2.2, for each scenario, the last recourse actions defining the end of the second-stage are represented by the ellipses occurring at the end of production period twelve.

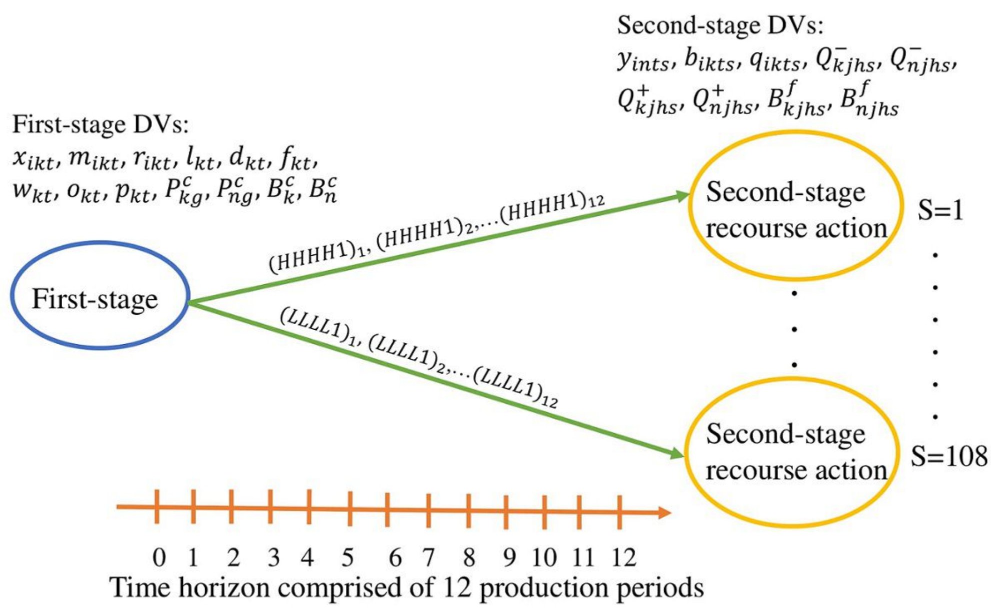

Figure 2.2: Scenario tree for two-stage stochastic programming model

In the APP problem described in Section 2.1, some of the recourse actions after a given scenario occurs are amount of each product to store in inventory, amount of each product to backorder and amount of energy to store daily in the BSS. Note that a difference between two-stage stochastic programs and multi-stage stochastic programs is that first-stage decisions (i.e. production, labor and machine hours in all categories, siting and sizing of RE generation technologies, and BS capacity) are not modified over the periods in the time horizon. This would be the case of a manufacturing system in which it is costly to alter the production schedule or undesirable to revisit the mentioned first-stage decisions several times during a year. Furthermore, as mentioned in this section, the number of scenarios in the two-stage stochastic APP approach may grow significantly. Thus, this research looks to validate that the two-stage stochastic APP model is tractable with commercial solvers and an efficient modeling approach to the researched problem.

2.3 Stochastic APP models

This section presents extensive formulations of the two-stage stochastic programs that model two instances of the APP problem presented in Section 2.1. Model 1 - Island microgrid with BS and daily granularity corresponds to the instance in which the manufacturing system adopts RE, operates disconnected from the main grid (i.e. island), uses battery system, and satisfies daily energy requirements. Model 2 - Prosumer microgrid with BS and daily granularity corresponds to the instance in which the manufacturing system works as a RE prosumer and all the other problem characteristics are the same as listed in Model 1. Both models consider that the manufacturing system has a pre-specified percentage of defective product and rework and it will be included in two constraints of the models.

Table 2.1 provides the notation for the sets used in both models. Table 2.2 list the decision variables and their units. Tables 2.3 to 2.4 provide the notation, definition, and units for all the data or input parameter used in the models. The models are presented after the tables.

Table 2.1: Sets

Notation	Description
I, T, J	Set of products, production periods and days, respectively
G,S,K,N	Set of generation technologies, scenarios, factories and warehouses

Table 2.2: Decision variables

Notation	Description	Unit
x_{ikt}	Amount of product i produced at factory k in period t	item
m_{ikt}	Amount of product i defective at factory k in period t	item
r_{ikt}	Amount of product i rectified at factory k in period t	item
l_{kt}	Labor hours kept at factory k in period t	h/period
h_{kt},f_{kt}	Labor hours hired and layoff at factory k in period t	h/period
w_{kt}	Regular machine hours at factory k in period t	h/period
p_{kt},o_{kt}	Idle and Overtime machine hour at factory k in period t	h/period
P^c_{kg}	Capacity of generation technology g in factory k	MW
P^c_{ng}	Capacity of generation technology g in warehouse n	MW
B^c_k,B^c_n	Battery capacity in factory k and warehouse n	MWh/day
y_{ints}	Amount of inventory of product i stored at warehouse n in period t under scenario s	item
q_{ikts}, b_{ikts}	Amount of product i subcontracted and backordered at factory k in period t under scenario s	item
B^f_{kjs}, B^f_{njs}	Energy stored daily in battery at factory k and warehouse n at day j under scenario s	MWh/day
Q^-_{kjs},Q^-_{njs}, Q^+_{kjs},Q^+_{njs}	Energy sold (spilled for Model 1) and bought from factory k and warehouse n, at day j under scenario s	MWh/day

Table 2.3: Parameters

Notation	Description	Unit
c_{it}^x	Materials cost for product i at period t	\$/item
c_{it}^w	Transportation cost for product i at period t	\$/item
c_{it}^q	Subcontracting cost for product i at period t	\$/item
c_{it}^y	Inventory holding cost for product i at period t	\$/item
c_{it}^b	Backorder cost for product i at period t	\$/item
c_{it}^m	Defective cost for product i at period t	\$/item
c_{it}^r	Rectification cost for product i at period t	\$/item
c_t^l	Regular time labor hour cost at period t	\$/hour
c_t^h	Labor hiring hour cost at period t	\$/hour
c_t^f	Labor layoff hour cost at period t	\$/hour
ϕ_g	Capital recovery factor of generation technology g	N/A
ϕ_b	Capital recovery factor of battery b	N/A
c_g	Penalty cost or tax incentive of generation technology g	\$/MWh
b_g	Operating and maintenance (O&M) cost of generation technology g	\$/MWh
a_g	Capacity cost for generation technology g	\$/MW
a_b	Capacity cost of battery b	\$/MWh
τ_{gj}	Number of generation hours in day j for generation technology g	h/day
τ_g^*	Total number of generation hours for generation technology g over the entire production periods	hour
e_i^x	Energy consumed for producing one unit of product i	MWh/item
e_i^f	Energy consumed for storing one unit of product i	MWh/item
q^v	Electric vehicle energy intensity rate	MWh/kg/km
$p(s)$	Probability of scenario s	N/A
d_{kn}	Distance between factory k and warehouse n	km
β	Number of daily trips	trip/day
m^v	Vehicle self weight	kg
w_i	Unit weight of product i	kg/item
a_i	Unit labor hour required by product i	hour/item
u_i	Unit machine hour required by product i	hour/item
χ	Number of hours in a day	hour
δ	Daily operating hours of warehouse or factory	hour/day

Table 2.4: Parameters continuation

Notation	Description	Unit
L_k	Base electricity load of factory k	MW
L_n	Base electricity load of warehouse n	MW
B_k^{max}	Maximum battery capacity at factory k	MWh/day
B_n^{max}	Maximum battery capacity at warehouse n	MWh/day
$\|J_t\|$	Size of the set of days in period t	day
$\|J\|$	Number of days over the entire horizon	day
u^-	Profit from selling spilled energy	\$/MWh
u^+	Cost of buying energy	\$/MWh
α	Percentage of allowable workforce variation	%
ν	Allowable defective percentage from production	%
η	Allowable rectification percentage from defective items produced	%
m^v	Vehicle self weight	kg
w_i	Unit weight of product i	kg/item
a_b	Capacity cost of battery b	\$/MWh
D_{ikts}	Demand of product i in factory k in period t under scenario s	item/period
P_{kg}^{max}	Maximum capacity of generation technology g at factory k	MW
P_{ng}^{max}	Maximum capacity of generation technology g at warehouse n	MW
λ_{gkjs}	Capacity factor for generation technology g in factory k in day j under scenario s	N/A
λ_{gnjs}	Capacity factor for generation technology g in warehouse n, in day j under scenario s	N/A
δ	Daily operating hours of warehouse or factory	hour/day
Q_{kjs}^{max}	Maximum energy selling amount daily from factory k at day j under scenario s	MWh/day
Q_{njs}^{max}	Maximum energy selling amount daily from warehouse n, at day j under scenario s	MWh/day
MH_{ts}^{max}	Maximum machine capacity in period t under scenario s	hour/period
LH_{ts}^{max}	Maximum labor capacity in period t under scenario s	hour/period
m_{it}^{max}	Maximum defective amount of product i in period t	item/period
WH_t^{max}	Maximum inventory capacity in period t	item/period

2.3.1 Island microgrid with BS

Model 1 - Island microgrid with BS and daily granularity:

$$\begin{aligned}\min \quad z = &\sum_{i\in I}\sum_{k\in K}\sum_{t\in T}(c^x_{it}+c^w_{it})x_{ikt} + \sum_{i\in I}\sum_{k\in K}\sum_{t\in T}(c^m_{it}m_{ikt}+c^r_{it}r_{ikt})+\\
&\sum_{k\in K}\sum_{t\in T}(c_l l_{kt}+c_h h_{kt}+c_f f_{kt}) + \sum_{t=1}^{T}\sum_{i\in I}\sum_{k\in K}\sum_{s\in S}p(s)(c^b_{it}b_{ikts}+c^q_{it}q_{ikts})+\\
&\sum_{t=1}^{T}\sum_{i\in I}\sum_{n\in N}\sum_{s\in S}p(s)c^y_{it}y_{ints} + \sum_{k\in K}\sum_{g\in G}\phi_g a_g P^c_{kg} + \sum_{n\in N}\sum_{g\in G}\phi_g a_g P^c_{ng}+\\
&\sum_{k\in K}\frac{\phi_b a_b B^c_k}{\chi} + \sum_{n\in N}\frac{\phi_b a_b B^c_n}{\chi} + \sum_{k\in K}\sum_{g\in G}\sum_{s\in S}p(s)(b_g-c_g)\tau^*_g(\sum_{j\in J}\frac{\lambda_{gkjs}}{|J|})P^c_{kg}+\\
&\sum_{n\in N}\sum_{g\in G}\sum_{s\in S}p(s)(b_g-c_g)\tau^*_g(\sum_{j\in J}\frac{\lambda_{gnjs}}{|J|})P^c_{ng}\end{aligned} \tag{2.1}$$

$s.t.$

$$y_{int-1}-y_{ints}+x_{ikt}+q_{ikts}-b_{ikt-1}+b_{ikts}-m_{ikt}+r_{ikt}=D_{ikts}$$
$$\forall i\in I, t=1, \forall k\in K, \forall n\in N, \forall s\in S \tag{2.2}$$

$$y_{int-1s}-y_{ints}+x_{ikt}+q_{ikts}-b_{ikt-1s}+b_{ikts}-m_{ikt}+r_{ikt}=D_{ikts}$$
$$\forall i\in I, \forall t\in T\backslash\{1\}, \forall k\in K, \forall n\in N, \forall s\in S \tag{2.3}$$

$$\sum_{i\in I}(e^x_i+q^v d_{kn}w_i)\frac{x_{ikt}}{|J_t|}+\delta L_k+q^v\beta d_{kn}m^v+B^f_{kjs}-B^f_{kj-1}+Q^-_{kjs}$$
$$=\sum_{g\in G}\tau_{gj}\lambda_{gkjs}P^c_{kg}$$
$$j=1, t=1, \forall k\in K, \forall n\in N, \forall s\in S \tag{2.4}$$

$$\sum_{i\in I}(e^x_i+q^v d_{kn}w_i)\frac{x_{ikt}}{|J_t|}+\delta L_k+q^v\beta d_{kn}m^v+B^f_{kjs}-B^f_{kj-1s}+Q^-_{kjs}$$
$$=\sum_{g\in G}\tau_{gj}\lambda_{gkjs}P^c_{kg}$$
$$\forall t\in T, \forall j\in J\backslash\{1\}, \forall k\in K, \forall n\in N, \forall s\in S \tag{2.5}$$

Model 1 - Island microgrid with BS and daily granularity continue

$$\sum_{i \in I} e_i^f y_{ints}\left(\frac{j - \sum_{v=1}^{t-1} |J_v|}{|J_t|}\right) + \delta L_n + q^v \beta d_{nk} m^v + B_{njs}^f - B_{nj-1}^f + Q_{njs}^-$$
$$= \sum_{g \in G} \tau_{gj} \lambda_{gnjs} P_{ng}^c$$
$$j = 1, t = 1, \forall k \in K, \forall n \in N, \forall s \in S \tag{2.6}$$

$$\sum_{i \in I} e_i^f y_{ints}\left(\frac{j - \sum_{v=1}^{t-1} |J_v|}{|J_t|}\right) + \delta L_n + q^v \beta d_{nk} m^v + B_{njs}^f - B_{nj-1s}^f + Q_{njs}^-$$
$$= \sum_{g \in G} \tau_{gj} \lambda_{gnjs} P_{ng}^c$$
$$\forall t \in T, \forall j \in J \backslash \{1\}, \forall k \in K, \forall n \in N, \forall s \in S \tag{2.7}$$

$$\sum_{i \in I} a_i x_{ikt} = l_{kt}$$
$$\forall k \in K, \forall t \in T, \tag{2.8}$$

$$l_{kt} \leq LH_{kts}^{max}$$
$$\forall k \in K, \forall s \in S, \forall t \in T \tag{2.9}$$

$$l_{kt} = l_{kt-1} + h_{kt} - f_{kt}$$
$$\forall k \in K, \forall t \in T \tag{2.10}$$

$$h_{kt} + f_{kt} \leq \alpha l_{kt-1}$$
$$\forall k \in K, \forall t \in T \tag{2.11}$$

$$\sum_{i \in I} u_i x_{ikt} = w_{kt}$$
$$\forall k \in K, \forall t \in T \tag{2.12}$$

$$w_{kt} \leq MH_{kts}^{max}$$
$$\forall k \in K, \forall s \in S, \forall t \in T \tag{2.13}$$

Model 1 - Island microgrid with BS and daily granularity continue

$$w_{kt} = w_{kt-1} + o_{kt} - p_{kt} \qquad \forall k \in K, \forall t \in T \tag{2.14}$$

$$\nu x_{ikt} = m_{ikt} \qquad \forall k \in K, \forall i \in I, \forall t \in T \tag{2.15}$$

$$\eta m_{ikt} = r_{ikt} \qquad \forall k \in K, \forall i \in I, \forall t \in T \tag{2.16}$$

$$0 \leq m_{ikt} - r_{ikt} \leq m_{ikt}^{max} \qquad \forall i \in I, \forall k \in K, \forall t \in T \tag{2.17}$$

$$\sum_{i \in I} y_{ints} \leq WH_t^{max} \qquad \forall n \in N, \forall s \in S, \forall t \in T \tag{2.18}$$

$$0 \leq P_{kg}^c \leq P_{kg}^{max} \qquad \forall k \in K, \forall g \in G \tag{2.19}$$

$$0 \leq P_{ng}^c \leq P_{ng}^{max} \qquad \forall n \in N, \forall g \in G \tag{2.20}$$

$$B_k^c \leq B_k^{max} \qquad \forall k \in K \tag{2.21}$$

$$B_n^c \leq B_n^{max} \qquad \forall n \in N \tag{2.22}$$

$$0 \leq B_{kjs}^f \leq B_k^c \qquad \forall k \in K, \forall s \in S, j \in J_t \tag{2.23}$$

$$0 \leq B_{njs}^f \leq B_n^c \qquad \forall n \in N, \forall s \in S, j \in J_t \tag{2.24}$$

$$B_{k0}^f = B_k^c \qquad \forall k \in K, j = 0 \tag{2.25}$$

$$B_{n0}^f = B_n^c \qquad \forall n \in N, j = 0 \tag{2.26}$$

$$x_{ikt}, m_{ikt}, r_{ikt} \geq 0 \qquad \forall i \in I, \forall k \in K, \forall t \in T \tag{2.27}$$

$$h_{kt}, f_{kt}, l_{kt}, w_{kt}, p_{kt}, o_{kt} \geq 0 \qquad \forall k \in K, \forall t \in T \tag{2.28}$$

$$b_{ikts}, q_{ikts} \geq 0 \qquad \forall i \in I, \forall k \in K, \forall t \in T, \forall s \in S \tag{2.29}$$

$$y_{ints} \geq 0 \qquad \forall i \in I, \forall n \in N, \forall t \in T, \forall s \in S \tag{2.30}$$

Model 1 - IM with BS and daily granularity, the first-stage strategic decisions are the size of the generation technologies at the factories and warehouses, (P_{kg}^c and P_{ng}^c), and the BS to install at each factory and warehouse, (B_k^c and B_n^c). The first-stage also has operational decisions to take for the twelve months time horizon. They are the amount of finished product to produce (x_{ikt}), number of labor hours

(l_{kt}), labor hiring hours (h_{kt}), labor layoff hours (f_{kt}), regular time machine hours (w_{kt}), machine overtime (o_{kt}), and machine idletime (p_{kt}). Recourse actions for each scenario are subcontracting (q_{ikts}), inventory (y_{ints}), backorder of final product (b_{ikts}), and daily energy spills in the factory and warehouse, (Q^{-}_{kjs} and Q^{-}_{njs}). The stochastic parameters in the model are the product demand (D_{ikts}), maximum machine hour capacity (MH^{max}_{kts}), maximum labor hour capacity (LH^{max}_{kts}), and the capacity factors (λ_{gkjs} and λ_{gnjs}). The capacity factors (CF) capture the wind speed and weather conditions at the geographical locations selected for the microgrid's installation. These CF affect the power output of the wind turbine (WT) and solar photovoltaic (PV) generation technologies at factories and warehouses (P^{c}_{kg} and P^{c}_{ng}). The objective function in equation 2.1 is to minimize the total expected cost comprised of production and energy related costs. Over the planning horizon given by the size of the set T, there is a cost to produce and transport product between the factory and warehouse, classify product as defective and rectify part of it, backorder, subcontract, store inventory in the warehouse, pay labor wages, and hire and fire labor. There is also an annualized cost to install, operate and maintain the RE technologies. Constraints 2.2 to 2.3 are the production-demand balance equations for the first period and the remaining ones, respectively. They ensure that the sum of produced, subcontracted and rectified product, inventory left from previous period, and current amount of product put in backorder equals to the sum of product demand, defective items, current inventory and backorder for previous period. In a nutshell, these equations balance the flow between the total amount of product going in and out in each production period. Constraints 2.4 to 2.5 represent the daily energy balance equations for the factory in the first production period and the remaining ones, respectively. They show that in each day and scenario, the sum of energy: (a) consumed by the factory in production and electric vehicle transportation, (b) needed to satisfy a base load, (c) stored in the battery, and (d) spilled, if needed, must be equal to the energy generation in conjunction with the energy stored in the battery from the previous day. Constraints 2.6 to 2.7 represent the daily energy balance equations for the warehouse in the first production period and the remaining ones, respectively. They show that, in each day and scenario, energy needed to: (a) store product in the warehouse, (b) send vehicles back to the factories, (c) satisfy the warehouse base load, and (d) spilled, if needed, must be equal to the energy generation in conjunction with the energy stored in the battery from the previous day. Constraints 2.8 to 2.9 indicate that the labor hours consumed to produce the products must be equal to the labor hours adopted for each production period, which must not exceed the maximum hours of labor capacity in each scenario. Constraints 2.10 to 2.11 update the work force level in each period considering hiring and firing , and satisfy criteria regarding the maximum amount of labor hired and fired in each period. Constraint 2.12 guarantees that the total machine hours consumed to produce the products must be equal to the machine hours adopted in each production period. Constraint 2.13 requires that the adopted machine hours not exceed the maximum hours of machine capacity available in each scenario. Constraint 2.14 updates the machine hours in each period by adding the overtime hours and subtracting the downtime hours. Constraints 2.15 to 2.16 define the amount of defective production and rectified items. Constraint 2.17 limits the amount of defective product. Constraint 2.18 represents the inventory capacity constraint. Constraints 2.19 to 2.20 are bounds to the technology generation capacity installed in the factory and warehouse, respectively. Constraints 2.21 to 2.22 are bounds to the battery capacity installed in the factory and warehouse, respectively. Constraints 2.23 to 2.24 ensure that the level of energy in the battery does not exceed the battery capacity. Constraints 2.25 to 2.26 define initial conditions for the battery in the factory and warehouse, respectively. Constraints 2.27 to 2.30 represent the sign constraints.

2.3.2 Prosumer model

Model 2 - Prosumer microgrid with BS and daily granularity

$$
\begin{aligned}
\min \quad z = & \sum_{i\in I}\sum_{k\in K}\sum_{t\in T}(c^x_{it}+c^w_{it})x_{ikt} + \sum_{i\in I}\sum_{k\in K}\sum_{t\in T}(c^m_{it}m_{ikt}+c^r_{it}r_{ikt}) + \\
& \sum_{k\in K}\sum_{t\in T}(c_l l_{kt}+c_h h_{kt}+c_f f_{kt}) + \sum_{t=1}^{T}\sum_{i\in I}\sum_{k\in K}\sum_{s\in S}p(s)(c^b_{it}b_{ikts}+c^q_{it}q_{ikts}) + \\
& \sum_{t=1}^{T}\sum_{i\in I}\sum_{n\in N}\sum_{s\in S}p(s)c^y_{it}y_{ints} + \sum_{k\in K}\sum_{g\in G}\phi_g a_g P^c_{kg} + \sum_{n\in N}\sum_{g\in G}\phi_g a_g P^c_{ng} + \\
& \sum_{k\in K}\frac{\phi_b a_b B^c_k}{\chi} + \sum_{n\in N}\frac{\phi_b a_b B^c_n}{\chi} + \sum_{k\in K}\sum_{g\in G}\sum_{s\in S}p(s)(b_g-c_g)\tau^*_g(\sum_{j\in J}\frac{\lambda_{gkjs}}{|J|})P^c_{kg} + \\
& \sum_{n\in N}\sum_{g\in G}\sum_{s\in S}p(s)(b_g-c_g)\tau^*_g(\sum_{j\in J}\frac{\lambda_{gnjs}}{|J|})P^c_{ng} - \sum_{k\in K}\sum_{j\in J}\sum_{s\in S}p(s)u^-\frac{Q^-_{kjs}}{\chi} + \\
& \sum_{k\in K}\sum_{j\in J}\sum_{s\in S}p(s)u^+\frac{Q^+_{kjs}}{\chi} - \sum_{n\in N}\sum_{j\in J}\sum_{s\in S}p(s)u^-\frac{Q^-_{njs}}{\chi} + \\
& \sum_{n\in N}\sum_{j\in J}\sum_{s\in S}p(s)u^+\frac{Q^+_{njs}}{\chi} \qquad (2.31)
\end{aligned}
$$

$s.t.$

$$
\begin{aligned}
& y_{int-1} - y_{ints} + x_{ikt} + q_{ikts} - b_{ikt-1} + b_{ikts} - m_{ikt} + r_{ikt} = D_{ikts} \\
& \qquad \forall i \in I, t=1, \forall k \in K, \forall n \in N \qquad (2.32)
\end{aligned}
$$

$$
\begin{aligned}
& y_{int-1s} - y_{ints} + x_{ikt} + q_{ikts} - b_{ikt-1s} + b_{ikts} - m_{ikt} + r_{ikt} = D_{ikts} \\
& \qquad \forall i \in I, t \in T\backslash\{1\}, \forall k \in K, \forall n \in N, \forall, \forall s \in S \qquad (2.33)
\end{aligned}
$$

$$
\begin{aligned}
& \sum_{i\in I}(e^x_i + q^v d_{kn} w_i)\frac{x_{ikt}}{|J_t|} + \delta L_k + q^v \beta d_{kn} m^v + B^f_{kjs} - B^f_{kj-1} + Q^-_{kjs} \\
& = \sum_{g\in G}\tau_{gj}\lambda_{gkjs}P^c_{kg} + Q^+_{kjs} \\
& \qquad j=1, t=1, \forall k \in K, \forall n \in N, \forall s \in S \qquad (2.34)
\end{aligned}
$$

Model 2 - Prosumer microgrid with BS and daily granularity continue

$$\sum_{i\in I}(e_i^x + q^v d_{kn} w_i)\frac{x_{ikt}}{|J_t|} + \delta L_k + q^v \beta d_{kn} m^v + B_{kjs}^f - B_{kj-1s}^f + Q_{kjs}^-$$
$$= \sum_{g\in G}\tau_{gj}\lambda_{gkjs}P_{kg}^c + Q_{kjs}^+$$
$$\forall t \in T, \forall j \in J\backslash\{1\}, \forall k \in K, \forall n \in N, \forall s \in S \tag{2.35}$$

$$\sum_{i\in I} e_i^f y_{ints}\left(\frac{j - \sum_{v=1}^{t-1}|J_v|}{|J_t|}\right) + \delta L_n + q^v \beta d_{nk} m^v + B_{njs}^f - B_{nj-1}^f + Q_{njs}^-$$
$$= \sum_{g\in G}\tau_{gj}\lambda_{gnjs}P_{ng}^c + Q_{njs}^+$$
$$j = 1, t = 1, \forall k \in K, \forall n \in N, \forall s \in S \tag{2.36}$$

$$\sum_{i\in I} e_i^f y_{ints}\left(\frac{j - \sum_{v=1}^{t-1}|J_v|}{|J_t|}\right) + \delta L_n + q^v \beta d_{nk} m^v + B_{njs}^f - B_{nj-1s}^f + Q_{njs}^-$$
$$= \sum_{g\in G}\tau_{gj}\lambda_{gnjs}P_{ng}^c + Q_{njs}^+$$
$$\forall t \in T, \forall j \in J\backslash\{1\}, \forall k \in K, \forall n \in N, \forall s \in S \tag{2.37}$$

$$\sum_{i\in I} a_i x_{ikt} = l_{kt}$$
$$\forall k \in K, \forall t \in T \tag{2.38}$$

$$l_{kt} \leq LH_{kts}^{max}$$
$$\forall k \in K, \forall s \in S, \forall t \in T \tag{2.39}$$

$$l_{kt} = l_{kt-1} + h_{kt} - f_{kt}$$
$$\forall k \in K, \forall t \in T \tag{2.40}$$

$$h_{kt} + f_{kt} \leq \alpha l_{kt-1}$$
$$\forall k \in K, \forall t \in T \tag{2.41}$$

Model 2 - Prosumer microgrid with BS and daily granularity continue

$$\sum_{i \in I} u_i x_{ikt} = w_{kt} \qquad \forall k \in K, \forall t \in T \tag{2.42}$$

$$w_{kt} \leq MH_{kts}^{max} \qquad \forall k \in K, \forall s \in S, \forall t \in T \tag{2.43}$$

$$w_{kt} = w_{kt-1} + o_{kt} - p_{kt} \qquad \forall k \in K, \forall t \in T \tag{2.44}$$

$$\nu x_{ikt} = m_{ikt} \qquad \forall k \in K, \forall i \in I, \forall t \in T \tag{2.45}$$

$$\eta m_{ikt} = r_{ikt} \qquad \forall k \in K, \forall i \in I, \forall t \in T \tag{2.46}$$

$$0 \leq m_{ikt} - r_{ikt} \leq m_{ikt}^{max} \qquad \forall i \in I, \forall k \in K, \forall t \in T \tag{2.47}$$

$$\sum_{i \in I} y_{ints} \leq WH_t^{max} \qquad \forall n \in N, \forall s \in S, \forall t \in T \tag{2.48}$$

$$0 \leq P_{kg}^c \leq P_{kg}^{max} \qquad \forall k \in K, \forall g \in G \tag{2.49}$$

$$0 \leq P_{ng}^c \leq P_{ng}^{max} \qquad \forall n \in N, \forall g \in G \tag{2.50}$$

$$B_k^c \leq B_k^{max} \qquad \forall k \in K \tag{2.51}$$

$$B_n^c \leq B_n^{max} \qquad \forall n \in N \tag{2.52}$$

$$0 \leq B_{kjs}^f \leq B_k^c \qquad \forall k \in K, \forall s \in S, j \in J_t \tag{2.53}$$

$$0 \leq B_{njs}^f \leq B_n^c \qquad \forall n \in N, \forall s \in S, j \in J_t \tag{2.54}$$

$$B_{k0}^f = B_k^c \qquad \forall k \in K, j = 0 \tag{2.55}$$

$$B_{n0}^f = B_n^c \qquad \forall n \in N, j = 0 \tag{2.56}$$

$$Q_{kjs}^- \leq Q_{kjs}^{max} \qquad \forall k \in K, j \in J, s \in S \tag{2.57}$$

$$Q_{njs}^- \leq Q_{njs}^{max} \qquad \forall n \in K, j \in J, s \in S \tag{2.58}$$

$$x_{ikt}, m_{ikt}, r_{ikt} \geq 0 \qquad \forall i \in I, \forall k \in K, \forall t \in T \tag{2.59}$$

$$h_{kt}, f_{kt}, l_{kt}, w_{kt}, p_{kt} \geq 0 \qquad \forall k \in K, \forall t \in T \tag{2.60}$$

$$b_{ikts}, q_{ikts} \geq 0 \qquad \forall i \in I, \forall k \in K, \forall t \in T, \forall s \in S \tag{2.61}$$

$$y_{ints} \geq 0 \qquad \forall i \in I, \forall n \in N, \forall t \in T, \forall s \in S \tag{2.62}$$

The two-stage stochastic model, Model 2 - Prosumer microgrid with BS and daily granularity, presented in this section is quite similar to the model presented in Section 2.3.1. The only difference is that the model presented in this section assumes the factory and warehouse are energy prosumers and it affects the objective function and the energy balance constraints. The objective function in equation 2.30 minimizes production and energy related expected costs. Production related terms included costs incurred to produce and transport product between the factory and warehouse, classify product as defective and rectify part of it, backorder, subcontract, store inventory in the warehouse, pay labor wages, and hire and fire labor. There is also an annualized cost to install, operate and maintain the RE technologies, acquire the BS, and buy energy to the grid over the time horizon given by the size of the set T. The RE sold by the factory and warehouse to the grid is a revenue in the objective function. The daily energy balance constraints for the factory and warehouse are updated to include energy buying and RE selling terms. Constraints 2.34 to 2.35, represent the daily energy balance equations for the factory in the first day of the first production period and the remaining ones, respectively. They show that in each day and scenario, the sum of energy: (a) consumed by the factory in production and electric vehicle transportation, (b) needed to satisfy a base load, (c) stored in the battery, and (d) sold must be equal to the energy generation, in conjunction with the energy stored in the battery from the previous day and the energy bought to the main grid. Constraints 2.36 to 2.37 represent the daily energy balance equations for the warehouse in the first day of the first production period and the remaining ones, respectively. They show that, in each day and scenario, the sum of energy to: (a) store product in the warehouse, (b) send vehicles back to the factories, (c) satisfy the warehouse base load, (d) store in the battery, and (d) sell to the grid must be equal to sum of RE generated, energy bought to the main grid, and energy stored in the battery from the previous day.

Constraints 2.57 to 2.58 require that the amount of energy sold by the factory and warehouse does not exceed a predefined maximum capacity. Constraints 2.32 to 2.33, 2.38 to 2.56, and 2.59 to 2.62 are exactly the same ones already explained for Model 1.

2.3.3 Models' assumptions

The two-stage stochastic APP model instances presented in this chapter have the following assumptions:

- Demand of products, machine hour capacity, labor hour capacity, wind profile and weather conditions are uncertain over the next production periods but historical data will permit to construct probability distributions to incorporate them in the models as different scenarios
- Labor hours and machine hours capacity are just for the factories
- The company adopting the microgrid system has no budget limitations
- Loss of energy in battery is negligible and thus not relevant to incorporate in the model
- The company is willing to engage in a feed-in tariff plan with the local utility company
- In the prosumers model instance, there are no imitations on the amount of RE prosumers can sell to the main grid
- Set-up costs are negligible and thus not relevant to incorporate in the model
- Trucks have enough capacity to transport all the products produced daily to the warehouse using a single trip

- All costs behave strictly linear
- If the number of types of products produced is large they can be grouped into families
- Products are simple to manufacture and thus constraints related to labor and machine hours are stated as if the production process is single-step.

2.4 Estimation of uncertain parameters in the models

2.4.1 Estimation of product demands

Model 1 - Island microgrid with BS and daily granularity and Model 2 - Prosumer microgrid with BS and daily granularity are implemented assuming two types of probability distributions (i.e discrete uniform and triangular) for the product demand. For the triangular distribution three different types are studied: (1) a distribution with mode value closely equal to the mean of the discrete uniform distribution assumed, (2) a distribution with mode 10% higher than the one in (1), and (3) a distribution with mode 10% lower the one in (1).

Table 2.5: Probability distributions for generating the product demands

Type	Distribution name	Product	Demand	Comments
1	Discrete uniform	A B	U [500, 800] U [600, 900]	Mean 650 for product A Mean 750 for product B
2	Triangular	A B	[500, 657, 800] [600, 770, 900]	Mode closely equal mean in Type 1
3	Triangular	A B	[500, 723, 800] [600, 847, 900]	Mode 10% higher than in Type 2
4	Triangular	A B	[500, 591, 800] [600, 693, 900]	Mode 10% lower than in Type 2

Table 2.5 summarizes the product demand distributions implemented in the

models. For the Triangular distribution the 3 demand values provided in the table are minimum, mode, and maximum.

2.4.2 Estimation of machine hours capacity

Machine failure and maintenance are examples of factors mainly responsible for fluctuations on the machine hours capacity over the production periods. In this thesis work, it is assumed that machine hours capacity may follow any of the three discrete uniform distributions listed in Table 2.6.

Table 2.6: Probability distributions for generating the machine hours capacity

Case	Hours
Low	U [150,633, 152,714]
Medium	U [152,855, 155,716]
High	U [155,997, 159,258]

The three possible cases for the machine hours are included in the scenarios of the two-stage APP models. This thesis work mainly focuses on energy intensive and labor intensive manufacturing companies such as wafer manufacturing, air separation process, and aluminum refinery. The parameter values for the machine hours capacity are chosen in a way that resembles the ones in these industries.

2.4.3 Estimation of labor hours capacity

Most of the existing research papers consider the labor hour capacity as a fixed parameter, but in practice, training, absenteeism, physical fatigue, etc. make the labor hours capacity uncertain over the production periods. In this research work, it is assumed that labor hours capacity may follow any of the three discrete uniform distributions listed in Table 2.7. The three possible cases for the labor hours are included in the scenarios of the two-stage APP models.

Table 2.7: Discrete uniform distribution for generating labor hours capacity

Case	Hours
Low	U [46,004, 46,101]
Medium	U [46,102, 46,307]
High	U [46,314, 46,492]

2.4.4 Estimation of WT capacity factor

This thesis uses the models presented in the literature review, Section 1.3, to estimate WT capacity factors (CF). Hourly wind speed data collected from (WeatherUnderground, 2019) at $h_g = 10m$ in years 2013, 2014, and 2015, and equations 1.1 and 1.2 are used to estimate a WT electric power. First, v_h is computed as in equation 1.1 at $h = 80m$ height, as it is the typical tower height of a modern WT system. The assumed value for the Hellman exponent or k-value is 0.27. Once v_h is computed, its value is used in equation 1.2 to compute $P_w(v_h)$. The assumed value for v_r and P_m are 12m/s and 1MW, respectively. Then the WT capacity factors are computed using equation 1.3.

Real wind speed data collected hourly from (WeatherUnderground, 2019) in years 2013, 2014, and 2015 for the cities of Phoenix and San Francisco was used to compute three different sets of daily WT capacity factors (CF) for a lapse of 365 days (i.e., the whole year). The daily CF result from averaging the hourly capacity factors computed for the cities of Phoenix and San Francisco using equation 1.3. The CF computed used 26,280 observations (365 days*24 hours/day*3 sets) for the wind speed.

Table 2.8 presents the annual mean, standard deviation, and median of the WT capacity factors for San Francisco. Similarly, Table 2.9 presents the annual mean, standard deviation and median of the WT capacity factors computed for Phoenix. These global statistics indicate that mean WT capacity factor of San Francisco is

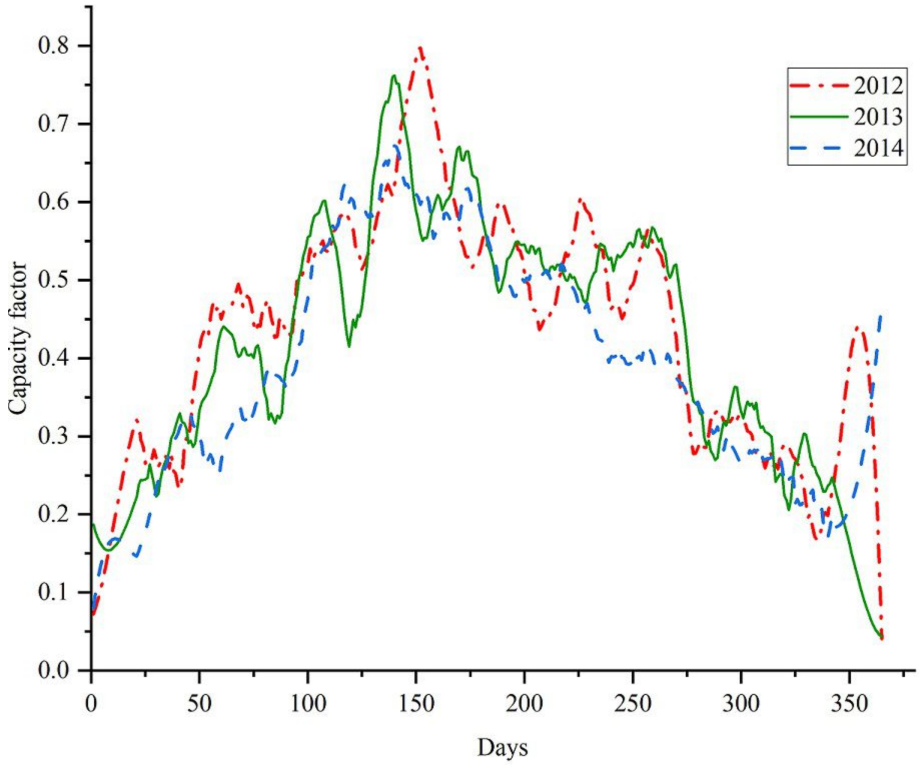

Figure 2.3: San Francisco average daily WT capacity factor

Table 2.8: San Francisco wind turbine capacity factor analysis

Year	Mean	St. Deviation	Median
2012	0.4348	0.2429	0.4122
2013	0.4175	0.2531	0.4299
2014	0.3904	0.2145	0.3736

approximately 172.51% higher than the mean WT capacity factor of Phoenix. From table 2.8 it is evident that San Francisco has a stronger wind profile than Phoenix. Figure 2.3 and Figure 2.4 show that, for any given day, there is variability in the capacity factor computed for the years 2013, 2014, and 2015. By including these 3 sets of CF in the APP models this variability is captured, and it may produce more robust optimal solutions for the models.

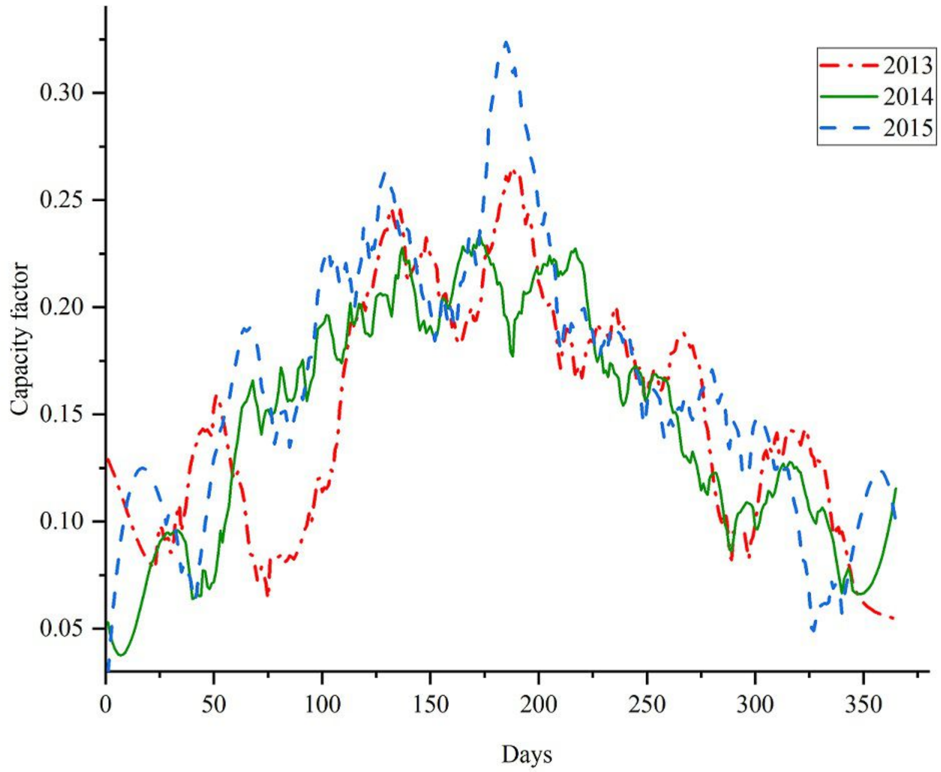

Figure 2.4: Phoenix average daily WT capacity factor

Table 2.9: Phoenix WT capacity factor analysis

Year	Mean	St. Deviation	Median
2013	0.1494	0.1054	0.1142
2014	0.1470	0.0979	0.1181
2015	0.1660	0.1148	0.1363

2.4.5 Estimation of solar PV capacity factor

This thesis uses the four-step procedure presented in the literature review, Section 1.4, to estimate PV capacity factors (CF). The definitions for the parameters and variables used in the four-step procedure to estimate the PV capacity factors are listed in Appendix A Table 5.1. All the equations used for the estimation of the PV capacity factors were presented in Section 1.4. In the computations of the CF for the cities of San Francisco and Phoenix, P_{PV}^{Max} was assumed 160W, the efficiency, η, as 0.2, the PV size, A, equal to $1m^2$, and the solar PV operating temperature, T_0, as 45°C. Table 5.2 in Appendix A lists twenty weather condition or states along with the corresponding value for W_t. Note that W_t varies between 0 and 1 to mimic, for instance, a clear, a partly cloudy, or an overcasting day (Lave and Kleissl, 2011).

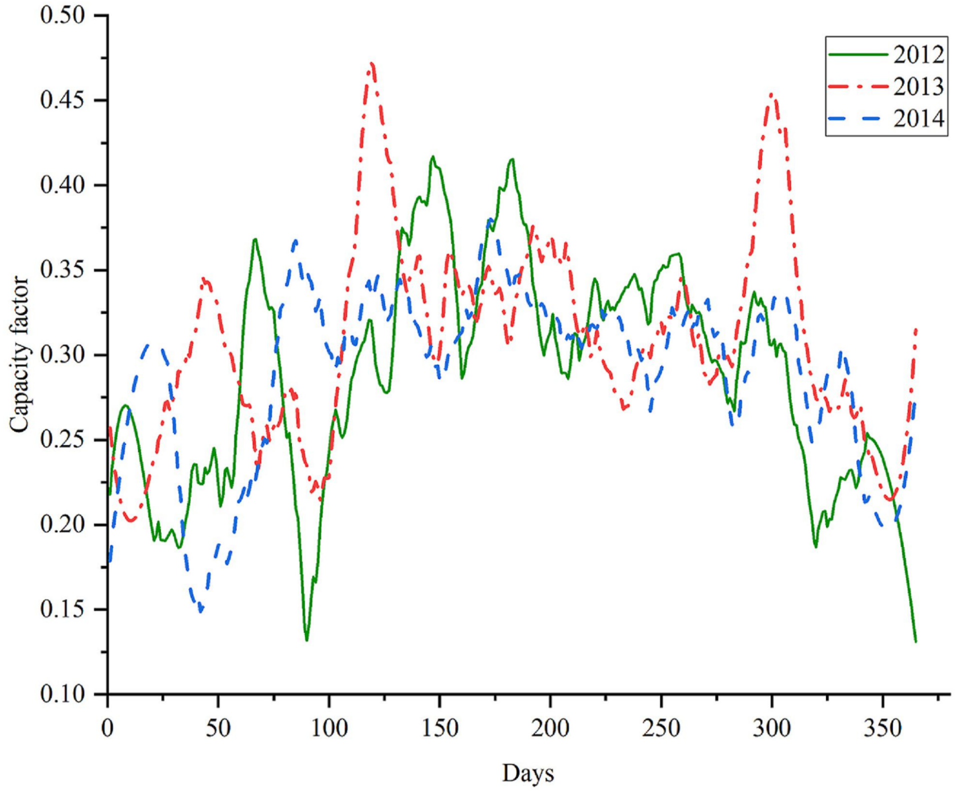

Figure 2.5: San Francisco average daily PV capacity factor

Table 2.10: San Francisco PV capacity factor analysis

Year	Mean	St. Deviation	Median
2012	0.2880	0.1395	0.2867
2013	0.3089	0.1340	0.3099
2014	0.2909	0.1215	0.3024

In this thesis work, hourly weather conditions were collected by undergraduate students for the cities of San Francisco and Phoenix. The author of this thesis used

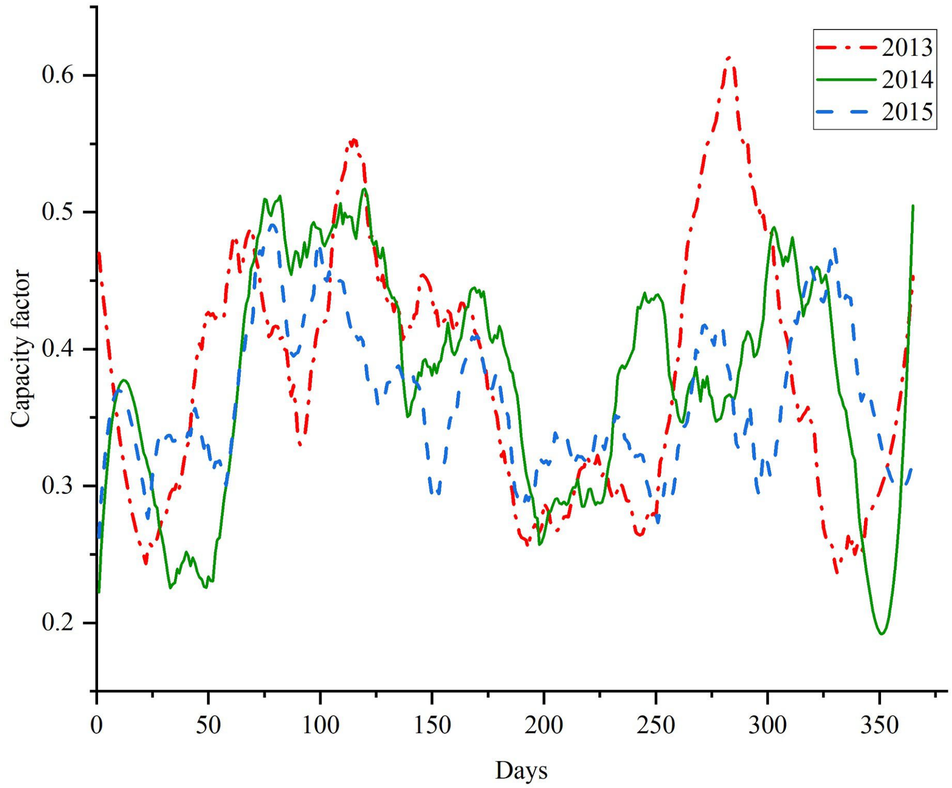

Figure 2.6: Phoenix average daily PV capacity factor

Table 2.11: Phoenix PV capacity factor analysis

Year	Mean	St. Deviation	Median
2013	0.3818	0.1630	0.3539
2014	0.3760	0.1587	0.3538
2015	0.3631	0.1555	0.3554

the four-step procedure described in Section 1.4 to compute the solar PV output and the CF for San Francisco and Phoenix. The hourly CF were averaged to compute daily CF and input them into the two-stage stochastic APP models. Table 5.18 to 5.38 in appendix represent the daily capacity factor of WT and PV of different cities. Table 2.10 presents the mean, standard deviation and median of the PV capacity factors computed for San Francisco for the years 2012, 2013, and 2014, respectively. Similarly, Table 2.11 presents the mean, standard deviation, and median of the PV capacity factors of Phoenix for the years 2013, 2014, and 2015, respectively. From the statistical analysis, it is found that mean PV capacity factor of Phoenix is approximately 26.27% higher than the mean PV capacity factor of San Francisco. Figures 2.5 and Figure 2.6 also show variability in the daily PV capacity factors computed in years 2013, 2014, and 2015. By including these 3 scenarios for the PV capacity factors in the APP models, this variability is captured, and it may produce the more robust optimal solutions for the models.

2.5 Numerical experiments single factory and single warehouse

2.5.1 Values for input parameters

In the numerical experiments with Model 1 - Island microgrid with BS and daily granularity and Model 2 - Prosumer microgrid with BS and daily granularity, the number of production periods, $|T|$, is assumed equal to 12, and each period, t, corresponds to a month. The factory is located in San Francisco and the warehouse is located in Phoenix. Both factory and warehouse run 24 hours a day. The total number of different products to produce, $|I|$, is assumed equal to 2. Demands for each product can be at any of two possible settings (i.e. low or high) over the time horizon. Machine and labor hour capacity can be at any of 3 settings each, and the are 3 sets of estimated WT and PV capacity factors. Then the total number of scenarios in the models is $(2 \times 2 \times 3 \times 3 \times 3) = 108$ scenarios. The reader is encouraged to go back to subsection 2.2.1 where the scenario approach implemented in the APP models was explained. The products are labeled as Product A and Product B. The demand values for products A and B are generated from uniform probability distribution Type 1 provided in Section 2.4.1. Table 5.3 in Appendix B, lists the set of actual values used for the demands for products A and B at the high and low levels. The values used for the machine and labor hour parameters are presented in Appendix B Table 5.10 to 5.13. All the values for the production and energy related parameters are listed in appendix B table 5.14 to 5.15. The sources for assuming the values for RE related parameters are: capital cost of WT (Stehly et al., 2019), PV (NREL, 2021), tax incentive (WINDExchange, 2021), energy selling price (EIA, 2021), energy buying price (EIA, 2021), M&O costs of the WT, PV and the capital recovery factors for WT, PV and BS (Anderson et al., 2017).

2.6 Computational results - base case

If the terms related to BS are dropped from the objective function and constraints in Model 1 - Island microgrid with BS and daily granularity, it converts to an island microgrid without BS. The computational results in this chapter, are for Model 1 without BS and with BS, labeled shortly as IM without BS and IM with BS, and for Model 2 - Prosumer microgrid with BS and daily granularity labeled shortly as Prosumer. Model 1 cases help to assess the impacts of BS on achieving a zero-carbon manufacturing environment. All models were coded using the AMPL mathematical programming language and solved through the CPLEX solver. The numerical experiments were conducted using a Dell Inspiron 13 7000 (1.80 GHz Intel(R) Core(TM) i5-8265U processor (quad core), 8GB RAM, 500GB hard drive with a 64-bit windows 10 operating system). Computation times are presented in Table 2.12 for different APP models presented in this chapter.

Table 2.12: Computational time comparison

APP Model	AMPL user time (sec)	Total solve time (sec)
IM without BS	7.94	31.28
IM with BS	11.53	103.67
Prosumer	13.77	113.91

The AMPL user time is defined as the user CPU seconds used by the AMPL process itself (Fourer et al., 1990). The solve system time is defined as the operating system

CPU seconds used by the latest solve command, including reading and writing files. The solve user is the time spend by the latest process outside the operating system. The total solve time (solve system time plus solve user time) seems a comprehensive way to appraise the models computational time as seen from the definitions.

The three two-stage stochastic APP models used in the computational results are summarized in Table 2.13 and Figure 2.7.

Table 2.13: Comparison of decision variables and constraints

APP Model	Decision variables	Constraints
IM without BS	86,122	1,609,031
IM with BS	164,750	1,688,093
Prosumer	243,590	1,766,933

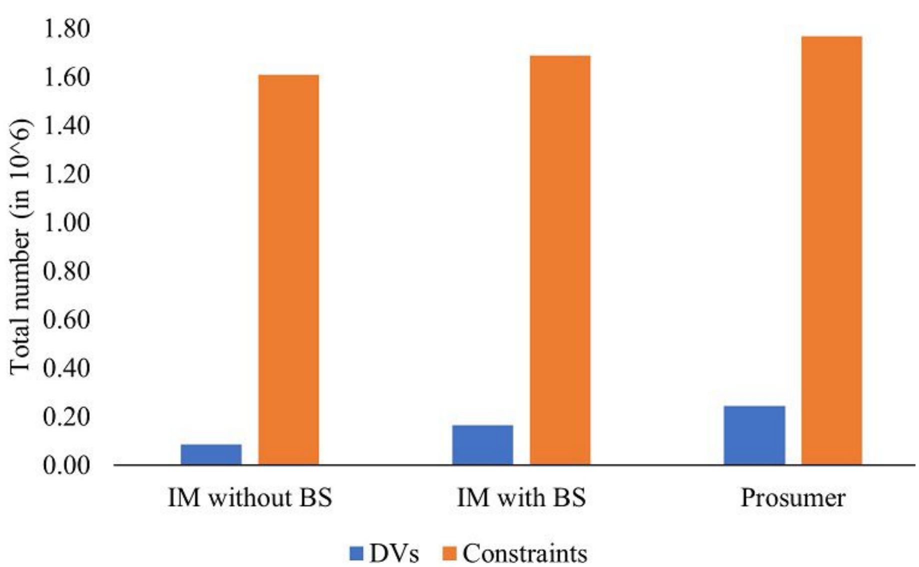

Figure 2.7: Comparison of decision variables and constraints

Besides the total expected annual costs of the models, the levelized cost of energy (LCOE) is also computed as a performance measure to compare the models. The next subsection explains the way the LCOE is computed for each model.

2.6.1 Levelized cost of energy (LCOE)

The levelized cost of energy is defined as the cost of producing one MWh of energy. It is considered as the main indicator to decide if a renewable energy project is attractive or not compared to the conventional sources of energy. Since the range for the actual cost of traditional sources of energy is $50-$100 per MWh, the goal is to obtain an LCOE value within this range. In this thesis work, the LCOE for islanded microgrid operation is calculated with the following equation (Shea and Ramgolam, 2019)

$$LCOE = \frac{\text{Total cost of energy production (\$)}}{\text{Total energy produced (MWh)}}$$

The total cost of energy production is the sum of installation, operation and maintenance costs, and carbon credits for the renewables over the entire production period. The total energy production is the total energy generated in the same period by the renewables in factory and warehouse. In this thesis work, the following equation is used to calculate the LCOE for the prosumer model:

$$LCOE = \frac{\text{Total cost of energy production} + \text{Total cost of energy purchased}}{\text{Total energy produced (MWh)} + \text{Total energy purchased (MWh)}}$$

Table 2.14: Levelized cost of energy

APP Model	LCOE	Unit
IM without BS	48.37	$/MWh
IM with BS	64.91	$/MWh
Prosumer	36.40	$/MWh

Table 2.14 and Figure 2.8 present the resulting LCOE's for the 3 implemented models. The table shows that all models have LCOE's below the $50-$100 cost range for non-renewable energy. The table also shows that the prosumer model has

the lowest LCOE followed by the island without BS. These LCOE results show that for all the cases it is cheaper to operate a facility and the warehouse with RE installation rather than using conventional energy from a main grid.

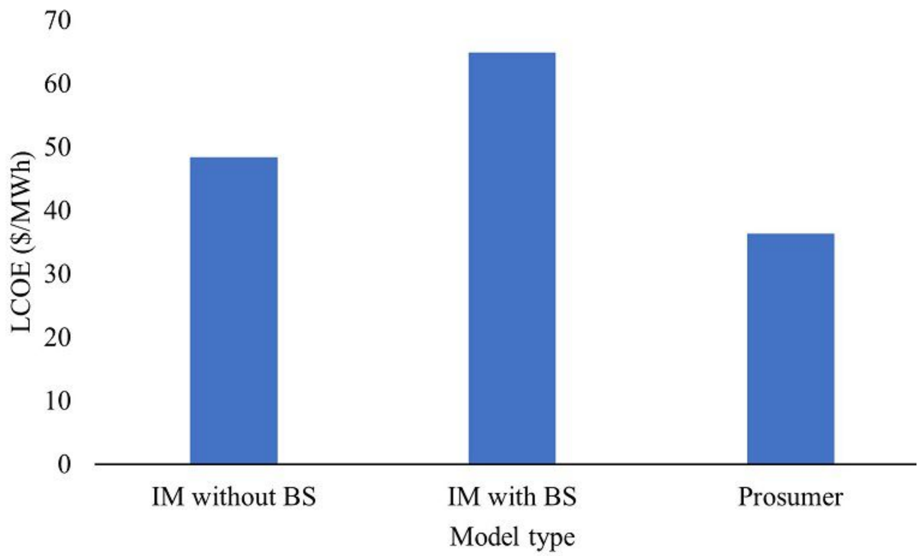

Figure 2.8: Comparison of levelized cost of energy

2.6.2 Energy production comparison

The total energy production (MWh/year) over the whole planning horizon for all the models is shown in Figure 2.9. Table 2.15 shows that the prosumer model produced less energy than the islanded microgrid cases. The main reason behind producing less energy is that the prosumer model now can buy energy from the outside energy sources. The amount of energy bought by the prosumer model at the factory and warehouse is 2,639 MWh and 2,225 MWh respectively and it totals to 4,864 MWh.

2.6.3 Technology installation at factory

The RE technology installation (MW) at the San Francisco factory over the whole planning horizon is shown in Table 2.16 and Figure 2.10. Though San

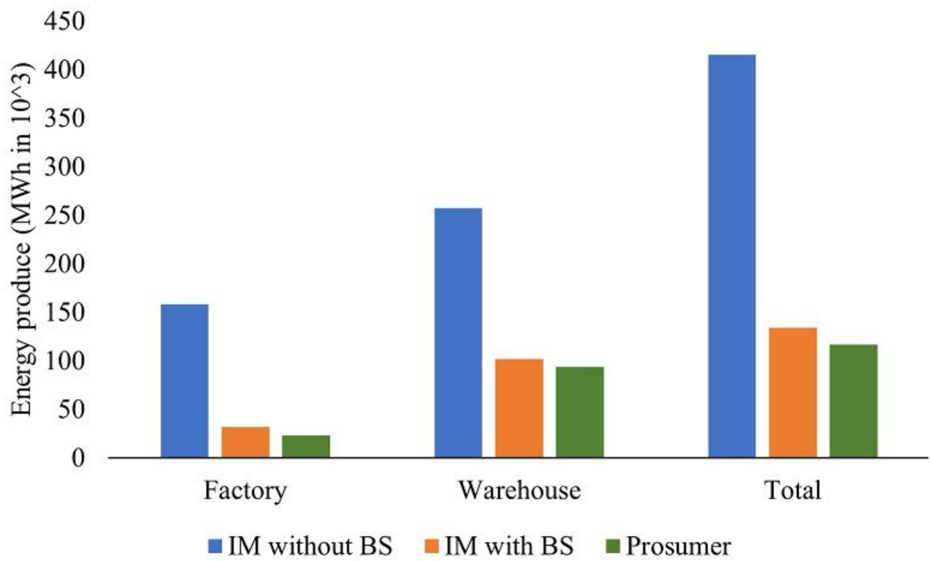

Figure 2.9: Energy production comparison

Table 2.15: Energy production

Model	Factory	Warehouse	Total
IM without BS	158,083	256,999	415,082
IM with BS	32,105	101,830	133,935
Prosumer	22,864	93,864	116,729

Francisco has better WT capacity factors than PV capacity factors, all cases install more PV than WT capacity. The main reasons for this result are that there is a PV has carbon incentive of \$25/MWh and that the PV installation cost is less than the WT installation cost (i.e., \$1.0M vs. \$1.5M).

Table 2.16: Technology installation at factory

Model	WT	PV	Total
IM without BS	13.23	84.91	98.14
IM with BS	0	24.77	24.77
Prosumer	2.93	9.45	12.37

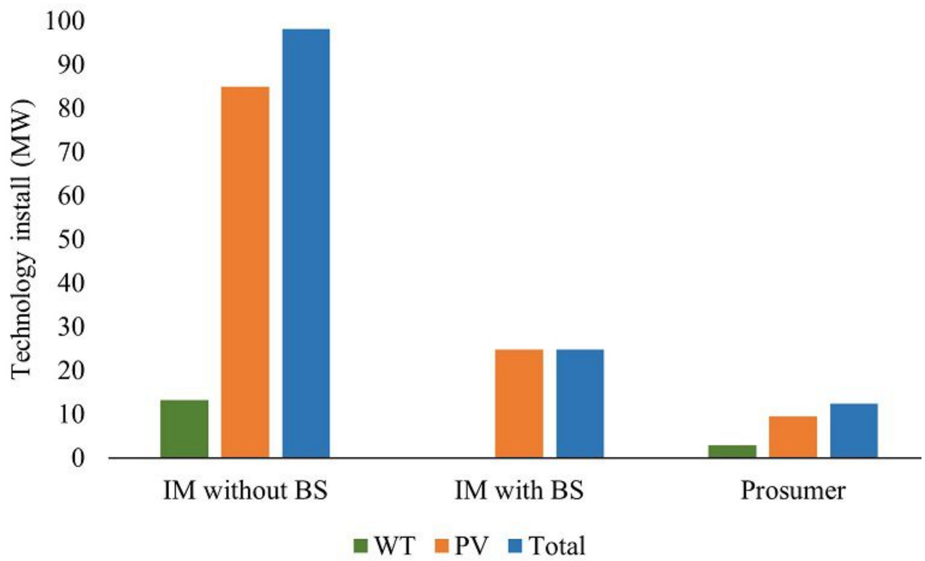

Figure 2.10: Technology installation at factory

2.6.4 Technology installation at warehouse

The technology installation at Phoenix warehouse (MW) over the whole planning horizon for all the cases is shown in Table 2.17 and Figure 2.11. Phoenix has better PV capacity factors than WT capacity factors. PV installation cost is less than WT installation cost and PV has carbon incentive. It explains PV is prefered over WT in all models.

Table 2.17: Technology installation at warehouse

Model	WT	PV	Total
IM without BS	19.72	140.77	160.49
IM with BS	0	62.22	62.22
Prosumer	0	57.35	57.35

2.6.5 Cost comparison

The annual expected cost comparison shows that the prosumer model also outperforms the IM models. Detailed results are in Table 2.18 and Figure 2.12.

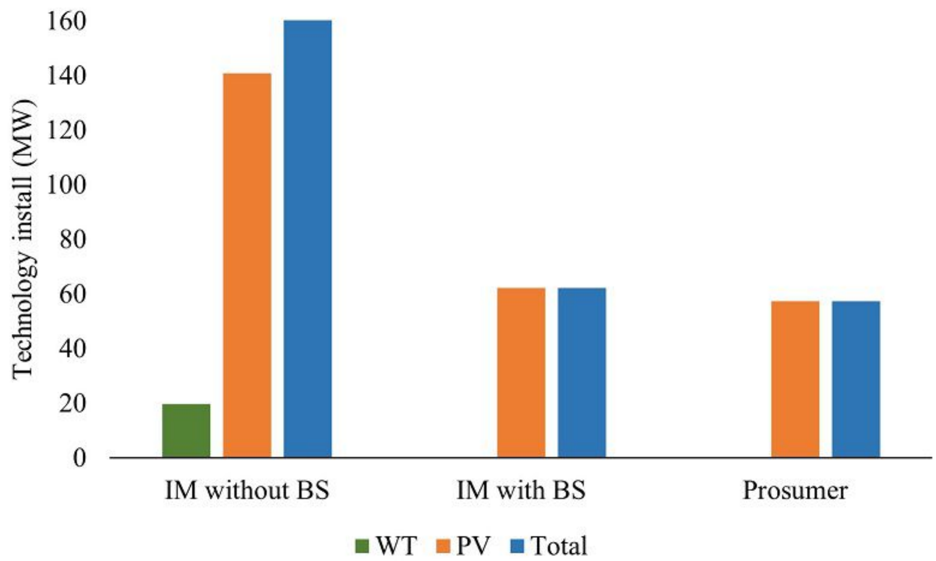

Figure 2.11: Technology installation at warehouse

The IM APP model without BS has an expected cost of $\$28,591,046$, IM APP model with BS has an expected cost of $\$17,131,084$ and the prosumer model has an expected cost of $\$12,727,622$. The energy cost of the prosumer model is $\$4,429,559$ which is 35% of the total cost.The energy cost of the IM without BS model is $\$20,076,339$, which is 70% of the total cost. For the IM with BS, such cost is $\$8,693,140$, which is 50.74%. These numbers evidence the benefits of selling RE to the main grid in the prosumer model.

Table 2.18: Annual cost breakdown

Cost element	IM without BS	IM with BS	Prosumer
Production Cost	$ 6,764,885	$ 6,795,653	$ 6,770,626
Energy Cost	$ 20,076,339	$ 8,693,140	$ 4,429,559
Backorder Cost	$ 273,444	$ 210,945	$ 214,238
Transportation Cost	$ 394,505	$ 396,236	$ 400,950
Subcontracting Cost	$ 1,080,260	$ 1,035,110	$ 912,105
Inventory Cost	$ 1,613	$ 0	$ 144
Total	$ 28,591,046	$ 17,131,084	$ 12,727,622

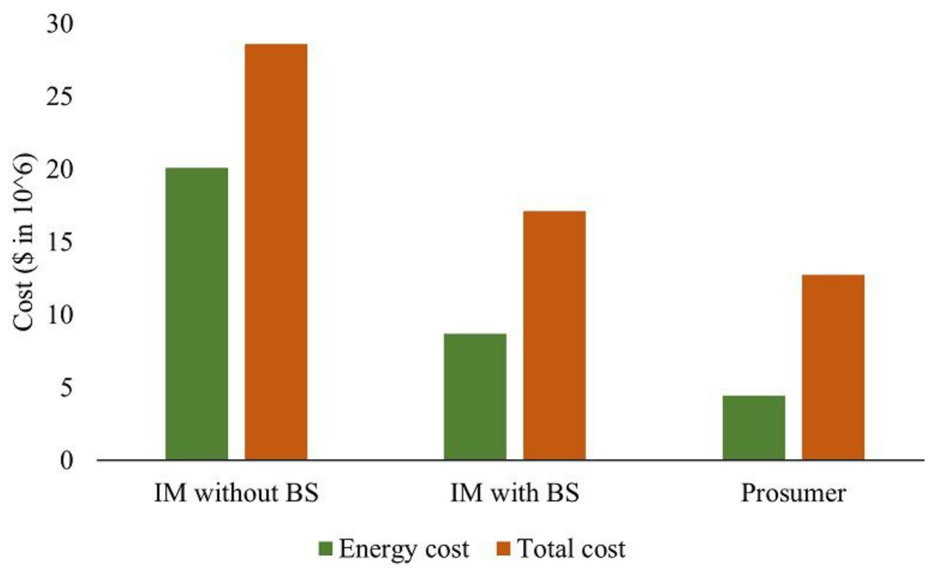

Figure 2.12: Energy cost and total cost comparison

2.7 Sensitivity analysis using DOE

Sensitivity analysis determines how changes in model parameters impacts the output of a model. An efficient way to perform sensitivity analysis is through statistical design of experiments (DOE). In this thesis work, the author experimented with the Model 2 - Prosumer microgrid with BS and daily granularity by performing a full four-factorial design to determine the critical factors affecting different model results. The factors considered in the DOE are type of demand distribution for the products, PV installation cost, carbon incentives for PV, and probability distribution for the 108 scenarios included in the two-stage stochastic model. The number of levels for each of these factors mentioned is 4, 3, 3, and 3, respectively. One replication or run was performed in each experimental condition. Hence, the DOE required to solve the prosumer model $4 \times 3 \times 3 \times 3 = 108$ times and each run will be named a case in the reminder of this chapter. Note that it is just as a coincidence that the number of scenarios included in the prosumer stochastic model is 108 and the number of experimental runs in the DOE is also

108. The levels selected for each of the factors included in the DOE are explained as follows. The DOE considers the four types of product demand distribution: discrete uniform and three different types of triangular distribution presented in Table 2.5 (Type 1, Type2, Type3, Type 4), three PV cost values (\$1,000,000; \$750,000 and \$500,000), three types of carbon incentive (\$30/MWh, \$25/MWh and \$15/MWh) and three levels for the probability distribution of the model scenarios (level 1, level 2, level 3). The levels for the mentioned factors are summarized in Appendix C Table 5.16, and the actual values chosen for product demands under each type of distribution are in Tables 5.3 to 5.5 in appendix B. The levels used for the last factor result after classifying each of the 108 scenarios in the two-stage stochastic model into 3 categories, labeled as low, medium and high. The classification is based on the total sum of the rankings given to product demands, machine and labor hours available in the scenario. A total of 22 scenarios were classified in the low category, 64 in the medium one, and 22 in the high one. Level 1 is a case where the sum of the probabilities for the low and high scenarios in the model is about equal to the probability for the medium scenarios (i.e., L(0.2037), M (0.5926), H(0.2037). Level 2 corresponds to a pessimistic case where the 22 scenarios falling under the low category have about 80% probability of occurrence and the probabilities for the other two scenarios is the same. Level 3 is an optimistic case where the 22 scenarios falling under the high category have about 80% probability of occurrence and the probabilities for the other two scenarios is the same. Note that the base case analyzed in the previous subsection (i.e., 2.6) is Case 1. It has product demand distribution as uniform or Type 1, PV cost \$1,000,000, carbon incentive \$25, and probability scenario as Level 1: L(0.2037), M(0.5926), H(0.2037).

2.7.1 Total cost comparison

Figure 2.13 shows that case 71 (probability distribution for scenarios: L 0.7995, M 0.1088, H 0.0917, probability distribution for product demands: Product A Tri(500,591,800) and Product B Tri(600,693,900), PV cost \$500,000/MW and PV incentives \$30/MWh has the lowest expected cost (\$1,957,550). This case has high probabilities for the scenarios categorized as low, product demand follows triangular distribution where the mode is 10% lower than the base case, the PV cost is at the lowest value assumed and the PV costs incentives are at the highest value assumed. Since some of these, especially the last two, are favorable conditions, it explains the resulting low expected cost. On the other hand, case 81 (probability distribution for

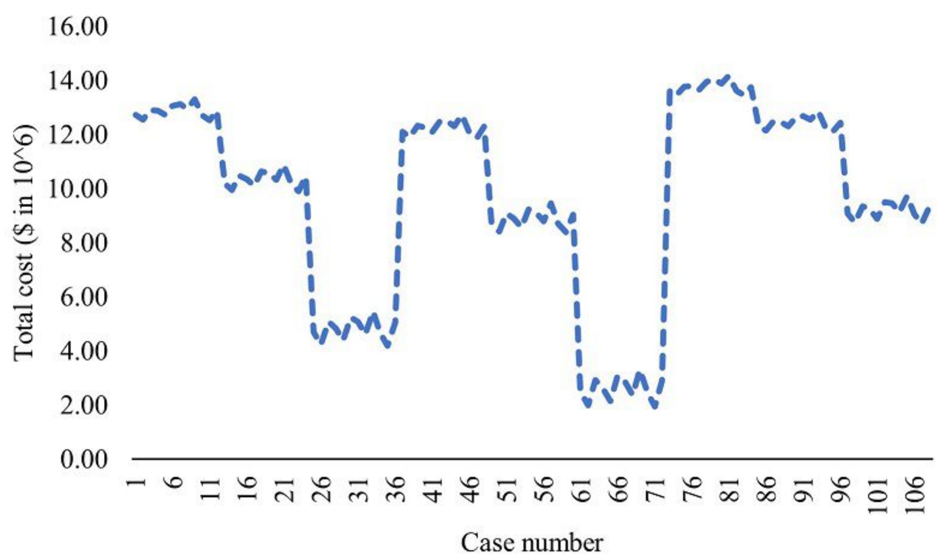

Figure 2.13: Total cost comparison

scenarios: L 0.0917, M 0.1088, H 0.7995, probability distribution for product demands: Product A Tri(500,723,800), Product B Tri(600,847,900), PV installation cost \$1,000,000/MW and PV incentives \$15/MWh has the highest cost of \$14,175,300. This case has high probability for scenarios classified as high, higher probability of high product demand since the product demand follows triangular distribution where the mode is 10% higher than the base case, PV cost at the highest level of \$1000,000 and carbon incentive at the lowest level of \$15/MWh. Thus, such case has multiple unfavorable conditions and it explains the resulting high total cost. The increase in cost vs. the base case is 111.37% and vs. the case with the lowest cost is 724.13%.

2.7.2 WT and PV installation at factory

Cases 75 to 84 in Figure 2.14 are the only ones where the factory install more WT than PV. This result is explained because in those cases, the PV cost is at the highest or costlier level of \$1,000,000/MW and the carbon incentive for PV is at the lowest level of \$15/MWh. Because in San Francisco the average wind capacity factor is higher than the average PV capacity factor, WT is attractive and also cost effective for those cases. Among the cases that installed the largest amount of PV are cases 25-35, in which PV installation cost is at the lowest level of \$500,000/MW and the PV incentives at the level of \$25/MWh. Also, cases 61-72, in which PV installation cost was also at the lowest level and the incentives are at the highest level of \$30/MWh.

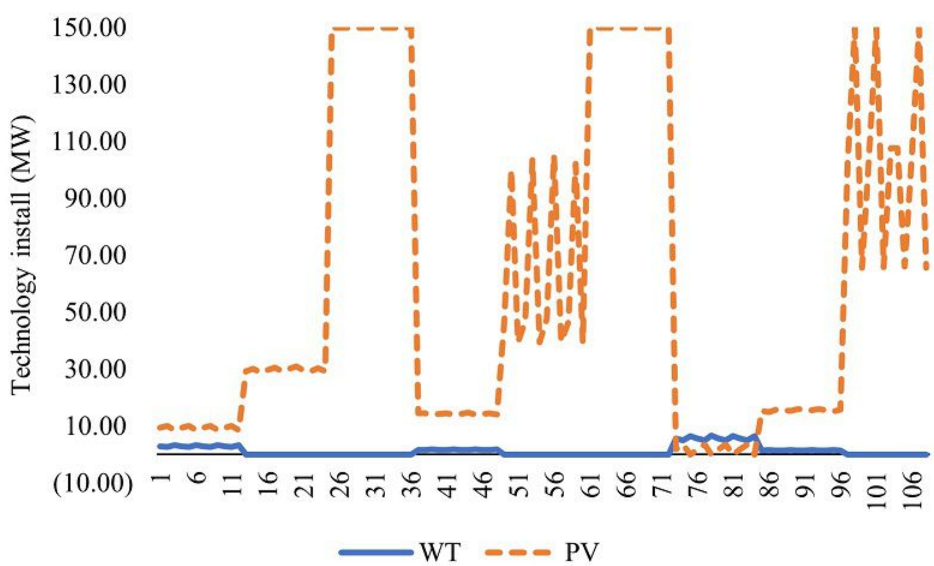

Figure 2.14: WT and PV installation at factory

2.7.3 WT and PV installation at warehouse

The warehouse is located at Phoenix where the PV capacity factor is stronger than the WT capacity factor. PV installation cost is lower than the WT installation cost and for PV there is also a carbon incentive. For all these favorable reasons, as shown in Figure 2.15 the warehouse in all cases installs PV and no WT. Cases 13-36 have PV cost in medium-low values such as \$750,000/MW or \$500,000/MW and high level of incentives for PV (\$25/MWh). Since the warehouse is an energy prosumer, in those cases there is an incentive to adopt higher PV capacity to sell extra energy generated. A similar PV installation capacity is observed for cases 49-70 where PV cost is also \$750,000/MW or \$500,000/MW and the incentives for PV are even higher (\$30/MWh). However, this result may suggest that incentives higher than \$25/MWh do not motivate the warehouse to adopt more PV even if it is an energy prosumer.

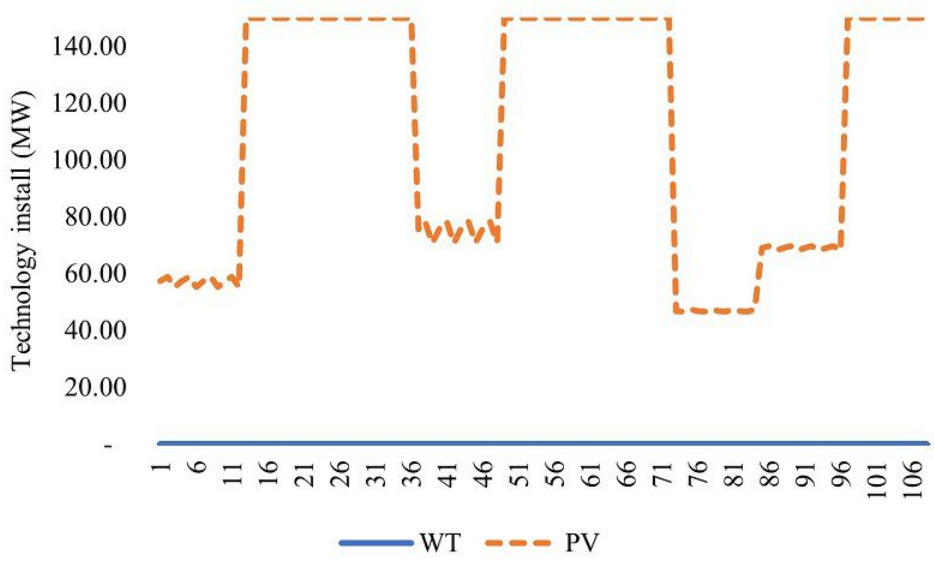

Figure 2.15: WT and PV installation at warehouse

2.7.4 Battery storage installation at factory

From case 25 to 36, 50 to 72 and 98 to 107 in figure 2.16, the prosumer model does not install BSS. In these cases the PV installation cost is 500,000 or 750,000 and the carbon incentive is \$30. The high adoption of PV that Figure 2.14 in Section 2.7.1 shows for these cases, suggest that the factory prefers PV as a buffer instead of acquiring BS because of the high battery cost, the low installation cost of PV, and the high PV incentives.

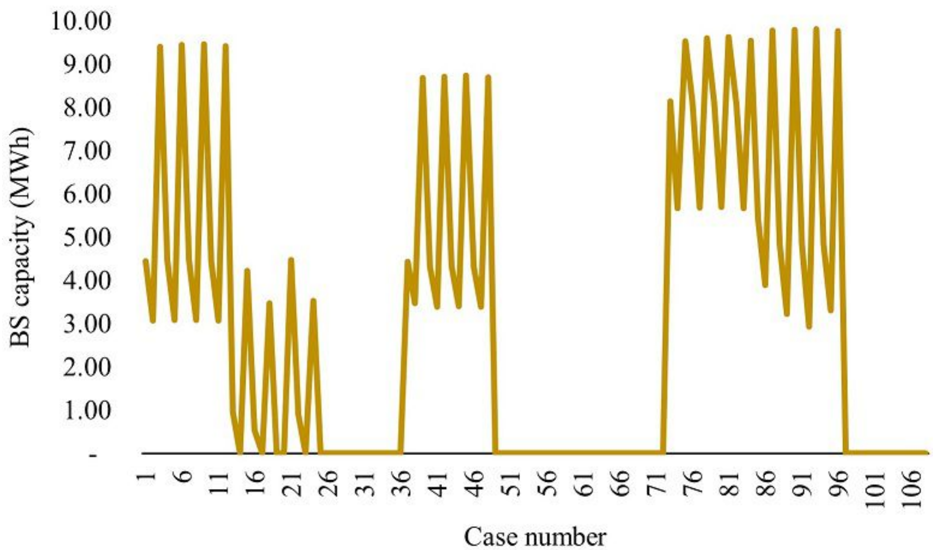

Figure 2.16: BS installation at factory

2.7.5 Battery storage installation at warehouse

From case 13 to 36, 50 to 72 and 98 to 107 in Figure 2.17, the prosumer APP model does not install BSS. From this behavior it is observed that when the PV installation cost is \$500,000 the model does not install BS. Similar situation happen, when the carbon incentive is greater than or equal to \$25 and the PV installation cost is \$750,000.

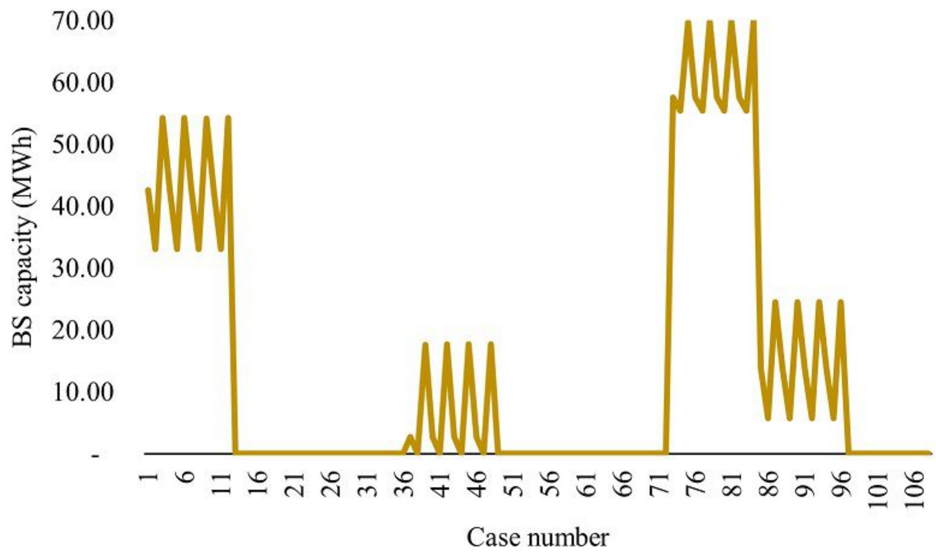

Figure 2.17: BS installation at warehouse

2.7.6 Amount of energy bought at factory

In Figure 2.18, from case 25 to 36 and 61 to 72, the amount of energy the prosumer model buys at the factory is very close to zero.

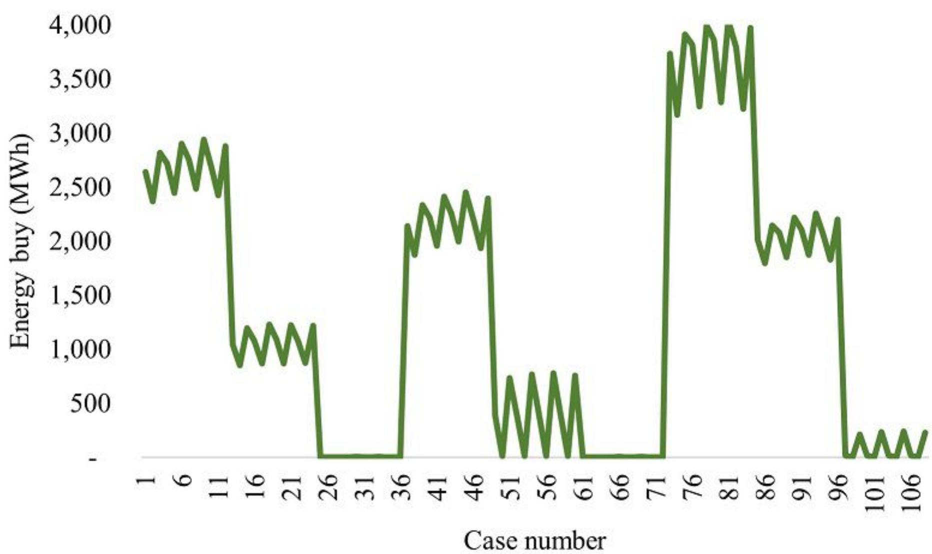

Figure 2.18: Energy buying amount at factory

In these cases, the PV installation cost is \$500,000 and the carbon incentive is \$25/MWh or \$30/MW motivating the energy prosumer to adopt large amount PV to consume or sell and avoid to purchase energy. On the contrary, in case 81 the model buy the highest amount of energy at the factory. In this case, the PV installation cost is $1,000,000, the carbon incentive is $15, the product demand follows triangular distribution where the mode is 10% more than the base case, and the probability distribution for the scenarios in the model is skewed to the high side (i.e. Low 0.0917, M 0.1088, H 0.7995). Thus, the factory is facing a highly energy demanding situation where buying larger amounts of energy ends preferable to increase the PV installation.

2.7.7 Energy selling amount from factory

In Figure 2.19 cases such as 26, 62 and 98 the APP model sell the largest amounts of energy at the factory. In these cases, the PV cost is $500,000. The product demand follows discrete uniform distribution and the probability distribution for the scenarios in the models indicates that there is higher probability for low product demand. All these conditions are very favorable to the prosumer facility for selling energy.

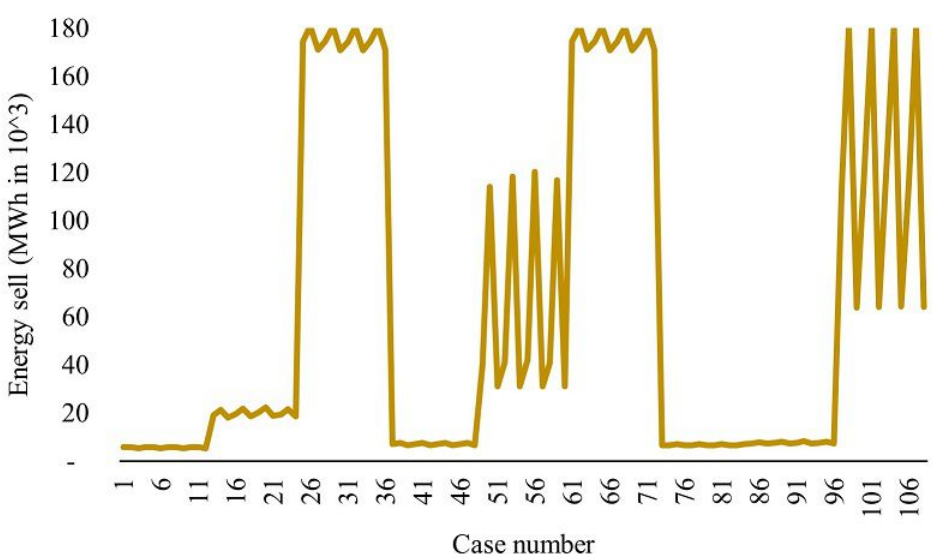

Figure 2.19: Energy selling amount from factory

2.7.8 Energy buying amount at warehouse

In figure 2.20 cases 13 to 36, 50 to 72 and 98 to 107, the APP model buy the least energy at warehouse. In these cases, the PV installation cost is $500,000 and $750,000 respectively and the carbon incentive is $25 and $30 respectively. Then the warehouse has high incentive to adopt enough energy to consume and sell avoiding the need to buy energy. On the contrary, in cases 74 to 83 the warehouse buy high amounts of energy, especially in case 81. In cases 74 to 83, the PV installation cost is high, $1,000,000, and the carbon incentive is low, $15. Thus the warehouse made a conservative adoption of RE capacity that at occasions required energy purchasing.

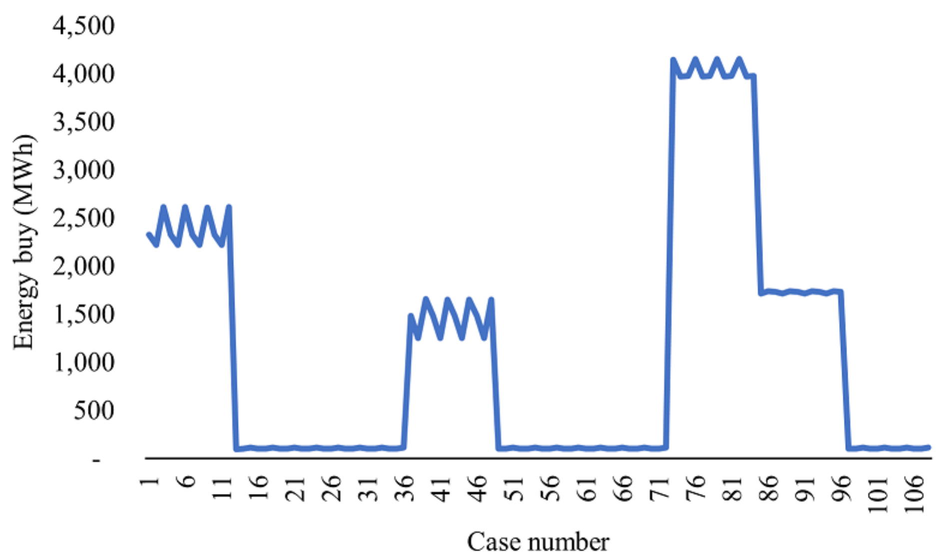

Figure 2.20: Energy buying amount at warehouse

2.7.9 Energy selling amount from warehouse

The behaviour of Figure 2.21 is opposite to the one in the previous subsection, energy buying from warehouse. In Figure 2.21, from case 13 to 36, 50 to 72 and 98 to 107, the APP model sells the highest amounts of RE. In these cases, the PV installation costs and incentives favour the selling energy option. The PV installation cost is $500,000 and $750,000 respectively and the carbon incentive is

$25 and $30 respectively. In case 81, the model sells the lowest amount of energy. In case 74 to 83, the PV installation cost is $1,000,000 and the carbon incentive is $15. The high cost and low incentives for adopting more PV than needed precludes the warehouse to buy extra RE capacity to sell energy.

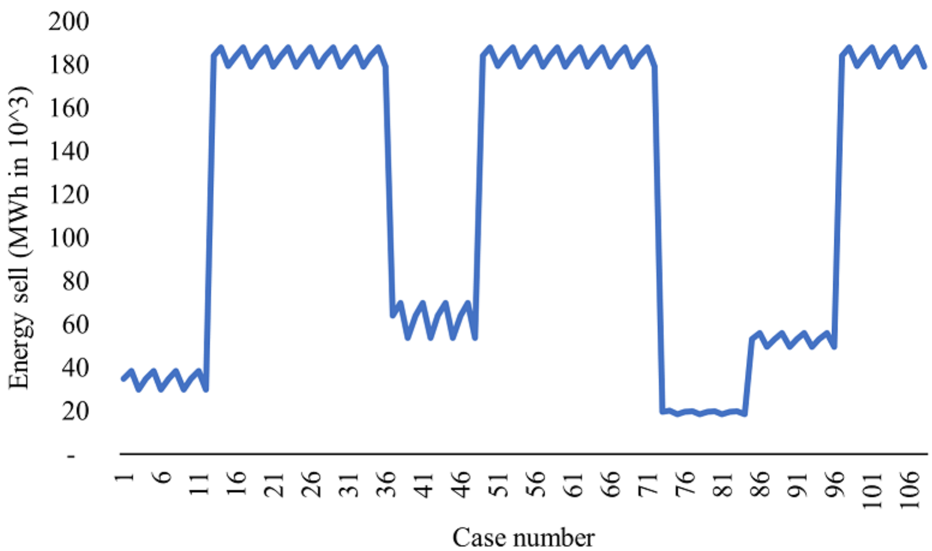

Figure 2.21: Energy selling amount from warehouse

The computational results presented in Section 2.6 with Model 1 - Island microgrid (IM) with and without BS, Model 2 - Prosumer microgrid with BS demonstrated that the it is possible to decarbonize the exemplified manufacturing system consisting of a single factory and a single warehouse. For all APP models, it was proven that the facilities can balance the energy required to operate or sell to the main grid with RE produced, RE stored or energy purchased to the main grid on a daily basis. The LCOE values computed make feasible an affordable integration of RE into the manufacturing system, particularly in Model 2 - Prosumer microgrid with BS. The sensitivity analysis performed in Section 2.7 with Model 2 - Prosumer microgrid with BS, particularly the one for expected total cost presented in Figure 2.13, showed that departures of the base case assumed values for product demand distribution type, probability distribution for the scenarios in the model, PV cost and PV incentives contributed to identify a high number of additional cases or experimental conditions (i.e. 87/107 cases or 81.31%) where the total cost of the system remained the same or lower.

3. APP CONSIDERING HOURLY ENERGY REQUIREMENTS

In this chapter, the author of this thesis researches the case in which the company must satisfy the energy requirements in an hourly basis (i.e. hourly time granularity). For the daily time granularity considered in the previous chapter, the capacity factors for WT and solar PV were averaged over 24 hours of a day. However, solar PV generates zero electricity at night. Therefore, average daily capacity factors do not accurately reflect the real conditions. Also, wind profile and weather conditions are highly dynamic and stochastic, changing frequently over the hours. Thus, an average daily capacity factor may distort the real stochastic pattern of wind profile and weather conditions. Because one of the research question's in this thesis is the one regarding the manufacturing system's feasibility to achieve zero carbon manufacturing operations, developing models that include hourly capacity factors is crucial. Furthermore, the results in the previous chapter have shown that capacity factors variability have enormous impact on decision making regarding capacity of the renewables and BS. Thus, the direct inclusion of hourly capacity factors in the two-stage stochastic APP models helps the decision maker to install more appropriate WT, PV, and BS capacity avoiding extra costs.

In this chapter, the problem is also enlarged to consider the company as one with multiple facilities or a supply chain. By considering more geographical locations or cities in the United States, it is possible to perform a wider evaluation of the feasibility to replace the usage of fossil fuels and accelerates eco-friendly operations to achieve net-zero carbon manufacturing operations. This chapter is organized as follows. Section 3.1 presents the aggregate production planning (APP) problem researched in this chapter and the related research questions. Section 3.2 provides the mathematical formulations for two APP model instances developed in this chapter. The model instances are: (1) Island microgrid (IM) adopting battery storage (BS) to satisfy hourly energy requirements and (2) Prosumer microgrid adopting BS to satisfy hourly energy requirements. The mathematical formulation presented for each instance is the extensive formulation of the two-stage stochastic program with recourse. Section 3.3 describes how the uncertain parameters product demand, machine and labor hours capacity are represented and it elaborates on the procedures to compute the capacity factors (CF) for wind turbines (WT) and solar photovoltaics (PV). Section 3.4 provides details about the numerical experiment and computational results. This chapter does not have a methodology section because the stochastic programming methodology explained in Section 2.2 also applies in this chapter.

3.1 Problem statement and research questions

The system researched in this chapter resembles to the one presented in Figure 2.1 in the previous chapter, but there are two differences.

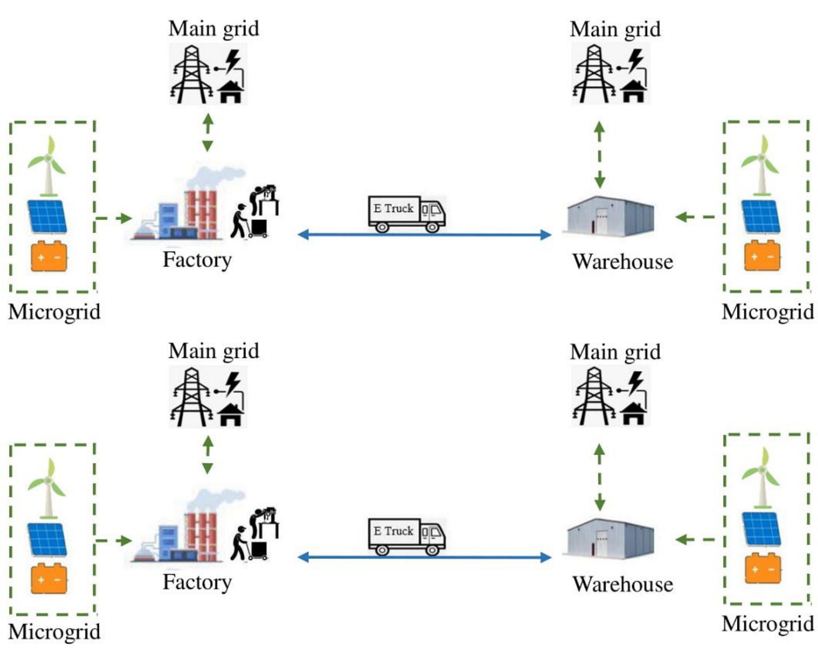

Figure 3.1: Onsite microgrid install at multiple factories and warehouses

The first difference between the problem stated in this chapter and the one in the previous one is the number of factories and warehouses considered. In this chapter, three factories are located at San Francisco, Austin and Boston. Furthermore, three warehouses are located at Phoenix, Dallas and New York. A second difference is the time granularity considered for the satisfaction of energy requirements at the facilities. In this chapter, the facilities satisfy the energy requirements hourly instead of daily.
The research in this chapter aims to solve the following two questions:

- Given that the facilities must satisfy energy requirements on an hourly basis, is it still possible to decarbonize the manufacturing operations and warehouse facilities with RE integration?
- Given that the facilities must satisfy energy requirements on an hourly basis, is it still feasible to integrate RE into manufacturing and warehouse operations with affordable levelized cost of energy (LCOE)?

3.2 Two stage stochastic APP models

In this chapter, the two models with daily time granularity to satisfy energy requirements presented in Chapter 2 transform into models with hourly time granularity regarding energy requirements. A new set labeled as H is included to represent the hours of the year. Most of the decision variables and parameters in the new models are same as the ones in the daily models. Additional notation or modified descriptions for the decision variables and parameters are listed in Tables 3.1 and 3.2. The models are presented after the tables.

3.2.1 Decision variables of the APP models

Table 3.1: Decision variables

Notation	Description	Unit
Q^-_{kjhs}	Energy sold (spilled for Model 1) from factory k at day j in hour h under scenario s	MWh/hour
Q^-_{njhs}	Energy sold (spilled for Model 1) from warehouse n at day j in hour h under scenario s	MWh/hour
Q^+_{kjhs}	Energy bought from the grid at factory k at day j in hour h under scenario s	MWh/hour
Q^+_{njhs}	Energy bought from the grid at warehouse n at day j in hour h under scenario s	MWh/hour
B^f_{kjhs}	Energy stored daily in battery at factory k at day j in hour h under scenario s	MWh/hour
B^f_{njhs}	Energy stored daily in battery at warehouse n at day j in hour h under scenario s	MWh/hour

3.2.2 Constraints of the APP models

Table 3.2: Parameters

Notation	Description	Unit
τ_{gjh}	Number of generation hours in day j in hour h for generation technology g	hour/day
λ^-_{gjhks}	Capacity factor for generation technology g in factory k in day j and hour h under scenario s	N/A
λ^-_{gjhns}	Capacity factor for generation technology g in warehouse n in day j and hour h under scenario s	N/A
u^-	Profit from selling spilled energy	\$/MWh
u^+	Cost of buying energy from main grid	\$/MWh
β_h	Number of trips in specific hour h	trip/hour
ξ	Daily operating hours of factory or warehouse	hour/day

3.2.3 Island microgrid with BS

Model 3 - Island microgrid with BS and hourly granularity:

$$
\begin{aligned}
\min \quad Z = & \sum_{i\in I}\sum_{k\in K}\sum_{t\in T}(c^x_{it}+c^w_{it})x_{ikt} + \sum_{i\in I}\sum_{k\in K}\sum_{t\in T}(c^m_{it}m_{ikt}+c^r_{it}r_{ikt})+ \\
& \sum_{k\in K}\sum_{t\in T}(c_l l_{kt}+c_h h_{kt}+c_f f_{kt}) + \sum_{t=1}^{T}\sum_{i\in I}\sum_{k\in K}\sum_{s\in S}p(s)(c^b_{it}b_{ikts}+c^q_{it}q_{ikts})+ \\
& \sum_{t=1}^{T}\sum_{i\in I}\sum_{n\in N}\sum_{s\in S}p(s)c^y_{it}y_{ints} + \sum_{k\in K}\sum_{g\in G}\phi_g a_g P^c_{kg} + \sum_{n\in N}\sum_{g\in G}\phi_g a_g P^c_{ng}+ \\
& \sum_{k\in K}\phi_b a_b B^c_k + \sum_{n\in N}\phi_b a_b B^c_n + \sum_{k\in K}\sum_{g\in G}\sum_{s\in S}p(s)(b_g-c_g)(\sum_{h\in H}\frac{\lambda_{gjhks}}{|H|})P^c_{kg}+ \\
& \sum_{n\in N}\sum_{g\in G}\sum_{s\in S}p(s)(b_g-c_g)(\sum_{h\in H}\frac{\lambda_{gjhns}}{|H|})P^c_{ng}
\end{aligned} \tag{3.1}
$$

$s.t.$

$$
y_{int-1} - y_{ints} + x_{ikt} + q_{ikts} - b_{ikt-1} + b_{ikts} - m_{ikt} + r_{ikt} = D_{ikts}
$$

$$
\forall i\in I, t=1, \forall k\in K, \forall n\in N, \forall s\in S \tag{3.2}
$$

$$
y_{int-1s} - y_{ints} + x_{ikt} + q_{ikts} - b_{ikt-1s} + b_{ikts} - m_{ikt} + r_{ikt} = D_{ikts}
$$

$$
\forall i\in I, \forall t\in T\backslash\{1\}, \forall k\in K, \forall n\in N, \forall, \forall s\in S \tag{3.3}
$$

$$
\sum_{i\in I}(e^x_i + q^v d_{kn} w_i)\frac{x_{ikt}}{\xi|J_t|} + L_k + q^v\beta_h d_{kn} m^v + B^f_{kjhs} - B^f_{kjh-1} + Q^-_{kjhs}
$$

$$
= \sum_{g\in G}\lambda_{gjhks}P^c_{kg}
$$

$$
j=1, h=1, t=1, \forall k\in K, \forall n\in N, \forall s\in S \tag{3.4}
$$

$$
\sum_{i\in I}(e^x_i + q^v d_{kn} w_i)\frac{x_{ikt}}{\xi|J_t|} + L_k + q^v\beta_h d_{kn} m^v + B^f_{kjhs} - B^f_{kjh-1s} + Q^-_{kjhs}
$$

$$
= \sum_{g\in G}\lambda_{gjhks}P^c_{kg}
$$

$$
\forall t\in T, \forall j\in J, \forall h\in H\backslash\{1\}, \forall k\in K, \forall n\in N, \forall s\in S \tag{3.5}
$$

Model 3 - Island microgrid with BS and hourly granularity continue

$$\sum_{i\in I} e_i^f y_{ints}(\frac{h-\sum_{v=1}^{t-1}|J_v\delta|}{|J_t|\delta}) + L_n + q^v\beta_h d_{nk}m^v + B_{njhs}^f - B_{njh-1}^f + Q_{njhs}^-$$
$$= \sum_{g\in G} \lambda_{gjhns} P_{ng}^c$$
$$j=1, h=1, t=1, \forall k \in K, \forall n \in N, \forall s \in S \tag{3.6}$$

$$\sum_{i\in I} e_i^f y_{ints}(\frac{h-\sum_{v=1}^{t-1}|J_v\delta|}{|J_t|\delta}) + L_n + q^v\beta_h d_{nk}m^v + B_{njhs}^f - B_{njh-1s}^f + Q_{njhs}^-$$
$$= \sum_{g\in G} \lambda_{gjhns} P_{ng}^c$$
$$\forall t \in T, \forall j \in J, \forall h \in H\backslash\{1\}, \forall k \in K, \forall n \in N, \forall s \in S \tag{3.7}$$

$$\sum_{i\in I} a_i x_{ikt} = l_{kt}$$
$$\forall k \in K, \forall t \in T \tag{3.8}$$

$$l_{kt} \leq LH_{kts}^{max}$$
$$\forall k \in K, \forall t \in T, \forall s \in S \tag{3.9}$$

$$l_{kt} = l_{kt-1} + h_{kt} - f_{kt}$$
$$\forall k \in K, \forall t \in T \tag{3.10}$$

$$h_{kt} + f_{kt} \leq \alpha l_{kt-1}$$
$$\forall k \in K, \forall t \in T \tag{3.11}$$

$$\sum_{i\in I} u_i x_{ikt} = w_{kt}$$
$$\forall k \in K, \forall t \in T \tag{3.12}$$

$$w_{kt} \leq MH_{kts}^{max}$$
$$\forall k \in K, \forall t \in T, \forall s \in S \tag{3.13}$$

Model 3 - Island microgrid with BS and hourly granularity continue

$$w_{kt} = w_{kt-1} + o_{kt} - p_{kt} \qquad \forall k \in K, \forall t \in T \qquad (3.14)$$

$$\nu x_{ikt} = m_{ikt} \qquad \forall k \in K, \forall i \in I, \forall t \in T \qquad (3.15)$$

$$\eta m_{ikt} = r_{ikt} \qquad \forall k \in K, \forall i \in I, \forall t \in T \qquad (3.16)$$

$$0 \leq m_{ikt} - r_{ikt} \leq m_{ikt}^{max} \qquad \forall i \in I, \forall k \in K, \forall t \in T \qquad (3.17)$$

$$\sum_{i \in I} y_{ints} \leq WH_t^{max} \qquad \forall n \in N, \forall t \in T, \forall s \in S \qquad (3.18)$$

$$0 \leq P_{kg}^c \leq P_{kg}^{max} \qquad \forall k \in K, \forall g \in G \qquad (3.19)$$

$$0 \leq P_{ng}^c \leq P_{ng}^{max} \qquad \forall n \in N, \forall g \in G \qquad (3.20)$$

$$B_k^c \leq B_k^{max} \qquad \forall k \in K \qquad (3.21)$$

$$B_n^c \leq B_n^{max} \qquad \forall n \in N \qquad (3.22)$$

$$0 \leq B_{kjhs}^f \leq B_k^c \qquad \forall k \in K, \forall s \in S, j \in J_t, h \in H \qquad (3.23)$$

$$0 \leq B_{njhs}^f \leq B_n^c \qquad \forall n \in N, \forall s \in S, j \in J_t, h \in H \qquad (3.24)$$

$$B_{k0}^f = B_k^c \qquad \forall k \in K, j = 0 \qquad (3.25)$$

$$B_{n0}^f = B_n^c \qquad \forall n \in N, j = 0 \qquad (3.26)$$

$$Q_{kjhs}^- \leq Q_{kjhs}^{max} \qquad \forall k \in K, j \in J, h \in H, s \in S \qquad (3.27)$$

$$Q_{njhs}^- \leq Q_{njhs}^{max} \qquad \forall n \in K, j \in J, h \in H, s \in S \qquad (3.28)$$

$$x_{ikt}, m_{ikt}, r_{ikt} \geq 0 \qquad \forall i \in I, \forall k \in K, \forall t \in T \qquad (3.29)$$

$$h_{kt}, f_{kt}, l_{kt}, w_{kt}, p_{kt} \geq 0 \qquad \forall k \in K, \forall t \in T \qquad (3.30)$$

$$b_{ikts}, q_{ikts} \geq 0 \qquad \forall i \in I, \forall k \in K, \forall t \in T, \forall s \in S \qquad (3.31)$$

$$y_{ints} \geq 0 \qquad \forall i \in I, \forall n \in N, \forall t \in T, \forall s \in S \qquad (3.32)$$

The explanation of the objective function and constraints for the Model 3 - Island microgrid with BS and hourly granularity presented above is exactly the same as the one provided for the IM Model 1 in the previous chapter. However, in the objective function of Model 3, the subscript used in the sum involving the parameters λ_{gjhks} and λ_{gjhns} changes because now the time granularity is hourly. Also, the subscript h is added in the constraints that balance the energy requirements in the factory and warehouse (i.e., constraints 3.4, 3.5, 3.6 and 3.7) to consider that the energy is balanced at every hour of the entire time horizon (i.e., year).

3.2.4 Prosumer without TOU

Model 4 - Prosumer microgrid with BS, without TOU, and hourly granularity:

$$\begin{aligned}
\min \quad Z = & \sum_{i\in I}\sum_{k\in K}\sum_{t\in T}(c^x_{it}+c^w_{it})x_{ikt} + \sum_{i\in I}\sum_{k\in K}\sum_{t\in T}(c^m_{it}m_{ikt}+c^r_{it}r_{ikt}) + \\
& \sum_{k\in K}\sum_{t\in T}(c_l l_{kt}+c_h h_{kt}+c_f f_{kt}) + \sum_{t=1}^{T}\sum_{i\in I}\sum_{k\in K}\sum_{s\in S} p(s)(c^b_{it}b_{ikts}+c^q_{it}q_{ikts}) + \\
& \sum_{t=1}^{T}\sum_{i\in I}\sum_{n\in N}\sum_{s\in S} p(s)c^y_{it}y_{ints} + \sum_{k\in K}\sum_{g\in G}\phi_g a_g P^c_{kg} + \sum_{n\in N}\sum_{g\in G}\phi_g a_g P^c_{ng} + \\
& \sum_{k\in K}\phi_b a_b B^c_k + \sum_{n\in N}\phi_b a_b B^c_n + \sum_{k\in K}\sum_{g\in G}\sum_{s\in S} p(s)(b_g-c_g)(\sum_{h\in H}\frac{\lambda_{gjhks}}{|H|})P^c_{kg} + \\
& \sum_{n\in N}\sum_{g\in G}\sum_{s\in S} p(s)(b_g-c_g)(\sum_{h\in H}\frac{\lambda_{gjhns}}{|H|})P^c_{ng} - \sum_{k\in K}\sum_{j\in J}\sum_{h\in H}\sum_{s\in S} p(s)u^- Q^-_{kjhs} + \\
& \sum_{k\in K}\sum_{j\in J}\sum_{h\in H}\sum_{s\in S} p(s)u^+ Q^+_{kjhs} - \sum_{n\in N}\sum_{j\in J}\sum_{h\in H}\sum_{s\in S} p(s)u^- Q^-_{njhs} + \\
& \sum_{n\in N}\sum_{j\in J}\sum_{h\in H}\sum_{s\in S} p(s)u^+ Q^+_{njhs}
\end{aligned} \tag{3.33}$$

$s.t.$

$$y_{int-1} - y_{ints} + x_{ikt} + q_{ikts} - b_{ikt-1} + b_{ikts} - m_{ikt} + r_{ikt} = D_{ikts}$$
$$\forall i \in I, t = 1, \forall k \in K, \forall n \in N, \forall s \in S \tag{3.34}$$

Model 4 - Prosumer microgrid with BS, without TOU, and hourly granularity continue

$$y_{int-1s} - y_{ints} + x_{ikt} + q_{ikts} - b_{ikt-1s} + b_{ikts} - m_{ikt} + r_{ikt} = D_{ikts}$$
$$\forall i \in I, \forall t \in T \backslash \{1\}, \forall k \in K, \forall n \in N, \forall, \forall s \in S \tag{3.35}$$

$$\sum_{i \in I}(e_i^x + q^v d_{kn} w_i)\frac{x_{ikt}}{\xi|J_t|} + L_k + q^v \beta_h d_{kn} m^v + B_{kjhs}^f - B_{kjh-1}^f + Q_{kjhs}^-$$
$$= \sum_{g \in G} \lambda_{gjhks} P_{kg}^c + Q_{kjhs}^+$$
$$j = 1, h = 1, t = 1, \forall k \in K, \forall n \in N, \forall s \in S \tag{3.36}$$

$$\sum_{i \in I}(e_i^x + q^v d_{kn} w_i)\frac{x_{ikt}}{\xi|J_t|} + L_k + q^v \beta_h d_{kn} m^v + B_{kjhs}^f - B_{kjh-1s}^f + Q_{kjhs}^-$$
$$= \sum_{g \in G} \lambda_{gjhks} P_{kg}^c + Q_{kjhs}^+$$
$$\forall t \in T, \forall j \in J, \forall h \in H \backslash \{1\}, \forall k \in K, \forall n \in N, \forall s \in S \tag{3.37}$$

$$\sum_{i \in I} e_i^f y_{ints}\left(\frac{h - \sum_{v=1}^{t-1} |J_v \delta|}{|J_t|\delta}\right) + L_n + q^v \beta_h d_{nk} m^v + B_{njhs}^f - B_{njh-1}^f + Q_{njhs}^-$$
$$= \sum_{g \in G} \lambda_{gjhns} P_{ng}^c + Q_{njhs}^+$$
$$j = 1, h = 1, t = 1, \forall k \in K, \forall n \in N, \forall s \in S \tag{3.38}$$

$$\sum_{i \in I} e_i^f y_{ints}\left(\frac{h - \sum_{v=1}^{t-1} |J_v \delta|}{|J_t|\delta}\right) + L_n + q^v \beta_h d_{nk} m^v + B_{njhs}^f - B_{njh-1s}^f + Q_{njhs}^-$$
$$= \sum_{g \in G} \lambda_{gjhns} P_{ng}^c + Q_{njhs}^+$$
$$\forall t \in T, \forall j \in J, \forall h \in H \backslash \{1\}, \forall k \in K, \forall n \in N, \forall s \in S \tag{3.39}$$

$$\sum_{i \in I} a_i x_{ikt} = l_{kt}$$
$$\forall k \in K, \forall t \in T \tag{3.40}$$

Model 4 - Prosumer microgrid with BS, without TOU, and hourly granularity continue

$$l_{kt} \leq LH^{max}_{kts} \qquad \forall k \in K, \forall t \in T, \forall s \in S \tag{3.41}$$

$$l_{kt} = l_{kt-1} + h_{kt} - f_{kt} \qquad \forall k \in K, \forall t \in T \tag{3.42}$$

$$h_{kt} + f_{kt} \leq \alpha l_{kt-1} \qquad \forall k \in K, \forall t \in T \tag{3.43}$$

$$\sum_{i \in I} u_i x_{ikt} = w_{kt} \qquad \forall k \in K, \forall t \in T \tag{3.44}$$

$$w_{kt} \leq MH^{max}_{kts} \qquad \forall k \in K, \forall t \in T, \forall s \in S \tag{3.45}$$

$$w_{kt} = w_{kt-1} + o_{kt} - p_{kt} \qquad \forall k \in K, \forall t \in T \tag{3.46}$$

$$\nu x_{ikt} = m_{ikt} \qquad \forall k \in K, \forall i \in I, \forall t \in T \tag{3.47}$$

$$\eta m_{ikt} = r_{ikt} \qquad \forall k \in K, \forall i \in I, \forall t \in T \tag{3.48}$$

$$0 \leq m_{ikt} - r_{ikt} \leq m^{max}_{ikt} \qquad \forall i \in I, \forall k \in K, \forall t \in T \tag{3.49}$$

$$\sum_{i \in I} y_{ints} \leq WH^{max}_{t} \qquad \forall n \in N, \forall t \in T, \forall s \in S \tag{3.50}$$

$$0 \leq P^{c}_{kg} \leq P^{max}_{kg} \qquad \forall k \in K, \forall g \in G \tag{3.51}$$

$$0 \leq P^{c}_{ng} \leq P^{max}_{ng} \qquad \forall n \in N, \forall g \in G \tag{3.52}$$

$$B^{c}_{k} \leq B^{max}_{k} \qquad \forall k \in K \tag{3.53}$$

$$B^{c}_{n} \leq B^{max}_{n} \qquad \forall n \in N \tag{3.54}$$

$$0 \leq B^{f}_{kjhs} \leq B^{c}_{k} \qquad \forall k \in K, \forall s \in S, j \in J_t, h \in H \tag{3.55}$$

$$0 \leq B^{f}_{njhs} \leq B^{c}_{n} \qquad \forall n \in N, \forall s \in S, j \in J_t, h \in H \tag{3.56}$$

$$B^{f}_{k0} = B^{c}_{k} \qquad \forall k \in K, j = 0 \tag{3.57}$$

$$B^{f}_{n0} = B^{c}_{n} \qquad \forall n \in N, j = 0 \tag{3.58}$$

$$Q^{-}_{kjhs} \leq Q^{max}_{kjhs} \qquad \forall k \in K, j \in J, h \in H, s \in S \tag{3.59}$$

$$Q^{-}_{njhs} \leq Q^{max}_{njhs} \qquad \forall n \in K, j \in J, h \in H, s \in S \tag{3.60}$$

Model 4 - Prosumer microgrid with BS, without TOU, and hourly granularity continue

$$x_{ikt}, m_{ikt}, r_{ikt} \geq 0 \qquad \forall i \in I, \forall k \in K, \forall t \in T \qquad (3.61)$$

$$h_{kt}, f_{kt}, l_{kt}, w_{kt}, p_{kt} \geq 0 \qquad \forall k \in K, \forall t \in T \qquad (3.62)$$

$$b_{ikts}, q_{ikts} \geq 0 \qquad \forall i \in I, \forall k \in K, \forall t \in T, \forall s \in S \qquad (3.63)$$

$$y_{ints} \geq 0 \qquad \forall i \in I, \forall n \in N, \forall t \in T, \forall s \in S \qquad (3.64)$$

The explanation of the objective function and constraints for the Model 4 - Prosumer microgrid with BS, whithout TOU, and hourly granularity presented above is exactly the same as the one provided for Model 2 - Prosumer microgrid with BS and daily granularity in the previous chapter. However, in the objective function of Model 4, the subscript used in the sum involving the parameters λ_{gjhks} and λ_{gjhns} changes because now the time granularity is hourly. Also, the subscript h is added in the constraints that balance the energy requirements in the factory and warehouse (i.e., constraints 3.36, 3.37, 3.38 and 3.39) to consider that the energy is balanced at every hour of the entire time horizon (i.e., year).

3.2.5 Model assumptions

The two-stage stochastic APP models presented in this chapter share the same assumptions provided in Section 2.3.3 in the previous chapter. Note that models in Chapters 2 and 3 are assuming that the company adopting the microgrids is not under a time of use (TOU) energy rate plan with the utility company. Besides, in this chapter it is assumed that the assignment of factories to warehouses is pre-determined. It means such transportation problem has been solved previously.

3.3 Estimation of uncertain parameters

3.3.1 Estimation of product demands

For the implementation of the hourly models presented in this chapter, the total number of factories, k, is assumed equal to 3. and the total number of warehouses n, is assumed equal to 3. The total number of different products to produce I, is assumed equal to 2. The number of production periods T, is assumed equal to 12, and each period t corresponds to a month. Discrete uniform distribution is assumed for the products' demand as listed in table 3.3.

Table 3.3: Distribution of product demands for different factories

Product	San Francisco	Austin	Boston
1	U [500, 800]	U [450, 550]	U [550, 650]
2	U [600, 900]	U [695, 810]	U [750, 850]

3.3.2 Estimation of machine hours capacity

In this chapter, it is assumed that machine hours capacity at the factories may follow any of the three discrete uniform distributions listed in Table 3.4. These three possible cases for the distribution of the machine hours capacity are included in the scenarios of Models 3 and 4 presented in this chapter.

Table 3.4: Distribution of machine hours capacity for different factories

Case	San Francisco	Austin	Dallas
Low	U [150,633, 152,714]	U [150,000, 152,700]	U [151,000, 153,700]
Medium	U [152,855, 155,716]	U [150,250, 150,500]	U [153,720, 155,800]
High	U [155,997, 159,258]	U [150,480, 151,000]	U [156,270, 160,450]

3.3.3 Estimation of labor hours capacity

In this chapter, it is assumed that labor hour capacity at the factories may follow any of the three discrete uniform distributions listed in Table 3.5. The three possible cases for the labor hour capacity are included in the scenarios of Models 3 and 4 presented in this chapter.

Table 3.5: Distribution of machine hours capacity for different factories

Case	San Francisco	Austin	Dallas
Low	U [46000, 46100]	U [46100, 46275]	U [46200, 46350]
Medium	U [46102, 46308]	U [46275, 46425]	U [46375, 46555]
High	U [46310, 46500]	U [46450, 46600]	U [46560, 46700]

3.3.4 Estimation of Austin WT capacity factor

The author of this thesis used the models presented in the literature review, Section 1.3, to estimate WT capacity factors (CF) to input to the models in this chapter. The estimation procedure is the same as explained in Section 2.4.4 in the previous chapter.

Table 3.6: Austin WT capacity factor analysis

City	Year	Mean	St. Deviation	Median
Austin	2013	0.3196	0.2032	0.2581
	2014	0.3525	0.1974	0.3047
	2015	0.3007	0.1904	0.2387

Real wind speed data collected hourly in different years for Austin (WeatherUnderground, 2019) was used to compute three different sets of hourly WT capacity factors (CF) for a lapse of 8760 hours (i.e. the whole year). In the computations, Equation 1.3 and 26,280 observations (365 days*24 hours/day*3

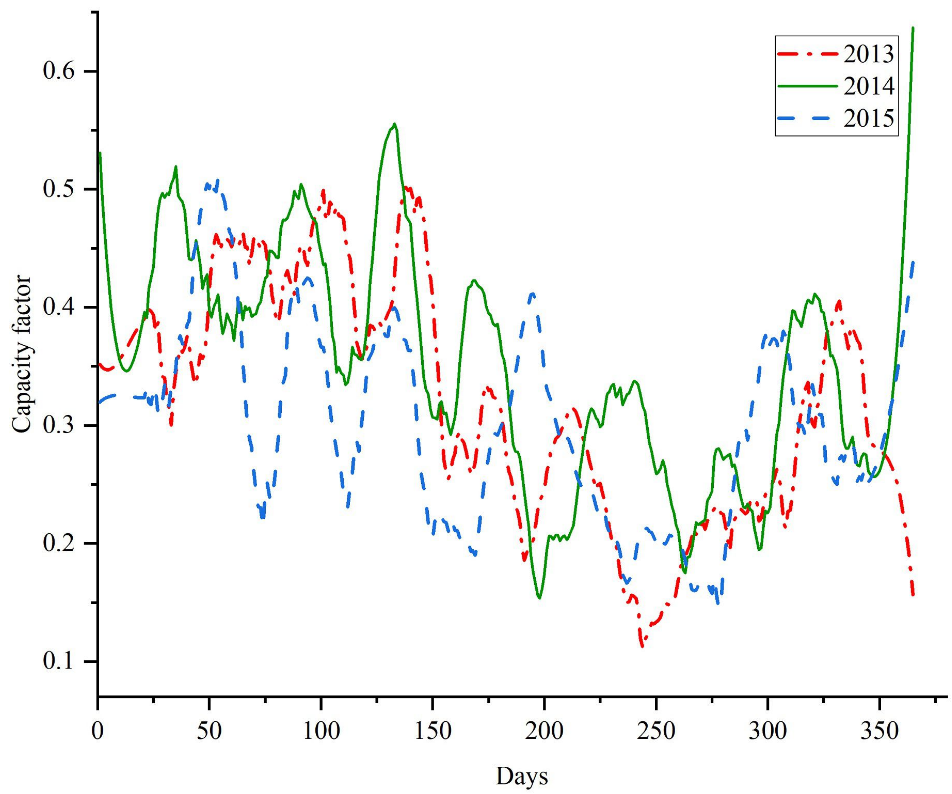

Figure 3.2: Austin average daily WT capacity factor

sets) for the wind speed are used. Table 3.6 presents the annual statistics (i.e., mean, standard deviation, and median) and Figure 3.2 represents the graphical representation of the WT capacity factors of Austin.

3.3.5 Estimation of Boston WT capacity factor

Real wind speed data collected hourly in different years for Boston (WeatherUnderground, 2019) was used to compute three different sets of hourly WT capacity factors (CF) for a lapse of 8760 hours (i.e. the whole year). The CF computed for Boston used equation 1.3 and 26,280 observations (365 days*24 hours/day*3 sets) for the wind speed. Table 3.7 presents the annual statistics (i.e., mean, standard deviation, and median) and Figure 3.3 represents the graphical representation of the WT capacity factors of Boston.

Table 3.7: Boston WT capacity factor analysis

City	Year	Mean	St. Deviation	Median
Boston	2013	0.4028	0.2444	0.3507
	2014	0.3956	0.2333	0.3443
	2015	0.4124	0.2260	0.3591

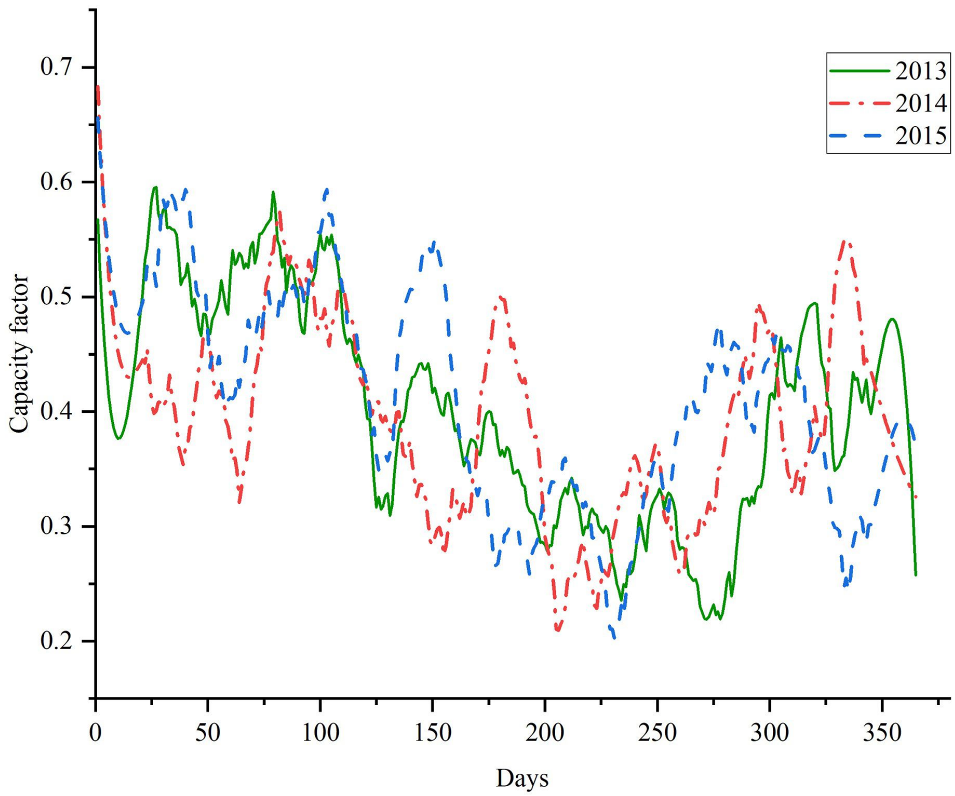

Figure 3.3: Boston average daily WT capacity factor

3.3.6 Estimation of Dallas WT capacity factor

Real wind speed data collected hourly in different years for Dallas (WeatherUnderground, 2019) was used to compute three different sets of hourly WT capacity factors (CF) for a lapse of 8760 hours (i.e. the whole year). The three sets of CF computed for Dallas used equation 1.3 and 26,280 observations (365 days*24 hours/day*3 sets) for the wind speed. Table 3.8 presents the annual statistics (i.e., mean, standard deviation, and median) and Figure 3.4 represents the graphical representation of the WT capacity factor of Dallas.

Table 3.8: Dallas WT capacity factor analysis

City	Year	Mean	St. Deviation	Median
Dallas	2013	0.4297	0.2577	0.3805
	2014	0.4632	0.2527	0.4263
	2015	0.3869	0.2295	0.3323

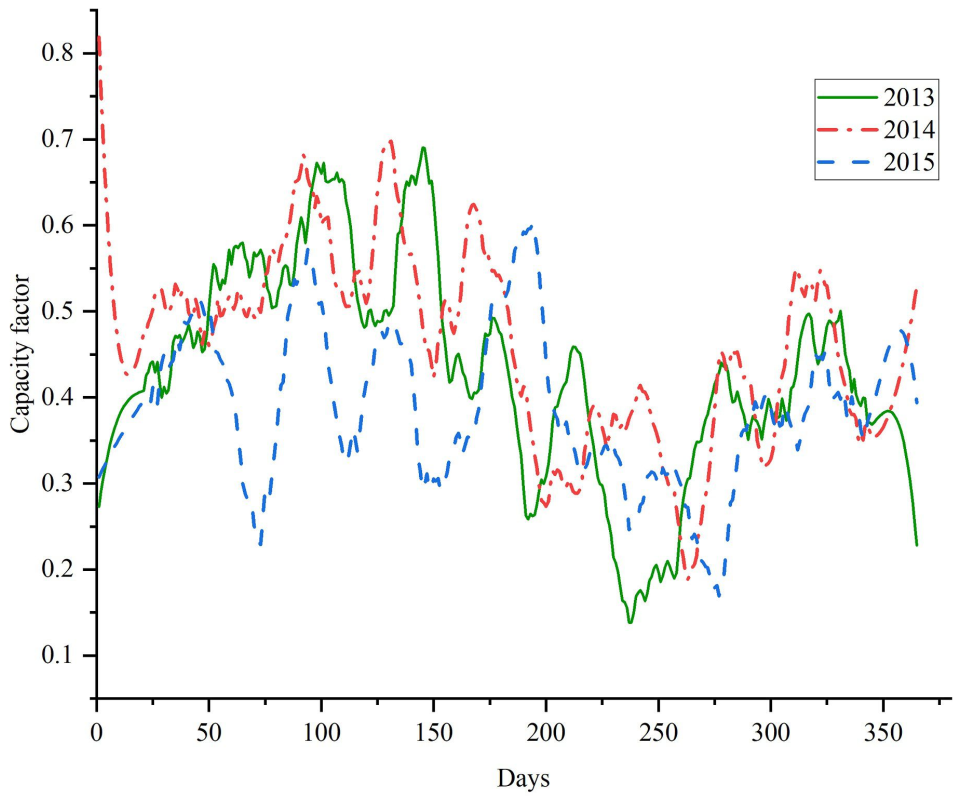

Figure 3.4: Dallas average daily WT capacity factor

3.3.7 Estimation of New York WT capacity factor

Real wind speed data collected hourly in different years for New York (WeatherUnderground, 2019) was used to compute three different sets of hourly WT capacity factors (CF) for a lapse of 8760 hours (i.e. the whole year). For the computations equation 1.3. and 26,280 observations (365 days*24 hours/day*3 sets) for the wind speed were used. Table 3.9 presents the annual statistics (i.e., mean, standard deviation and median) and Figure 3.5 represents the graphical representation of the WT capacity factors of New York.

Table 3.9: New York WT capacity factor analysis

City	Year	Mean	St. Deviation	Median
New York	2013	0.4777	0.2361	0.4407
	2014	0.4530	0.2404	0.3964
	2015	0.4515	0.2299	0.4195

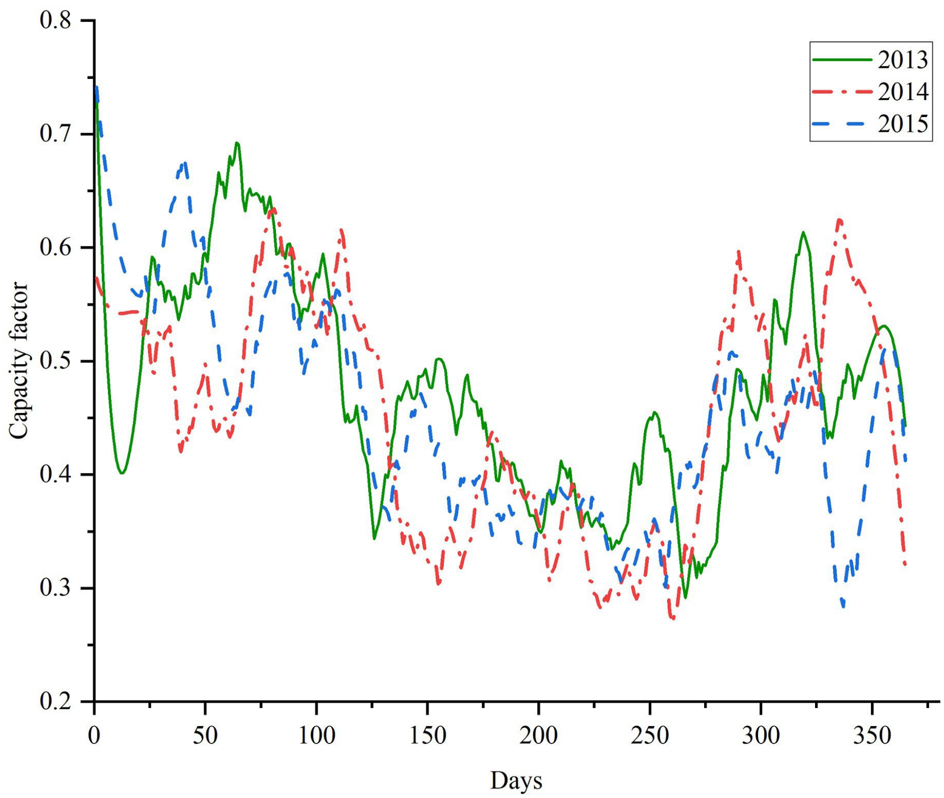

Figure 3.5: New York average daily WT capacity factor

3.3.8 Estimation of Austin solar PV capacity factor

The author of this thesis used again the four-step procedure presented in the literature review, Section 1.4, to estimate PV capacity factors (CF). The definitions for the parameters and variables used in the four-step procedure to estimate the PV capacity factors are listed in Appendix A Table 5.1. All the equations used for the estimation of the PV capacity factors were presented in Section 1.4. In the computations of the CF, P_{pv}^{Max} was assumed 160W, the efficiency, η, as 0.2, the PV size, A, equal to $1m^2$, and the solar PV operating temperature, T_0, as 45°C. Table 5.2 in Appendix A lists twenty weather condition or states along with the corresponding value for W_t. Note that W_t varies between 0 and 1 to mimic, for instance, a clear, a partly cloudy, or an overcasting day (Lave and Kleissl, 2011). Real weather conditions data collected hourly in different years for Austin (WeatherUnderground, 2019) was used to compute three different sets of hourly solar PV capacity factors (CF) for a lapse of 8760 hours (i.e. the whole year). The three different sets CF for Austin were computed using equation 1.13 and 26,280 observations (365 days*24 hours/day*3 sets) for the weather conditions. Table 3.10 presents the yearly statistics (i.e., mean, standard deviation, and median) and Figure 3.6 represents the graphical representation of the solar PV capacity factors of Austin.

Table 3.10: Austin solar PV capacity factor analysis

City	Year	Mean	St. Deviation	Median
Austin	2013	0.3273	0.1606	0.3263
	2014	0.2941	0.1534	0.2790
	2015	0.2766	0.1450	0.2742

3.3.9 Estimation of Boston solar PV capacity factor

Real weather conditions data collected hourly in different years for Boston (WeatherUnderground, 2019) was used to compute three different sets of hourly solar PV capacity factors (CF) for a lapse of 8760 hours (i.e. the whole year). The

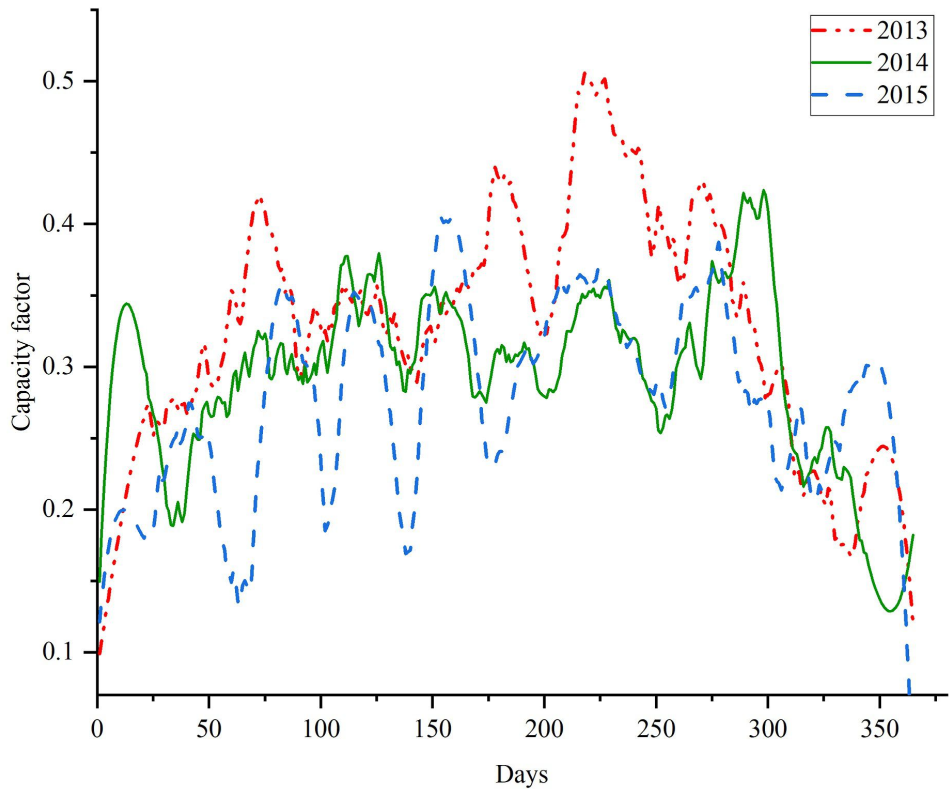

Figure 3.6: Austin average daily PV capacity factor

CF were computed using equation 1.13 and 26,280 observations (365 days*24 hours/day*3 sets) for the weather conditions. Table 3.11 presents the yearly statistics (i.e., mean, standard deviation, and median) and Figure 3.7 represents the graphical representation of the solar PV capacity factors of Boston.

Table 3.11: Boston solar PV capacity factor analysis

City	Year	Mean	St. Deviation	Median
Boston	2013	0.2453	0.1398	0.2276
	2014	0.2582	0.1578	0.2364
	2015	0.2618	0.1586	0.2319

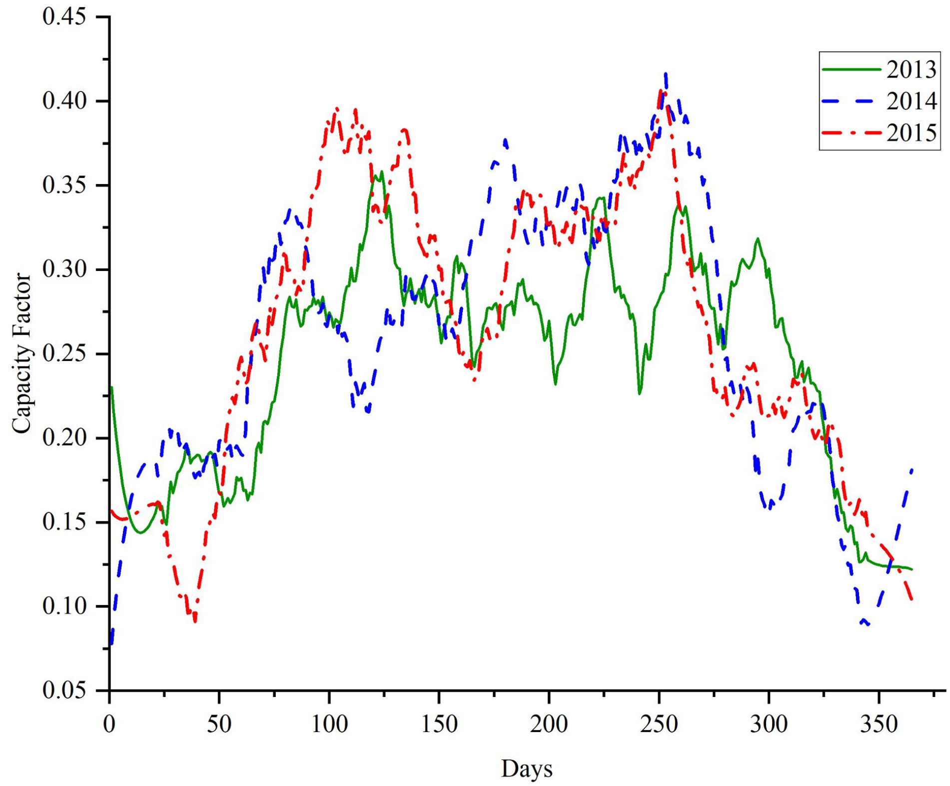

Figure 3.7: Boston average daily PV capacity factor

3.3.10 Estimation of Dallas solar PV capacity factor

Real weather conditions data collected hourly in different years for Dallas was used to compute three different sets of hourly solar PV capacity factors (CF) for a lapse of 8760 hours (i.e. the whole year). The CF were computed using equation 1.13 and 26,280 observations (365 days*24 hours/day*3 sets) for the weather conditions.

Table 3.12: Dallas solar PV capacity factor analysis

City	Year	Mean	St. Deviation	Median
Dallas	2013	0.2922	0.1503	0.2767
	2014	0.2671	0.1414	0.2339
	2015	0.2609	0.1264	0.2478

Table 3.12 presents the yearly statistics (i.e., mean, standard deviation, and

median) and Figure 3.8 represents the graphical representation of the solar PV capacity factors of Dallas.

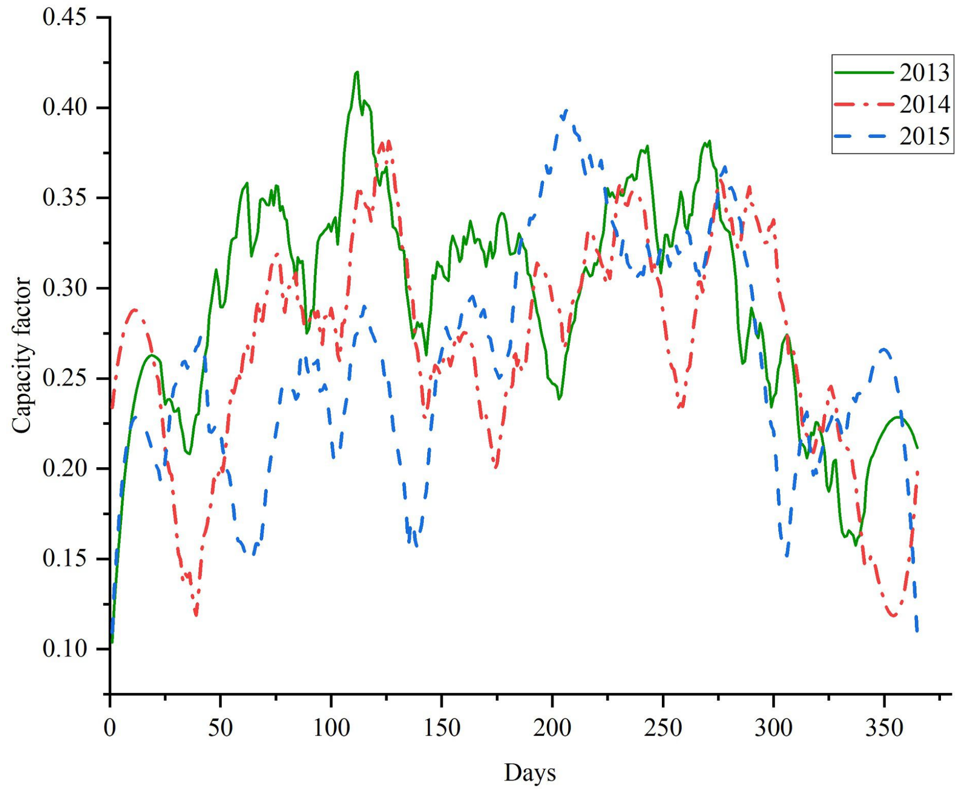

Figure 3.8: Dallas average daily PV capacity factor

3.3.11 Estimation of New York solar PV capacity factor

Real weather conditions data collected hourly in different years for New York (WeatherUnderground, 2019) was used to compute three different sets of hourly solar PV capacity factors (CF) for a lapse of 8760 hours (i.e. the whole year). The CF computed used equation 1.13 and 26,280 observations (365 days*24 hours/day*3 sets) for the weather conditions. Table 3.13 presents the yearly statistics (i.e., mean, standard deviation, and median) and Figure 3.9 represents the graphical representation of the solar PV capacity factors of New York.
All the figures presented in this section show that, for any given day, there is variability in the CF computed for the years 2013, 2014, and 2015. By including

Table 3.13: New York solar PV capacity factor analysis

City	Year	Mean	St. Deviation	Median
New York	2013	0.2277	0.1152	0.2105
	2014	0.2309	0.1304	0.2009
	2015	0.2328	0.1232	0.2077

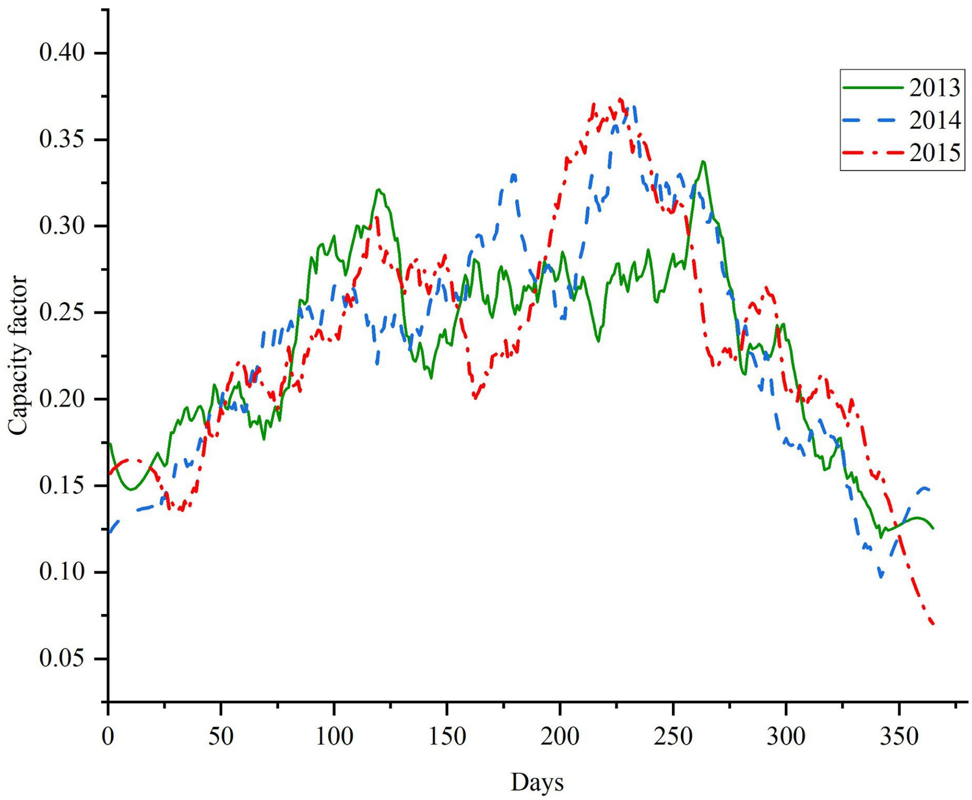

Figure 3.9: New York average daily PV capacity factor

these 3 sets of CF in the APP models, this variability is captured and it may produce more robust optimal solutions for the models.

Wind and solar generation can be classified into three categories: low if CF < 0.20, medium if $0.2 \leq$ CF < 0.40, and high if CF ≥ 0.40. Table 3.14 summarizes the climate statistics of the six cities selected for the research presented in this chapter. The statistics used all the CF computed for the years 2013 to 2015. The table indicates that all cities selected in this research, except Phoenix, have WT average capacity factors in the medium or high category. Besides, all cities have average PV

Table 3.14: Average capacity factor of WT and PV of six US cities

City	WT CF	CF category	PV CF	CF category
San Francisco	0.41	High	0.29	Medium
Austin	0.32	Medium	0.30	Medium
Boston	0.40	High	0.25	Medium
Phoenix	0.15	Low	0.37	Medium
Dallas	0.43	High	0.27	Medium
New York	0.46	High	0.23	Medium

Table 3.15: Median and standard deviation of WT and PV CF of six US cities

City	WT CF		PV CF	
	Median	St. Dev	Median	St. Dev
San Francisco	0.405	0.237	0.300	0.132
Austin	0.267	0.197	0.293	0.153
Boston	0.351	0.235	0.232	0.152
Phoenix	0.123	0.106	0.354	0.159
Dallas	0.380	0.247	0.253	0.139
New York	0.419	0.235	0.206	0.123

capacity factors in the medium category. Capacity factors for can be found in Appendix B. New York city hourly WT capacity factor figure can be found in Appendix B Figure 5.1.

3.4 Computational results - base case

The information provided in Section 2.5.1 in previous chapter regarding values for input parameters is also valid for this chapter. In the numerical experiments performed with the models in this chapter, demands for each of the two products (i.e., A and B) can be at any of two possible settings (i.e. low or high) over the time horizon. Machine and labor hour capacity can be at any of 3 settings each, and the are 3 sets of WT and PV capacity factors. Then the total number of scenarios in the models is $(2 \times 2 \times 3 \times 3 \times 3) = 108$ scenarios. The demand values for products A and B are generated from the probability distributions provided in Section 3.3.1. Tables 5.3 and 5.4 in Appendix B, list the set of actual values used for the demands for products A and B at the high and low levels. The values used for the machine and labor hour capacities in the model's scenarios are presented in Appendix B Table 5.10 to 5.13. All the values for the production and energy related parameters are listed in Appendix B table 5.14 to 5.15. The sources for assuming the values for RE related parameters are: capital cost of WT (Stehly et al., 2019), PV (NREL, 2021), tax incentive (WINDExchange, 2021), energy selling price (EIA, 2021), energy buying price (EIA, 2021), M&O costs of the WT, PV and the capital recovery factors for WT, PV and BS (Anderson et al., 2017).

The computational results in this chapter, are for Model 3 Island microgrid (IM) with BS and hourly granularity , labeled shortly as IM with BS, and for Model 4 - Prosumer microgrid with BS and hourly granularity, labeled shortly as Prosumer. The models were coded using the AMPL mathematical programming language and solved through the CPLEX solver. Table 3.16 presents the number of decision variables and constraints in each model. Because the models have a large number of decision variables and constraints it was necessary to run them in the Texas State University large memory nodes (1.5TB) in the LEAP cluster (LEAP, 2021). The LEAP Dell PowerEdge C6320 Cluster is configured with 120 compute nodes, each with 28 CPU cores via two (14-core) 2.4 GHz E5-2680v4 Intel Xeon (Broadwell) processors having 128 GB of memory and 400 GB of SSD storage per node (LEAP, 2021). Additionally, LEAP features two large memory (1.5 TB) nodes with 72 CPU cores via four(18-core) 2.4 GHz E7-8867 v4 Intel Xeon (Broadwell) processors. (LEAP, 2021). It was also necessary to follow the procedure for dealing with insufficient memory to run the CPLEX solver in AMPL available in "AMPL software website" (AMPL, 2021). The procedure decouples the three following steps: (1) generation of .nl file by AMPL, (2) solution of the model in .nl format by CPLEX, and (3) translation of the solution file generated by CPLEX using AMPL.

Table 3.16: Comparison of decision variables and constraints

Model - hourly granularity	Decision variables	Constraints
IM with BS	11,376,738	120,956,094
Prosumer	17,053,218	126,632,574

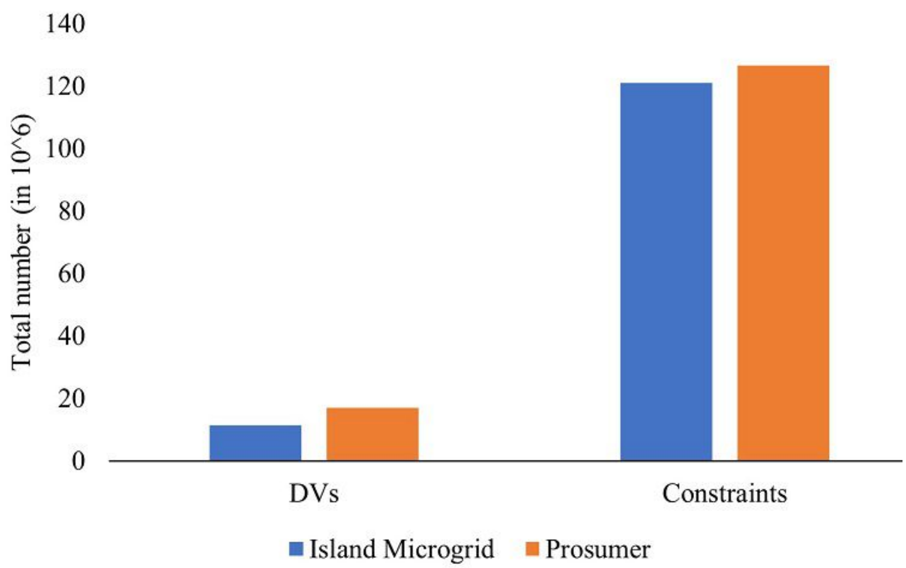

Figure 3.10: Decision variables and constraints

Besides the total expected annual costs of the models, the levelized cost of energy (LCOE) is also computed as a performance measure to compare the models. The way the LCOE is computed for Models 3 and 4 in this chapter is the same as for the island model and prosumer models in the previous chapter. It was explained in the numerical results, section 2.6 in previous chapter and thus this explanation is dropped from this chapter.

3.4.1 Levelized cost of energy (LCOE)

The levelized cost of energy is defined as the cost of producing one MWh of energy. It is considered as the main indicator to decide if a renewable energy project is attractive or not compared to the conventional sources of energy. Since the range for the actual cost of traditional sources of energy is $50-$100 per MWh, the goal is to obtain LCOE within this range. Table 3.17 presents the resulting LCOE's for the 2 implemented models.

Table 3.17: Levelized cost of energy

Model - hourly granularity	LCOE	Unit
IM with BS	80.86	$/MWh
Prosumer	38.73	$/MWh

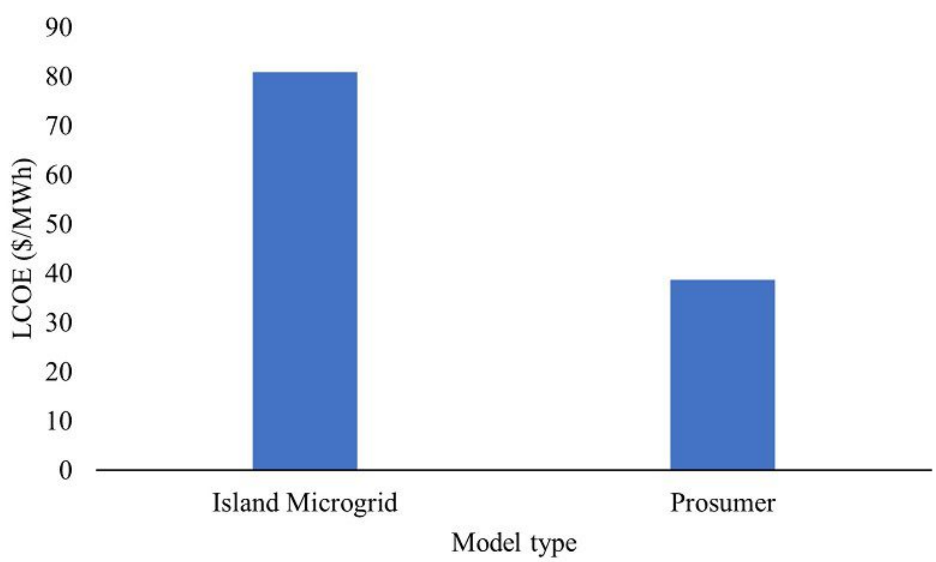

Figure 3.11: Levelized cost of energy

Table 3.17 shows that all models have LCOE's below the $50-$100 cost range for non-renewable energy. It also shows that the prosumer model has the lowest LCOE and that the magnitude of this value is much lower than the one for the IM with BS model. These LCOE results reveal that for both cases it is cheaper to operate the facilities with RE installation rather than purchasing energy from a main grid.

3.4.2 Energy production comparison

The total energy production (MWh/year) over the whole planning horizon for all the models is shown in table 3.18. The prosumer model produced less energy than the island microgrid one. The main reason behind producing less energy is that the prosumer model now can buy energy from the outside energy sources.

Table 3.18: Energy production

Model - hourly granularity	Factory	Warehouse	Total
IM with BS	337,573	594,187	931,760
Prosumer	75,273	329,411	404,684

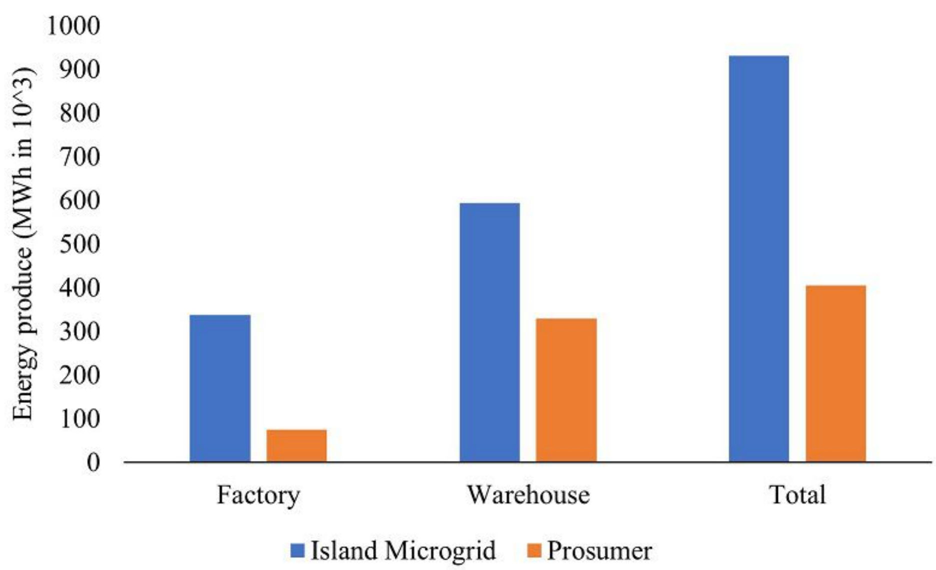

Figure 3.12: Energy production comparison

The amount of energy bought by the prosumer model at the factories and warehouses is 17,897 MWh and 63,824 MWh, respectively and it totals to 81,722 MWh. Furthermore, the amount of energy sold by the prosumer model at the factories and warehouses is 38,770 MWh and 213,966 MWh, respectively and it totals to 252,736 MWh.

3.4.3 Cost comparison

In the annual expected cost comparison, the prosumer model outperforms the island microgrid model. Detailed results are in Table 3.19 . Model IM with BS has higher annual expected total cost than the prosumer model. The cost of the prosumer model is 57.42% lower than the IM with BS.

Table 3.19: Annual cost breakdown

Cost element	IM with BS	Prosumer
Materials Cost	\$ 19,897,032	\$ 19,937,944
Energy Cost	\$ 75,339,170	\$ 18,840,457
Backorder Cost	\$ 486,545	\$ 459,496
Transportation Cost	\$ 1,152,740	\$ 1,186,850
Subcontracting Cost	\$ 2,910,350	\$ 2,065,430
Inventory Cost	\$ 0	\$ 0
Total	\$ 99,785,837	\$ 42,490,176

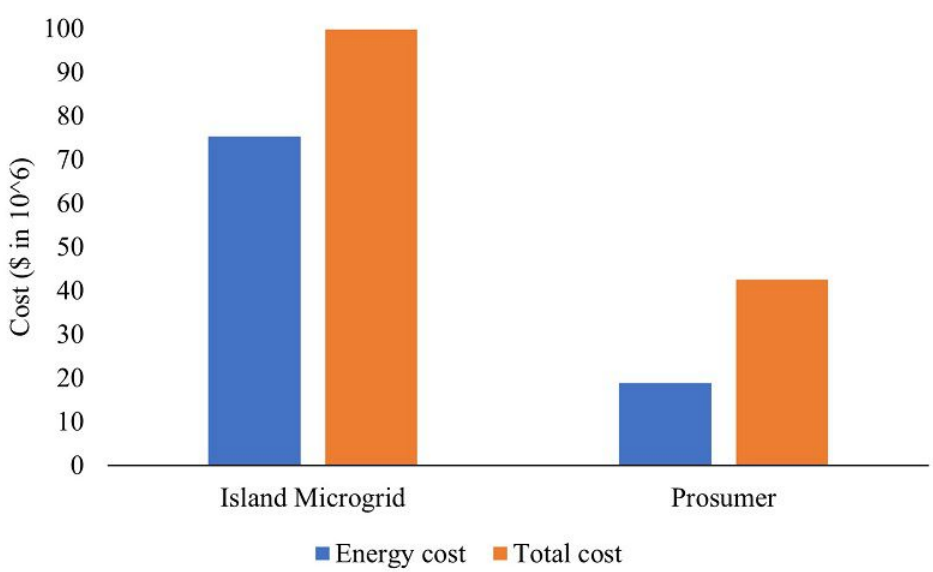

Figure 3.13: Energy cost and total cost comparison

The energy costs of the IM with BS and prosumer model are $\$75,339,170$ and

$18,840,457 which is 75.5% and 44.34%, respectively of the total cost. This result show that it is very significant to chose a prosumer model over an IM model.

3.4.4 Technology installation at factory

The technology installation at San Francisco, Austin and Boston over the whole planning horizon is shown in Table 3.20.

Table 3.20: Technology installation at factory

City	Model- hourly granularity	WT	PV	Total
San Francisco	IM with BS	26.26	41.29	67.55
	Prosumer	4.93	5.68	10.61
Austin	IM with BS	11.58	8.36	19.94
	Prosumer	5.17	5.78	10.94
Boston	IM with BS	17.96	71.65	89.61
	Prosumer	6.83	2.73	9.56

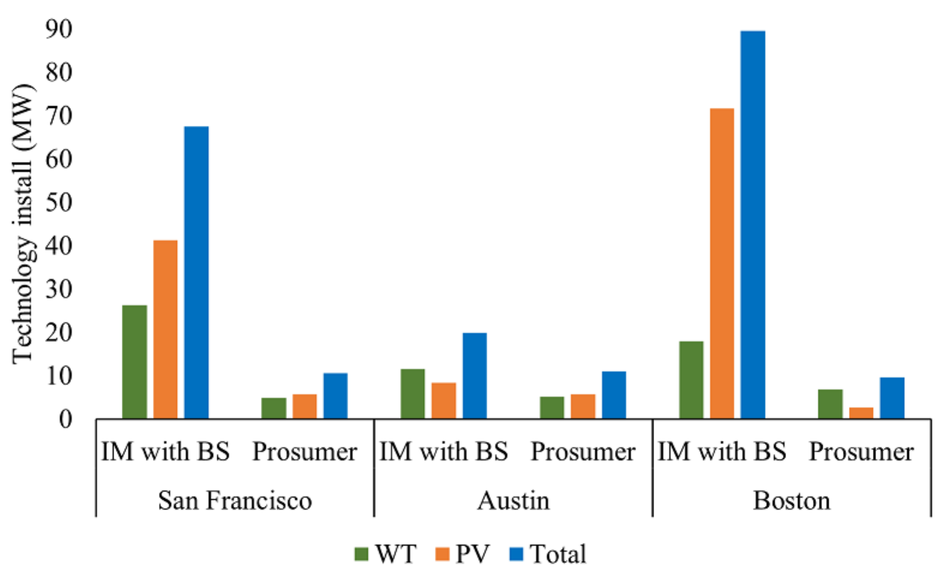

Figure 3.14: Technology installation at factory

The IM with BS model always installs overall more RE capacity than the prosumer model. It is because the IM with BS model needs to meet the energy demand by itself whereas the prosumer model can buy energy from main grid. Though San Francisco has better WT capacity factors than PV capacity factors, all models install more PV than WT capacity. The main reason for this result is that the PV has carbon incentive of \$25/MWh and the PV installation cost is less than the WT installation cost. These differences significantly influence the selection of PV over WT. For Boston, the prosumer model prefers to install more WT than PV because of the strong wind speed in this city favours the high production of RE to be sold. However, IM prefers to install more PV than WT because of the PV installation cost and PV carbon incentive of \$25/MWh.

3.4.5 Technology installation at warehouse

The technology installation at Phoenix, Dallas and New York over the whole planning horizon is shown in Table 3.21.

Table 3.21: Technology installation at warehouse

City	Model - hourly granularity	WT	PV	Total
Phoenix	IM with BS	21.52	121.85	143.37
	Prosumer	0	80.46	80.46
Dallas	IM with BS	27.49	68.40	95.89
	Prosumer	22.36	9.52	31.89
New York	IM with BS	31.07	51.56	82.63
	Prosumer	24.39	1.70	26.09

The IM with BS model always installs overall more RE capacity than the the prosumer model. It is because the IM with BS model needs to meet the energy demand by itself whereas the prosumer model can buy energy from main grid. For New York, the prosumer model prefers to install more WT than PV because of strong wind speed. However, the IM with BS model prefers to install more PV than WT because of lower PV installation cost and PV carbon incentive of \$25/MWh.

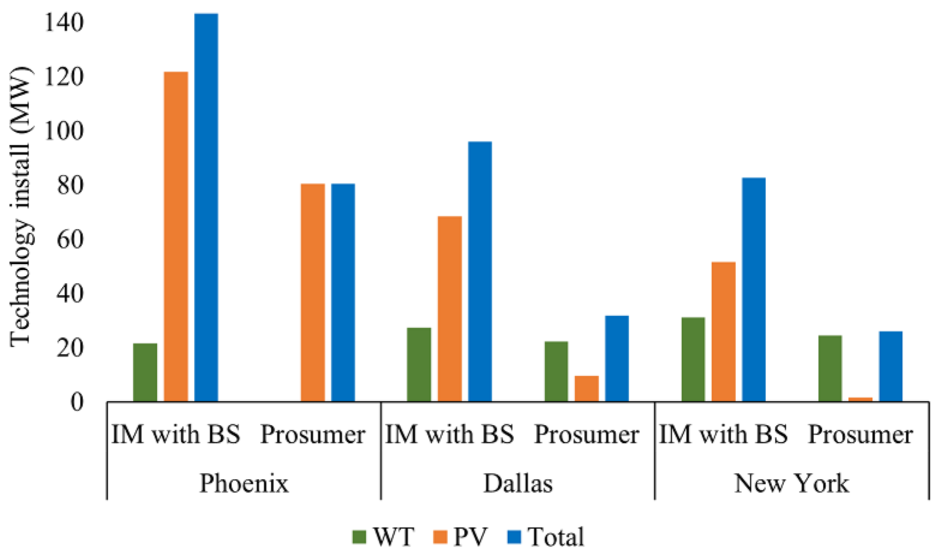

Figure 3.15: Technology installation at warehouse

3.4.6 BS installation at Factory

The BS installation at San Francisco, Austin and Boston over the whole planning horizon is shown in Table 3.22. The IM with BS model always installs BS whereas the prosumer model does not install BS. It is because the IM with BS model needs to meet the energy demand by itself whereas the prosumer model can buy energy from main grid and installing BS is not cost effective in this scheme (i.e., WT cost 1.5M \$/MW, PV cost 1.0M \$/MW, BS cost 0.5M \$/MWh, Carbon incentive 25 \$/MWh).

Table 3.22: BS installation at factory

City	Model- hourly granularity	BS
San Francisco	IM with BS	57.3
	Prosumer	0
Austin	IM with BS	57.3
	Prosumer	0
Boston	IM with BS	57.3
	Prosumer	0

3.4.7 BS installation at warehouse

The BS installation at Phoenix, Dallas and New York over the whole planning horizon is shown in Table 3.23. The IM with BS model always installs BS whereas the prosumer model does not install BS. It is because the IM with BS model needs to meet the energy demand by itself whereas the prosumer model can buy energy from main grid and installing BS is not cost effective in this scheme (i.e., WT cost 1.5M $/MW, PV cost 1.0M $/MW, BS cost 0.5M $/MWh, Carbon incentive 25 $/MWh).

Table 3.23: BS installation at warehouse

City	Model- hourly granularity	BS
San Francisco	IM with BS	91.7
	Prosumer	0
Austin	IM with BS	91.7
	Prosumer	0
Boston	IM with BS	91.7
	Prosumer	0

This chapter presented two-stage stochastic APP models that integrate RE (i.e., WT, PV, and BS) and consider hourly granularity to satisfy the energy requirements. The models were scaled up to consider that the company or supply chain operates multiple factories and multiple warehouses in different geographical locations. Two instances, island model (IM) with BS and prosumer are contrasted. The computational results show that the models proposed are tractable. The LCOE's for both models are affordable (i.e., $80.86/MWh for the IM with BS model and $38.73/MWh for the prosumer model). The LCOE of the prosumer model is 47.88% lower that the LCOE of the IM with BS model. The results in this chapter confirm the ones obtained in Ch. 2 regarding the cost advantages of the prosumer model if compated to an island model.

4. APP CONSIDERING HOURLY TOU

The problem researched in the first four sections of this chapter is an enhancement to the one researched in Chapter 3 and depicted in Figure 3.1. The enhancement is that in this chapter it is assumed that the company adopting the microgrid systems will operate under a time of use (TOU) energy rate plan under an agreement with the utility company. Then, the Model 4 - Prosumer microgrid with BS, without TOU, and daily granularity presented in the previous chapter is slightly modified. It will permit to assess the economical effect of a TOU plan for the manufacturing company installing the WT, PV, and BS microgrid system. In recent years, energy-intensive manufacturing industries are highly impacted by rising electricity costs. To handle this challenge, many energy suppliers have begun to implement the TOU strategy. TOU represents a huge opportunity to reduce electricity costs by shifting electricity usage from on-peak hours to off-peak or mid-peak hours. Time-of-use (TOU) electricity pricing has been implemented in many countries around the globe to encourage manufacturers to shift their electricity usage from peak periods to off-peak periods and ultimately alleviate the grid's burden during peak hours (Ding et al., 2015). Wang and Li (2013) study TOU in a production scheduling problem to minimize electricity consumption and costs under the constraint of meeting the production target during peak periods. Zhang et al. (2014) propose a time indexed integer programming formulation for an energy-conscious flow shop scheduling problem that looks to minimize electricity cost and the carbon footprint under TOU tariffs and without compromising production throughput. Fang et al. (2016) consider the time-of-use tariffs for solving the single machine scheduling problem while minimizing total electricity cost. Che et al. (2016) develop an efficient greedy insertion heuristic method for solving a

continuous time mixed-integer linear programming (MILP) model under time-of-use tariffs. Che et al. (2017) consider an unrelated parallel machine scheduling problem under the TOU tariffs to minimize the total electricity cost. After reviewing the time-of-use tariffs literature the author of this thesis found that most of the TOU tariffs application is in the field of scheduling problem. At the best of the author's knowledge, this thesis will be the first endeavour to implement TOU tariffs in an aggregate production planning problem that integrates onsite renewable microgrid to reduce carbon emissions in manufacturing and supply chain settings.
The research in this chapter aims to solve the following questions:

- Given that the facilities must satisfy energy requirements on an hourly basis, what is the effect brought to the manufacturing company if it engages in a time of use (TOU) energy rate? Is it still feasible to decarbonize the manufacturing operations and warehouse facilities with RE integration?

- If the facilities must satisfy energy requirements on an hourly basis and operate under TOU, is it still feasible to integrate microgrids coupled with WT, PV, and BS into the manufacturing and warehouse operations with affordable levelized cost of energy (LCOE)?

- What is the value of solving the APP with RE problem using two-stage stochastic programming instead of a deterministic modeling approach?

- What are differences in expected cost and LCOE values for all the models studied in this thesis work?

This chapter is organized as follows. Section 4.1 presents the mathematical formulation of Model 5 - Prosumer microgrid with BS and TOU - hourly granularity. The formulation is a extensive formulation of a two-stage stochastic program with recourse. Section 4.2 provides Model 5 computational results for the base case. Section 4.3 presents the sensitivity analysis performed on some of Model 5 parameters through design of experiments (DOE). Section 4.4 presents the statistical analysis of the DOE. Section 4.5 presents the computations of the value of the stochastic solution (VSS) for the prosumer models with BS and hourly granularity with and without TOU (i.e., Model 4 presented in previous chapter and Model 5 presented in this chapter) . Finally, Section 4.6 compares all the models researched in this thesis. Because the stochastic programming methodology explained in Section 2.2 also applies to the model presented Section 4.1 no methodology section is included in this chapter. Also, the procedures to compute the capacity factors (CF) for wind turbines (WT) and solar photovoltaics (PV) and to represent the uncertain parameters: product demand, machine and labor hours capacity are skipped since they correspond to the ones described in Section 3.3.

4.1 Prosumer model with BS and TOU - hourly granularity

As in the previous chapter, the set H is represents the hours of the year. All the other sets used are the same listed in Table 2.1 in Chapter 2. The notation for decision variables and parameters in Tables 2.2 to 2.4, and 3.1 to 3.2 also apply for this model. The additional parameter u_h^+ for this model defined in Table. TOU is considered only for purchasing energy from main grid. On-peak hours and off-peak hours are assumed from 8:01 AM to 8:00 PM and 8:01 PM to 8:00 AM, respectively. The values for purchasing energy in off-peak hours and on-peak hours are shown in Appendix B 5.15. The model is as follows.

Table 4.1: Parameters

Notation	Description	Unit
u_h^+	Cost of purchasing energy from main grid in hour h	\$/MWh

Model 5 - Prosumer microgrid with BS and TOU - hourly granularity:

$$\min \quad Z = \sum_{i\in I}\sum_{k\in K}\sum_{t\in T}(c^x_{it}+c^w_{it})x_{ikt} + \sum_{i\in I}\sum_{k\in K}\sum_{t\in T}(c^m_{it}m_{ikt}+c^r_{it}r_{ikt})+$$

$$\sum_{k\in K}\sum_{t\in T}(c_l l_{kt}+c_h h_{kt}+c_f f_{kt}) + \sum_{t=1}^{T}\sum_{i\in I}\sum_{k\in K}\sum_{s\in S}p(s)(c^b_{it}b_{ikts}+c^q_{it}q_{ikts})+$$

$$\sum_{t=1}^{T}\sum_{i\in I}\sum_{n\in N}\sum_{s\in S}p(s)c^y_{it}y_{ints} + \sum_{k\in K}\sum_{g\in G}\phi_g a_g P^c_{kg} + \sum_{n\in N}\sum_{g\in G}\phi_g a_g P^c_{ng}+$$

$$\sum_{k\in K}\phi_b a_b B^c_k + \sum_{n\in N}\phi_b a_b B^c_n + \sum_{k\in K}\sum_{g\in G}\sum_{s\in S}p(s)(b_g-c_g)(\sum_{h\in H}\frac{\lambda_{gjhks}}{|H|})P^c_{kg}+$$

$$\sum_{n\in N}\sum_{g\in G}\sum_{s\in S}p(s)(b_g-c_g)(\sum_{h\in H}\frac{\lambda_{gjhns}}{|H|})P^c_{ng} - \sum_{k\in K}\sum_{j\in J}\sum_{h\in H}\sum_{s\in S}p(s)u^-Q^-_{kjhs}+$$

$$\sum_{k\in K}\sum_{j\in J}\sum_{h\in H}\sum_{s\in S}p(s)u^+_h Q^+_{kjhs} - \sum_{n\in N}\sum_{j\in J}\sum_{h\in H}\sum_{s\in S}p(s)u^-Q^-_{njhs}+$$

$$\sum_{n\in N}\sum_{j\in J}\sum_{h\in H}\sum_{s\in S}p(s)u^+_h Q^+_{njhs} \tag{4.1}$$

$s.t.$

$$y_{int-1} - y_{ints} + x_{ikt} + q_{ikts} - b_{ikt-1} + b_{ikts} - m_{ikt} + r_{ikt} = D_{ikts}$$

$$\forall i\in I, t=1, \forall k\in K, \forall n\in N, \forall s\in S \tag{4.2}$$

$$y_{int-1s} - y_{ints} + x_{ikt} + q_{ikts} - b_{ikt-1s} + b_{ikts} - m_{ikt} + r_{ikt} = D_{ikts}$$

$$\forall i\in I, \forall t\in T\backslash\{1\}, \forall k\in K, \forall n\in N, \forall, \forall s\in S \tag{4.3}$$

$$\sum_{i\in I}(e^x_i + q^v d_{kn} w_i)\frac{x_{ikt}}{\xi|J_t|} + L_k + q^v\beta_h d_{kn} m^v + B^f_{kjhs} - B^f_{kjh-1} + Q^-_{kjhs}$$

$$= \sum_{g\in G}\lambda_{gjhks}P^c_{kg} + Q^+_{kjhs}$$

$$j=1, h=1, t=1, \forall k\in K, \forall n\in N, \forall s\in S \tag{4.4}$$

$$\sum_{i\in I}(e^x_i + q^v d_{kn} w_i)\frac{x_{ikt}}{\xi|J_t|} + L_k + q^v\beta_h d_{kn} m^v + B^f_{kjhs} - B^f_{kjh-1s} + Q^-_{kjhs}$$

$$= \sum_{g\in G}\lambda_{gjhks}P^c_{kg} + Q^+_{kjhs}$$

$$\forall t\in T, \forall j\in J, \forall h\in H\backslash\{1\}, \forall k\in K, \forall n\in N, \forall s\in S \tag{4.5}$$

Model 5 - Prosumer microgrid with BS and TOU - hourly granularity continue

$$\sum_{i\in I} e_i^f y_{ints}(\frac{h-\sum_{v=1}^{t-1}|J_v\delta|}{|J_t|\delta}) + L_n + q^v\beta_h d_{nk} m^v + B_{njhs}^f - B_{njh-1}^f + Q_{njhs}^-$$
$$= \sum_{g\in G} \lambda_{gjhns} P_{ng}^c + Q_{njhs}^+$$
$$j=1, h=1, t=1, \forall k\in K, \forall n\in N, \forall s\in S \tag{4.6}$$

$$\sum_{i\in I} e_i^f y_{ints}(\frac{h-\sum_{v=1}^{t-1}|J_v\delta|}{|J_t|\delta}) + L_n + q^v\beta_h d_{nk} m^v + B_{njhs}^f - B_{njh-1s}^f + Q_{njhs}^-$$
$$= \sum_{g\in G} \lambda_{gjhns} P_{ng}^c + Q_{njhs}^+$$
$$\forall t\in T, \forall j\in J, \forall h\in H\backslash\{1\}, \forall k\in K, \forall n\in N, \forall s\in S \tag{4.7}$$

$$\sum_{i\in I} a_i x_{ikt} = l_{kt}$$
$$\forall k\in K, \forall t\in T \tag{4.8}$$

$$l_{kt} \leq LH_{kts}^{max}$$
$$\forall k\in K, \forall t\in T, \forall s\in S \tag{4.9}$$

$$l_{kt} = l_{kt-1} + h_{kt} - f_{kt}$$
$$\forall k\in K, \forall t\in T \tag{4.10}$$

$$h_{kt} + f_{kt} \leq \alpha l_{kt-1}$$
$$\forall k\in K, \forall t\in T \tag{4.11}$$

$$\sum_{i\in I} u_i x_{ikt} = w_{kt}$$
$$\forall k\in K, \forall t\in T \tag{4.12}$$

Model 5 - Prosumer microgrid with BS and TOU - hourly granularity continue

$$w_{kt} \leq MH_{kts}^{max} \qquad \forall k \in K, \forall t \in T, \forall s \in S \tag{4.13}$$

$$w_{kt} = w_{kt-1} + o_{kt} - p_{kt} \qquad \forall k \in K, \forall t \in T \tag{4.14}$$

$$\nu x_{ikt} = m_{ikt} \qquad \forall k \in K, \forall i \in I, \forall t \in T \tag{4.15}$$

$$\eta m_{ikt} = r_{ikt} \qquad \forall k \in K, \forall i \in I, \forall t \in T \tag{4.16}$$

$$0 \leq m_{ikt} - r_{ikt} \leq m_{ikt}^{max} \qquad \forall i \in I, \forall k \in K, \forall t \in T \tag{4.17}$$

$$\sum_{i \in I} y_{ints} \leq WH_t^{max} \qquad \forall n \in N, \forall t \in T, \forall s \in S \tag{4.18}$$

$$0 \leq P_{kg}^c \leq P_{kg}^{max} \qquad \forall k \in K, \forall g \in G \tag{4.19}$$

$$0 \leq P_{ng}^c \leq P_{ng}^{max} \qquad \forall n \in N, \forall g \in G \tag{4.20}$$

$$B_k^c \leq B_k^{max} \qquad \forall k \in K \tag{4.21}$$

$$B_n^c \leq B_n^{max} \qquad \forall n \in N \tag{4.22}$$

$$0 \leq B_{kjhs}^f \leq B_k^c \qquad \forall k \in K, \forall s \in S, j \in J_t, h \in H \tag{4.23}$$

$$0 \leq B_{njhs}^f \leq B_n^c \qquad \forall n \in N, \forall s \in S, j \in J_t, h \in H \tag{4.24}$$

$$B_{k0}^f = B_k^c \qquad \forall k \in K, j = 0 \tag{4.25}$$

$$B_{n0}^f = B_n^c \qquad \forall n \in N, j = 0 \tag{4.26}$$

$$Q_{kjhs}^- \leq Q_{kjhs}^{max} \qquad \forall k \in K, j \in J, h \in H, s \in S \tag{4.27}$$

$$Q_{njhs}^- \leq Q_{njhs}^{max} \qquad \forall n \in K, j \in J, h \in H, s \in S \tag{4.28}$$

$$x_{ikt}, m_{ikt}, r_{ikt} \geq 0 \qquad \forall i \in I, \forall k \in K, \forall t \in T \tag{4.29}$$

$$h_{kt}, f_{kt}, l_{kt}, w_{kt}, p_{kt} \geq 0 \qquad \forall k \in K, \forall t \in T \tag{4.30}$$

$$b_{ikts}, q_{ikts} \geq 0 \qquad \forall i \in I, \forall k \in K, \forall t \in T, \forall s \in S \tag{4.31}$$

$$y_{ints} \geq 0 \qquad \forall i \in I, \forall n \in N, \forall t \in T, \forall s \in S \tag{4.32}$$

The explanation of the objective function and constraints for the Model 5 - Prosumer microgrid with BS and TOU - hourly granularity presented above is exactly the same as the ones provided for Model 4 - Prosumer microgrid with BS, without TOU, and hourly granularity, and Model 2 - Prosumer microgrid with BS and daily granularity. However, in the objective function of Model 5, the subscript h is added to the energy purchasing cost u_h^+ parameter used in the sums involving the energy purchasing decision variables Q_{kjhs}^+ and Q_{njhs}^+.

4.2 Computational results - base case

The information provided in Section 2.5.1 regarding values for model's input parameters is also valid for this chapter. Model 5 - Prosumer microgrid with BS and TOU - hourly granularity was coded using the AMPL mathematical programming language and solved through the CPLEX solver. The total number of scenarios in the Models is also 108 as detailed in the computational results section in previous chapter. The demand values for products A and B are generated from the probability distributions provided in Section 3.3.1. Tables 5.3 and 5.4 in Appendix B, list the set of actual values used for the demands for products A and B at the high and low levels. The values used for the machine and labor hour capacities in the model's scenarios are presented in Appendix B Table 5.10 to 5.13. Table 4.2 presents the number of decision variables and constraints in the model.

Table 4.2: Comparison of decision variables and constraints

Case	Total
Decision variables	17,053,218
Constraints	126,632,574

As mentioned in the previous section, TOU is considered only for purchasing energy from main grid. On-peak hours and off-peak hours are assumed from 8:01 AM to

8:00 PM and 8:01 PM to 8:00 AM, respectively. Besides the total expected annual costs of the model, the levelized cost of energy (LCOE) is also computed as a performance measure.

4.2.1 Levelized cost of energy (LCOE)

The levelized cost of energy is defined as the cost of producing one MWh of energy. It is considered as the main indicator to decide if a renewable energy project is attractive or not compared to the conventional sources of energy. Since the range for the actual cost of traditional sources of energy is $50-$100 per MWh, the goal is to obtain LCOE within this range. The resulting LCOE's for Model 5 - prosumer microgrid with BS, TOU - hourly granularity is $36.29, which is below the $50-$100 cost range for non-renewable energy. Thus, this resulting LCOE shows that Model 5 is feasible to decarbonize the company operations. It is cheaper to operate the facilities under the energy prosumer mode than relying entirely on conventional energy from the main grid.

4.2.2 Energy production, buy and sell comparison

The total energy production (MWh/year) over the whole planning horizon for the Model 5 - prosumer microgrid with BS, TOU - hourly granularity is shown in Table 4.3. From Table 4.3 it is evident that the prosumer hourly model with TOU tariffs prefers to sell RE rather than buy conventional energy because of the favourable weather conditions for the onsite renewable installation.

Table 4.3: Energy production, buy and sell

Case	Factories	Warehouses	Total
Total energy produce	58,435	273,176	331,611
Total energy buy	21,515	68,707	90,222
Total energy sell	25,553	162,620	188,173

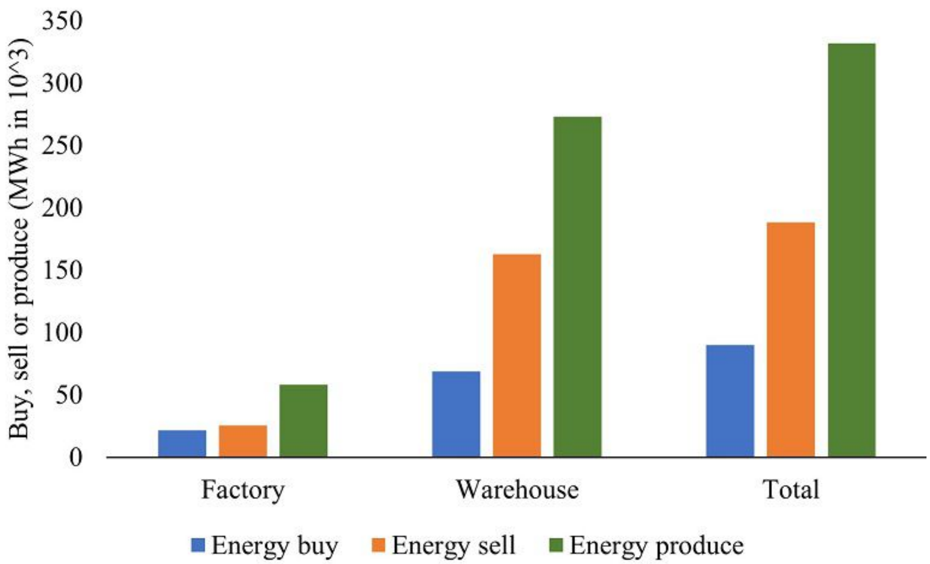

Figure 4.1: Energy produced, bought and sold

4.2.3 Technology installation at factory

The technology installation at San Francisco, Austin, and Boston over the whole planning horizon is shown in Table 4.4.

Table 4.4: Technology installation at factory

City	WT	PV	Total
San Francisco	2.92	6.61	9.53
Austin	2.99	7.05	10.04
Boston	4.85	3.59	8.44

Though San Francisco has better WT capacity factors than PV capacity factors, San Francisco and Austin install more PV than WT capacity. The main reason for this result is that the PV has carbon incentive of $25/MWh and the PV installation cost is less than the WT installation cost. Those factors have significant influence on the company's decision to chose PV over WT. For Boston, the model prefers to install more WT than PV because of strong wind speed. Though San Francisco has higher WT capacity factor than PV, it ended installing less WT than Boston because San Francisco has higher PV capacity factor than Boston.

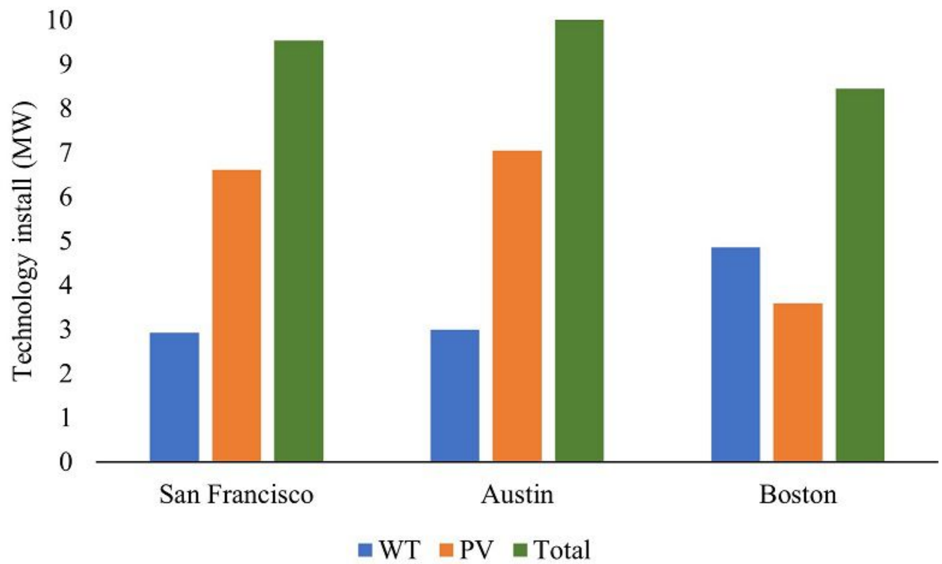

Figure 4.2: Technology installation at factory

4.2.4 Technology installation at warehouse

The technology installation at Phoenix, Dallas and New York over the whole planning horizon is shown in table 4.5.

Table 4.5: Technology installation at warehouse

City	WT	PV	Total
Phoenix	0	71.43	71.43
Dallas	15.20	12.60	27.80
New York	19.06	5.50	24.56

In Phoenix, the prosumer Model 5 does not install WT because the PV factor is much higher than the WT capacity factor and PV has low installation cost than WT. Despite of higher installation cost of WT, the prosumer model installs more WT than PV in Dallas and New York. This is because in Dallas and New York the WT capacity factor is higher than the PV capacity factor.

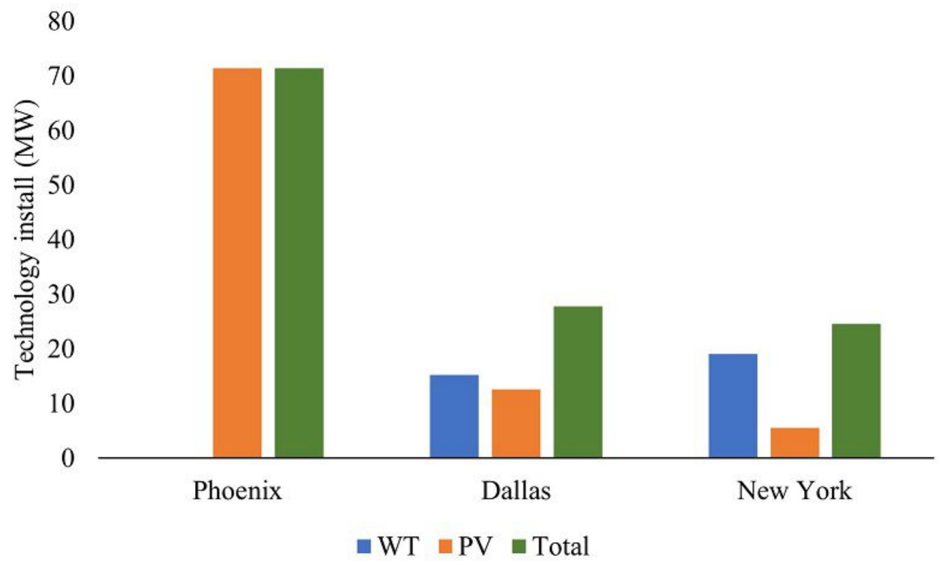

Figure 4.3: Technology installation at warehouse

4.2.5 Cost comparison

Detailed results of Model 5 costs elements are presented in Table 4.6. The proposed thesis work is focusing on energy intensive manufacturing companies. For Model 5, the resulting expected energy cost as percentage of the expected total cost is 39%.

Table 4.6: Annual cost breakdown

Cost element	Cost amount	Percentage
Materials Cost	\$ 19,937,944	51%
Energy Cost	\$ 15,309,347	39%
Backorder Cost	\$ 459,472	1%
Transportation Cost	\$ 1,186,850	3%
Subcontracting Cost	\$ 2,065,290	5%
Inventory Cost	\$ 0	0%
Total	\$ 38,958,903	100%

4.3 Sensitivity analysis using DOE

Sensitivity analysis determines how changes in model parameters impacts the output of a model. An efficient way to perform sensitivity analysis is through statistical design of experiments (DOE). In this chapter, a DOE is performed with the Model 5 - prosumer microgrid with BS, TOU - hourly granularity. A full four factorial design is performed to identify the critical factors affecting different model results. The factors considered in the DOE are type of demand distribution for the products, PV installation cost, carbon incentives for PV, battery cost, and probability distribution for the 108 scenarios included in the model. The number of levels for each of these factors mentioned is 2, 3, 3, 3 and 2, respectively. One replication or run was performed in each experimental condition. Hence, the DOE required to solve the prosumer model $2 \times 3 \times 3 \times 3 \times 2 = 108$ times and each run will be named a case in the reminder of this document. Note that it is just as a coincidence that the number of scenarios included in the model is 108 and the number of experimental runs in the DOE is also 108. It is also a coincidence that the number of runs in the DOE in this chapter ended equal to the number of runs for the DOE presented in Chapter 2.

The levels selected for each of the factors included in the DOE are as explained as follows. The DOE considers two types of product demand distribution: triangular distribution (mode value is 7% lower than the mean value of the discrete uniform distribution assumed in the base case, mode value is 7% higher than the mean value of the discrete uniform distribution assumed in the base case), three PV cost values ($1,000,000/MW; $750,000/MW and $500,000/MW), three types of carbon incentive ($30/MWh, $20/MWh and $10/MWh), three levels of BS cost ($500,000/MWh, $300,000/MWh and $150,000/MWh) and two levels for the probability distribution of the model scenarios. The levels for the mentioned factors are summarized Appendix B Table 5.17. The levels used for the probability distribution of the model scenarios were assigned after classifying each of the 108 scenarios included in the two-stage stochastic model into 3 categories labeled as low, medium and high. The classification is based on the total sum of the rankings given to product demands, machine and labor hours available in the scenario. A total of 22 scenarios were classified as low, 64 in the medium category and 22 in the high one. Level 1 corresponds to a pessimistic case where the 22 scenarios falling under the low category have about 80% probability of occurrence and the medium and high categories have equal probabilities. Level 2 is an optimistic case where the 22 scenarios falling under the high category have about 80% probability of occurrence and the medium and low categories have equal probabilities. Note that the base case analyzed in the previous section is Case 1, where the product demand follows discrete uniform distribution, PV cost $1,000,000/MW, PV carbon incentive $25/MWh, BS cost $500,000 /MWh, probability distribution (0.2037, 0.5926, 0.2037).

4.3.1 Total cost comparison

Figure 4.4 shows that case 75 (probability distribution for scenarios: L 0.7995, M 0.1088, H 0.0917, probability distribution for product demands: Product A and Product B follows triangular distribution where mean is -7% below than the base case (PV cost $500,000/MW and PV incentives $30/MWh) has the lowest expected cost ($47,921). This case has high probabilities for the scenarios categorized as low, product demand follows triangular distribution where the mean is 7% lower than the base case, the PV cost is at the lowest value assumed and the PV costs incentives are at the highest value assumed. Since some of these, especially the last two, are favorable conditions, it explains the resulting lower expected cost.
On the other hand, case 26 (probability distribution for scenarios: L 0.0917, M

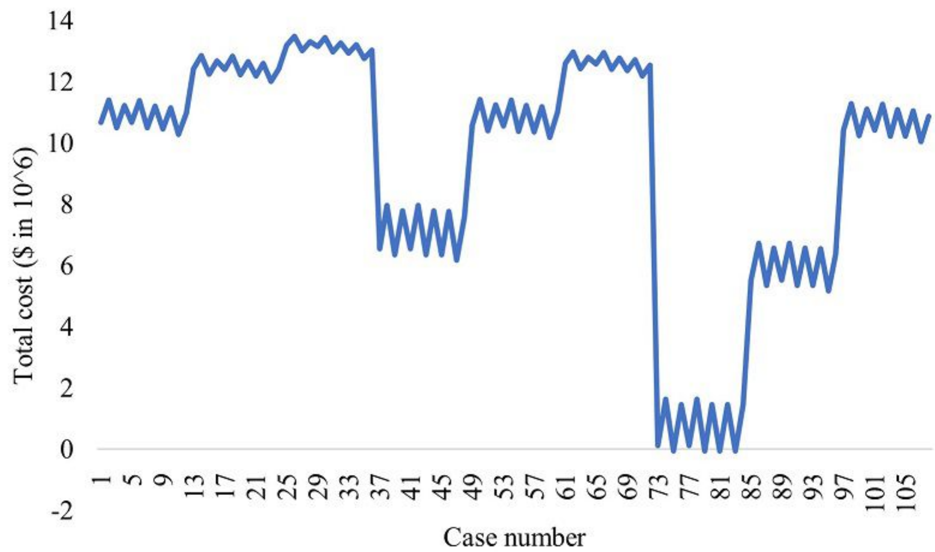

Figure 4.4: Total cost comparison

0.1088, H 0.7995, probability distribution for product demands: Product A and Product B follows triangular distribution where mode is +7% higher than base case, PV installation cost \$1,000,000/MW and PV incentives \$10/MWh) has the highest cost (\$13,487,400). This case has high probability for scenarios classified as high, higher probability of high product demand since the product demand follows triangular distribution where the mode is 7% higher than the base case, PV cost at the highest level of \$1000,000/MW and carbon incentive at the lowest level of \$10/MWh. Thus such case has multiple not favorable conditions and it explains the resulting high total cost.

4.3.2 WT and PV installation at Austin

Cases 25 to 36 in Figure 4.5 are the only ones where Austin install more WT than the PV. This result is explained because in those cases, the PV cost is at the highest or costlier level of \$1,000,000/MW and the carbon incentive for PV is at the lowest level of \$10/MWh. Because in Austin the average wind capacity factor is slightly higher than the average PV capacity factor, WT is attractive and also cost effective for those cases.

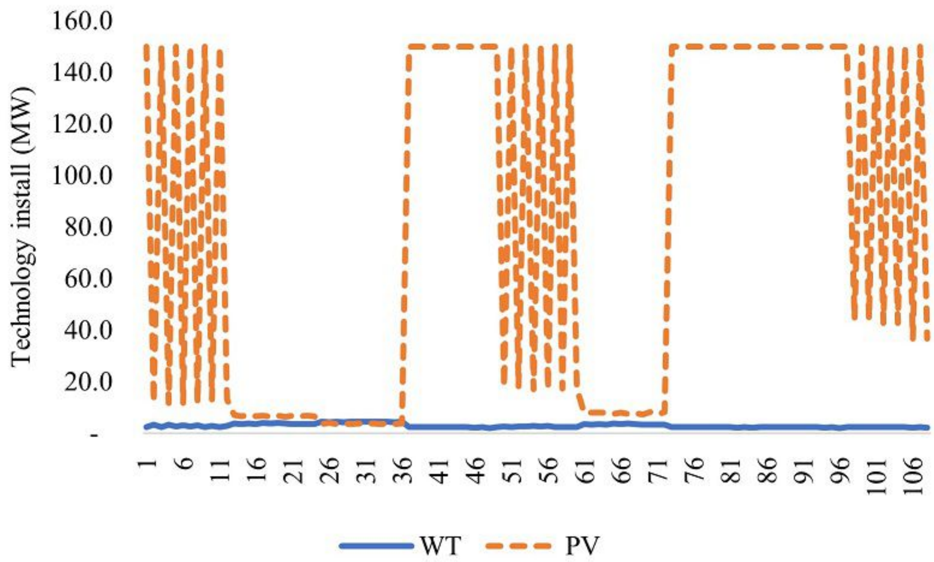

Figure 4.5: WT and PV installation at Austin

Among the cases that installed the largest amount of PV are for instance cases 37-49 in which PV installation cost is \$750,000/MW and the PV incentives are \$30/MWh and cases 73-97 in which PV installation cost was also at the lowest level of \$500,000/MW and the incentives are at the highest level of \$30/MWh.

4.3.3 WT and PV installation at Boston

Cases 1 to 36 in Figure 4.6 show that Boston installs more WT than the PV. This result is explained because in those cases, the PV cost is at the highest or costlier level of \$1,000,000/MW. Furthermore, in cases 61 to 72 in Figure 4.6 Boston installs more WT than the PV. This result is explained because in those cases, the PV cost is \$750,000/MW and the carbon incentive is \$10/MWh. Because in Boston the average wind capacity factor is higher than the average PV capacity factor, WT is attractive and also cost effective for those cases.

Among the cases that installed the largest amount of PV are for instance cases 37-49 in which PV installation cost is \$750,000/MW and cases 73-97 in which PV

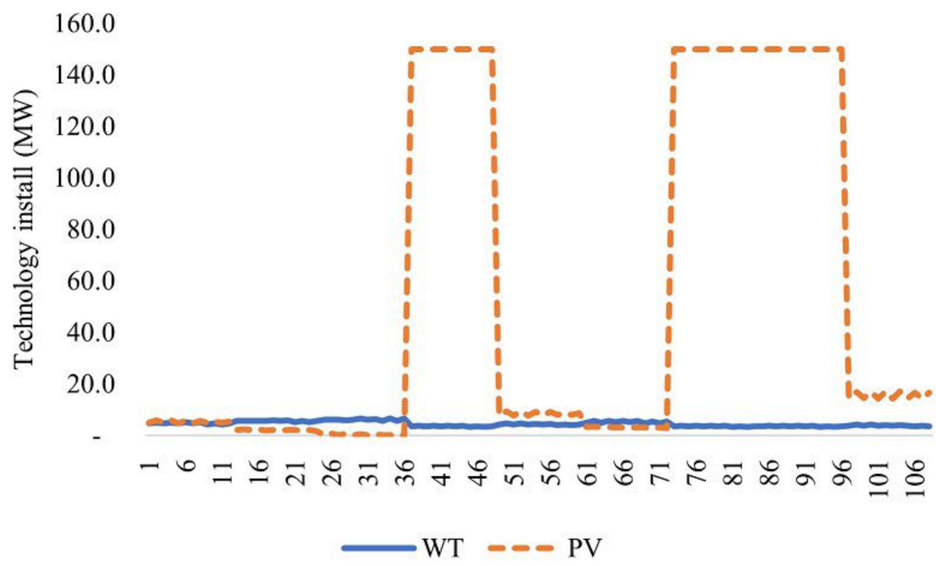

Figure 4.6: WT and PV installation at Boston

installation cost was also at the lowest level of \$500,000/MW to \$750,000/MW.

4.3.4 WT and PV installation at Dallas

Cases 25 to 36 in Figure 4.7 are the only ones where Dallas installs more WT than PV.

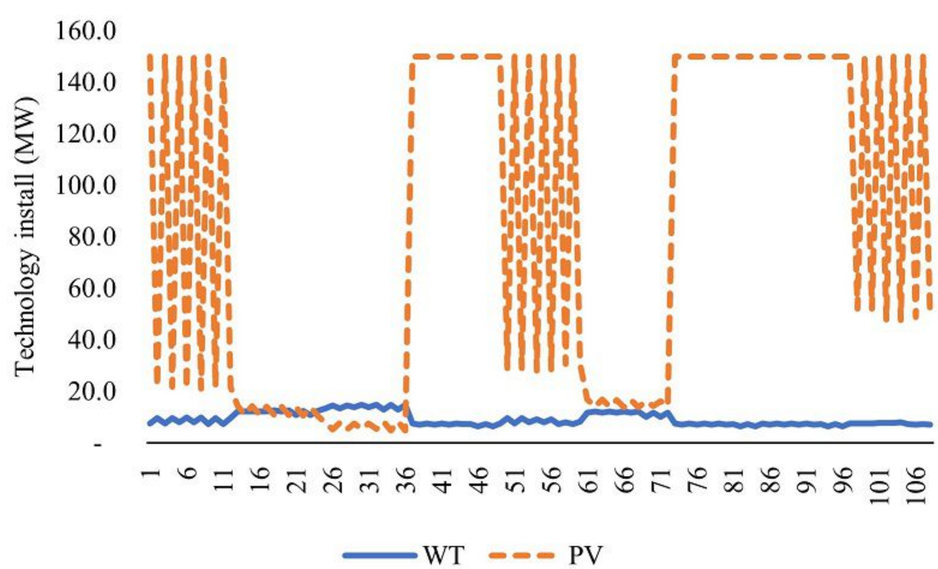

Figure 4.7: WT and PV installation at Dallas

This result is explained because in those cases, the PV cost is at the highest or costlier level of $1,000,000/MW and the carbon incentive for PV is at the lowest level of $10/MWh. Because in Dallas the average wind capacity factor is slightly higher than the average PV capacity factor, WT is attractive and also cost effective for those cases. Among the cases that installed the largest amount of PV are for instance cases 37-49 in which PV installation cost is $750,000/MW and the PV incentives are $30/MWh and cases 73-97 in which PV installation cost was also at the lowest level of $500,000/MW and the incentives are at the highest level of $30/MWh.

4.3.5 WT and PV installation at New York

Cases 37 to 48 in Figure 4.8 are the only ones where New York install more PV than WT. This result is explained because in those cases, the PV cost is at the low or less costlier level of $750,000/MW and the carbon incentive for PV is at the highest level of $30/MWh. Hence, lower PV cost and highest carbon incentive make solar PV attractive and also cost effective for those cases.

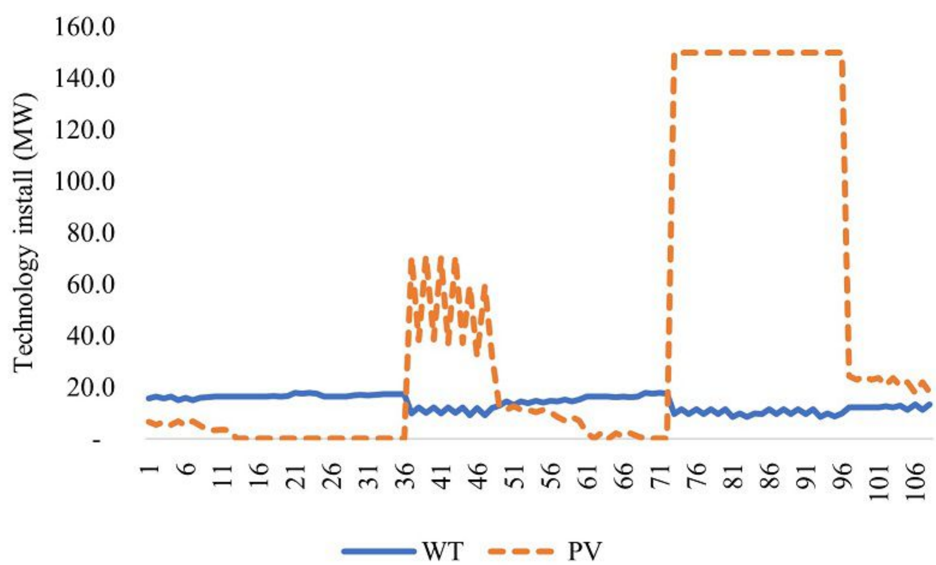

Figure 4.8: WT and PV installation at New York

Among the cases that installed the largest amount of PV are for instance cases 73-96 in which PV installation cost is \$500,000/MW and the PV incentives are \$20/MWh to \$30/MWh.

4.3.6 Energy buying amount at factory and warehouse

Figure 4.9 presents the amount of energy bought from factories and warehouses. The figure shows a relatively similar trend for factories and warehouses even if the oscillations for the energy bought in the factory are larger than in the warehouse. Lower amount of energy is needed in cases 10-12, 22-24 and so on where the BS cost is \$150,000/MWh. On those ranges factories and warehouses install highest capacity of BS. The stored energy in BS is used on those days where the lower wind speed and bad weather conditions are not good enough to meet the energy demand of the facilities.

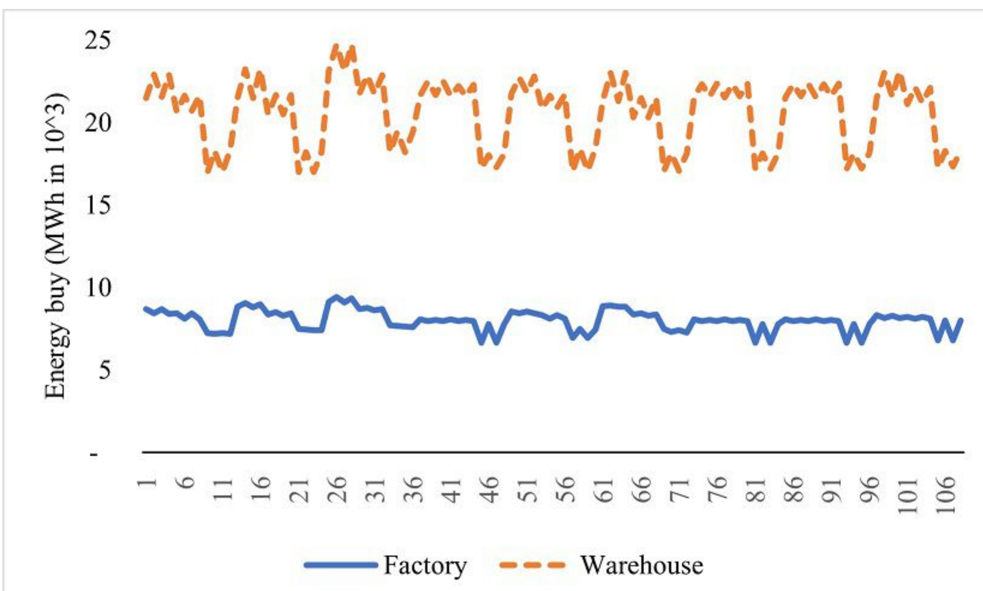

Figure 4.9: Energy buying amount at factory and warehouse

4.3.7 BS installation at factory and warehouse

Figure 4.10 presents the BS installation at factories and warehouses. The figure shows a relatively similar trend for factories and warehouses even if the oscillations for the energy bought in the factory are larger than in the warehouse. Highest capacity of BS is installed in cases 9-12, 21-24 and so on where the BS cost is \$150,000/MWh.

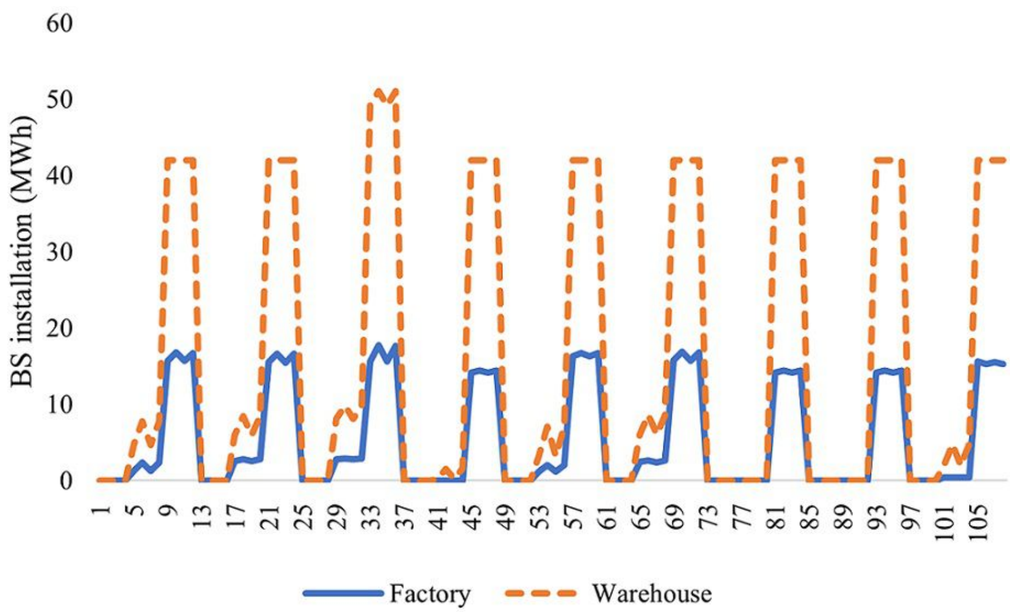

Figure 4.10: BS installation at factory and warehouse

4.3.8 Energy selling amount at factory and warehouse

Figure 4.11 presents the amount of energy bought by the factories and warehouses. There is a similar trend for energy sold from factory and warehouse. Cases 73-96, show the highest amount of energy sold from factory and warehouse. It is because in those cases the PV installation cost is \$500,000/MW and the carbon incentives are \$30/MWh and \$20/MWh. These are favorable conditions to adopt large RE capacity and sell extra energy generated. On the contrary, cases 13-36, show the lowest amount of energy sold from factory and warehouse. It is because in those cases the PV installation cost is \$1,000,000/MW and the carbon incentive is \$20/MWh and \$10/MWh, respectively. It is observed that facilities normally sell high amounts of energy when facing a low energy demanding case with the most appealing conditions for adopting larger amounts of renewable energy.

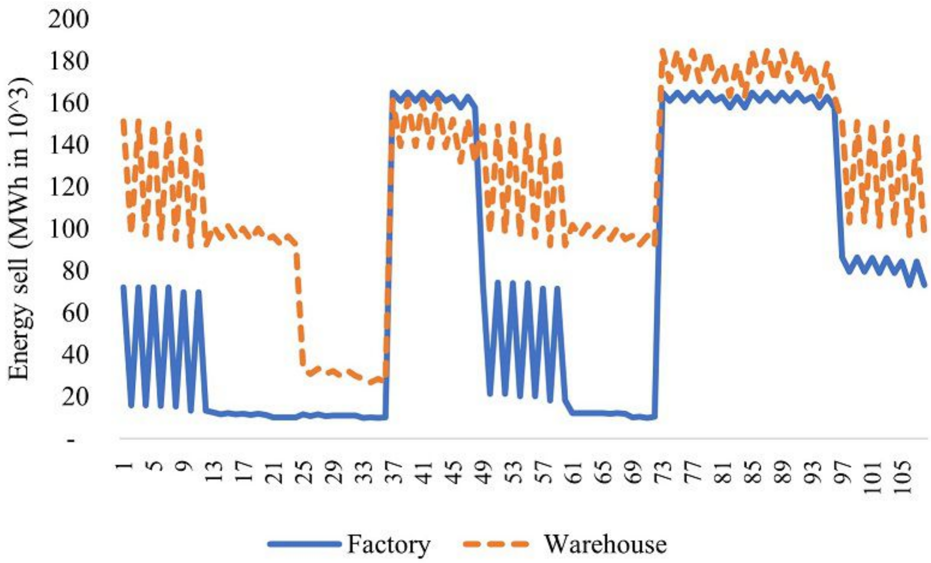

Figure 4.11: Energy selling amount at factory and warehouse

4.4 VSS for the hourly prosumer microgrid models

The value of a stochastic solution (VSS) allows a researcher to evaluate the goodness of a solution given by a stochastic model by comparing the stochastic model objective function value to the expected cost of a solution in which the random values for the uncertain inputs are replaced with the mean values (Escudero et al., 2007). For a maximization problem, the gain in expected objective function value from using a stochastic solution over one from a deterministic program is called the VSS (Birge, 1995). In linear programming, the optimal solution obtained from deterministic models falls toward extreme point solutions which rely on a limited set of activities (basic variables) and force a solution to meet critical constraints tightly (Birge, 1995). On the contrary, an optimal solution from a stochastic model allows for broader sets of activities and naturally impose penalties that enable solutions to meet critical constraints with some cushion to avoid costly violations (Birge, 1995). For practical problems in which a deterministic model cannot provide adequate solutions the VSS becomes quite significant. A mathematical formula to compute the VSS for a minimization problem is as follows (Escudero et al., 2007):

$$VSS = EEVS - RP \tag{4.33}$$

Where, EEVS is the expected cost of implementing the expected value solution and RP is the expected cost of the stochastic recourse problem. In this research, the expected cost of implementing the expected value solution (i.e. first term in the formula) is the expected cost of implementing a solution obtained from solving the model with a single-scenario that assumes the values for the uncertain parameters equal to the expected values. The expected cost of the stochastic recourse problem (i.e, second term in the formula) is the the expected cost of solving the two-stage stochastic model. Consequently, for the minimization problem in this research positive values of VSS are cost savings a decision maker incurs by implementing the two-stage stochastic model solution instead of the one from a deterministic model.

Table 4.7: VSS comparison for prosumer models - hourly granularity

Model type	EEVS ($)	RP ($)	VSS ($)
Prosumer without TOU	43,286,600	42,490,176	796,424
Prosumer with TOU	39,722,500	38,958,903	763,597

The VSS values for Model 4 - prosumer microgrid with BS, without TOU - and Model 5 - prosumer microgrid with BS and TOU are presented in table 4.7. Both models satisfy energy constraints under an hourly time granularity. The VSS for both models are very similar and practically significant since they are near to a million dollars per year.

4.5 Analysis of the design of experiments

This section provides further details about the statistical analysis of the design of Experiments (DOE) for Model 5 - Prosumer microgrid with BS and TOU - hourly granularity presented in the previous section. The analysis was done using Minitab and the General Linear Model (GLM) option available under the command Stat, ANOVA. The aim of the DOE is to learn which parameters in the model, which are named as factors in the DOE, significantly affect the model objective function value using a significance level of 5% (confidence level 95%). The model objective function is the total expected cost. It is desirable to identify the optimal levels of the factors in the DOE that reduce such expected cost. In this section, the expected cost will be abbreviated as total cost. The two categorical factors in the experiments are: products demand distributions and probability distribution for the model scenarios. The two levels (i.e., low and high) selected for these categorical factors are as mentioned in the previous section and also are displayed in Appendix B Table 5.17. The three experimental factors that in practice can be continuous were included in the GLM analysis as covariates. They are: PV cost, carbon incentive and battery cost. The three levels (i.e., low, medium and high) selected for the covariates are also as mentioned in the previous section and displayed in Table 5.17. Montgomery (2017) suggests to keep the number of factor levels low, if the purpose of the DOE is to screen which factors are significant. Following this suggestion, the number of factor levels in this DOE was set to 2 for the categorical factors and 3 for the covariates. Montgomery (2017) also mentions that the number of replications that the experimenter can perform may be small and, in some cases, restricted to a sample size equal to one because time and resources including computational ones are usually limited.

Minitab statistical software version 18 was used to generate and analyze the DOE. In the first model generated by Minitab, all the factors and covariates (i.e, PV cost, carbon incentive, battery cost, product demand distribution and probability distribution for the model scenarios) were included in the GLM. This model has an R-squared of 83.97%, but the residuals show non-constant variance. To correct the non-constant variance issue, the total cost (i.e. response variable) for all cases (i.e., experimental runs) was transformed to the natural logarithm of total cost plus a small constant ($47,921). Since there were a few cases where the model objective function ended with a small revenue, this transformation permitted to have all the costs positive and use the natural logarithm transformation. The variable total cost + 47,921 is named Small_Transformed_total_cost. The GLM on the natural logarithm of Small_Transformed_total_cost is successful on stabilizing the variance of the residuals, but the R-squared of the model is low (20.29%).

Further revision of the total costs in the experimental cases revealed that there are four cases or experimental runs with considerably high residuals. Then, it was explored if it was possible to adjust a better model to the remaining cases. Such model didn't require the addition of any constant, was performed on the total_cost, but still required a Box-Cox transformation to stabilize the variance. The Box-Cox transformation used was optimally selected by Minitab. In such model battery cost, products demand distribution type and probability distribution for the scenarios were non-significant factors to explain the variability in the total cost and to keep the lack of fit of the model at the lowest possible value, and consequently they were excluded from the model. After doing this step, a final GLM model with only PV cost and carbon incentive, and second-order terms and interactions was produced to explain the total cost variability. The ANOVA table, information concerning the statistical significance of the regression coefficients at a 5% significance level (95% confidence level), and the summary of the regression model reporting about the significance of the regression are shown in table 4.8 to 4.10. The final regression equation is presented between the last two tables mentioned. This last model has R-squared of 97.60%. Figures 4.12 and 4.13 show the normal probability plot and residuals vs. fits graphs to evaluate the assumptions of normality and constant variance of the residuals in GLM. Note that in the database provided to Minitab the levels of PV cost were coded as 1 =\$1,000,000/MW, 2=\$750,000/MW, and 3 =\$500,000/MW and the levels of carbon incentives for PV were coded as 1 =\$30/MWh, 2=\$20/MWh, and 3 =\$10/MWh.

Table 4.8: Analysis of variance for transformed response

Source	DF	Adj SS	Adj MS	F-value	P-value
PV_cost	1	6.4E+12	6.4E+12	23.91	0.000
Carbon_inc	1	2.1E+12	2.1E+12	7.69	0.000
PV_cost*PV_cost	1	3.0E+13	3.0E+13	112.69	0.000
Carbon_inc*Carbon_inc	1	5.9E+12	5.9E+12	21.95	0.000
PV_cost*Carbon_inc	1	1.4E+14	1.4E+14	532.47	0.000
Error	98	2.6E+13	2.7E+11	-	-
Lack-of-Fit	3	4.0E+12	1.3E+12	5.76	0.001
Pure Error	95	2.2E+13	2.3E+11	-	-
Total	103	1.2E+15	-	-	-

Table 4.9: Coefficients for transformed response

Term	Coef	SE Coef	T-value	P-value	VIF
Constant	11701645	608205	19.24	0.000	-
PV_cost	-2211662	452261	-4.89	0.000	51.83
Carbon_inc	1257407	453508	2.77	0.007	52.11
PV_cost*PV_cost	-1135379	106954	-10.62	0.000	46.91
Carbon_inc*Carbon_inc	-501088	106954	-4.69	0.000	47.85
PV_cost*Carbon_inc	1818976	78828	23.08	0.000	14.38

Final regression equation:

Total_ cost

$= 11701645 - 2211662$ PV_cost + 1257407 Carbon_inc

$-$ 1135379 PV_cost*PV_cost $-$ 501088 Carbon_inc*Carbon_inc

+ 1818976 PV_cost*Carbon_inc

Table 4.10: Model summary for transformed response

S	R-sq	R-sq(adj)	R-sq (pred)
0.517456	97.87%	97.76%	97.60%

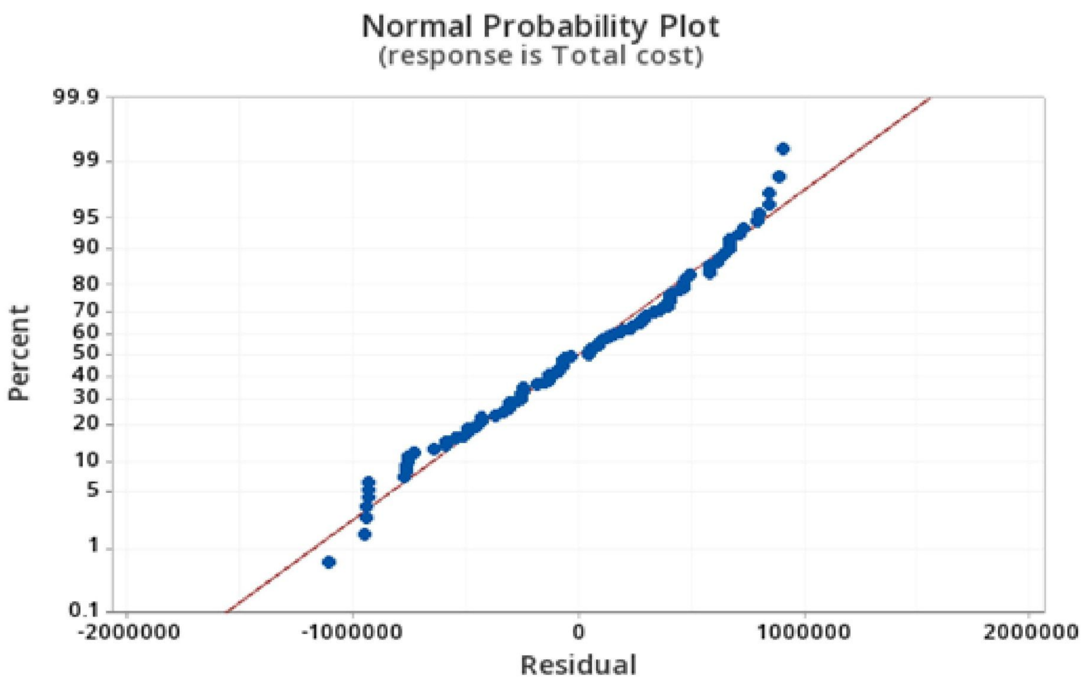

Figure 4.12: Normal probability plot

To predict a total cost it is necessary to plug in the final regression equation the PV cost and carbon incentive values in coded units (i.e., using the level numbers not their real values). It is desirable to get small values for the regression equation after plugging the PV cost and carbon incentive levels. The lowest level of carbon incentive (i.e., 1) and the highest level of PV cost (i.e. 3) will produce those lowest

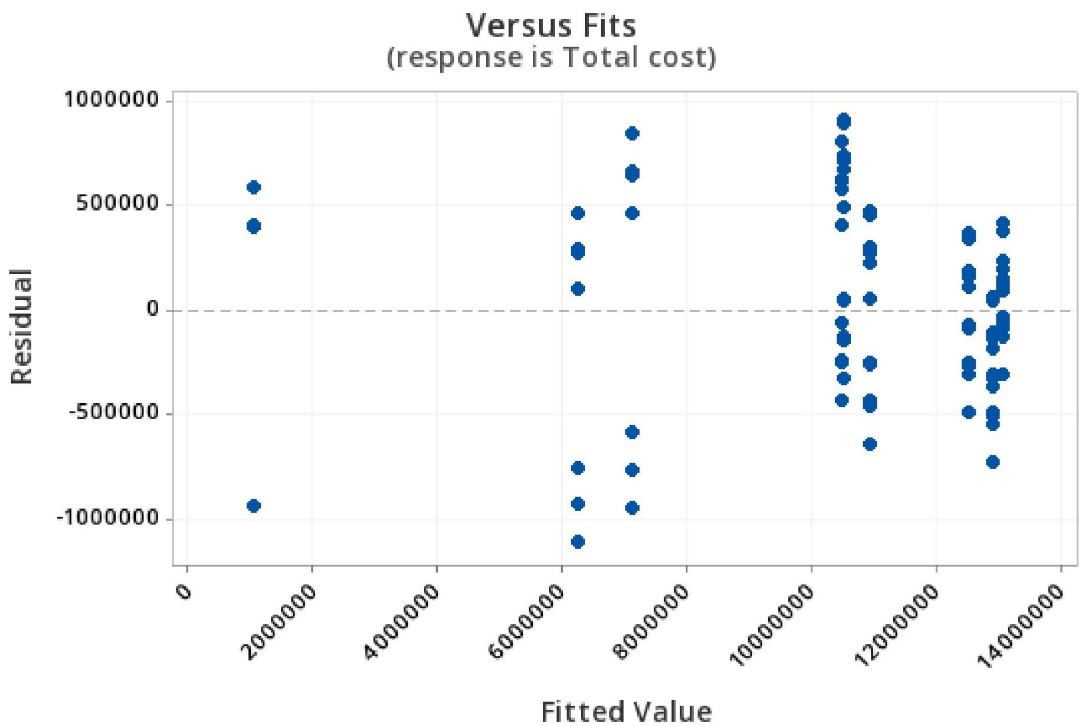

Figure 4.13: Residuals vs. Fits graph

values and consequently the lowest expected costs. This resulting equation agrees with the total expected cost results presented in the previous section that showed as the most favorable cases the ones with PV cost equal to $500,000/MW) and PV carbon incentives equal to $30). However, the model could be not the optimal one for predicting the expected total cost because it exhibits some lack-of-fit, even if the interactions and second-order level terms were included and Minitab found only one unusual residual. Such lack of fit can indicate that there are other factors not included in the model that could help to explain the variability in the total cost.

4.6 Hourly vs. daily models' comparison and analysis

This section provide a comparative analysis of all models presented in this thesis work.

4.6.1 Total cost comparison

Table 4.11 provides the expected cost for all the models researched in this thesis. Since all models have the option to adopt BS the words "with BS" were dropped from the model names. The abbreviated names for the models used in Figure 4.14 are given the third column of the table.

Table 4.11: Total cost comparison

Model	Time granularity	Notation	Expected total cost ($)
Island microgrid	Daily	IM daily	47,115,128
Prosumer without TOU	Daily	P daily	35,959,082
Island microgrid	Hourly	IM hourly	99,785,837
Prosumer without TOU	Hourly	P hourly	42,490,176
Prosumer with TOU	Hourly	P TOU hourly	38,958,903

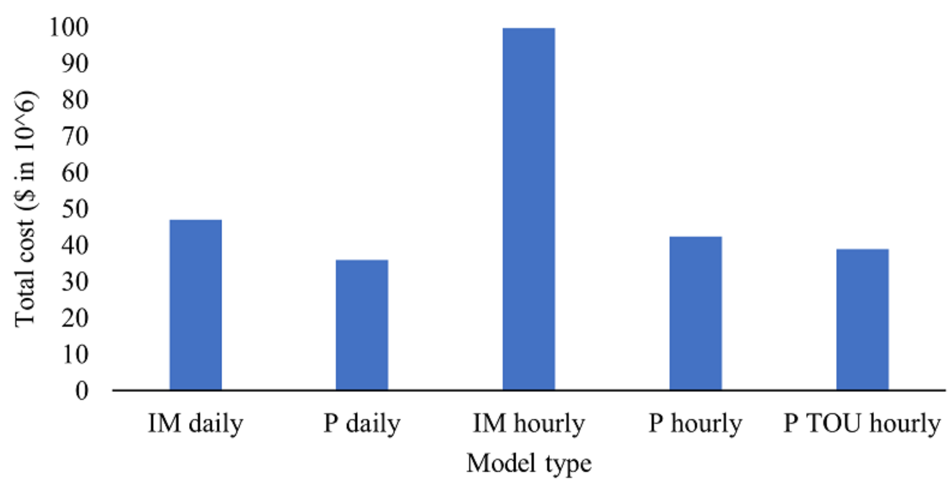

Figure 4.14: Total cost comparison

From table 4.11, it is evident that the prosumer models always outperform the island microgrid models. The lowest cost is seen in prosumer daily model without TOU tariffs. However, the expected costs of the hourly models are more accurate because they use directly the hourly capacity factors computed from the real weather database instead of using daily averages. In the daily models, the capacity factor used in the models objective function and energy constraints is the average of the 24 hours capacity factor. On the other hand, when models are converted from daily to hourly time granularity, the island microgrid hourly model is impacted by drastic changes due to the highly stochastic nature of the hourly weather conditions. The prosumer hourly model ends less impacted by the variation in weather conditions because it has the option of buying energy from the main grid. In poor weather conditions, the prosumer models prefer to buy energy from the main grid and install less microgrid to meet the energy demand of the facilities. In daily time granularity, 23.68% cost will be reduced if manufacturers transform from island mode to prosumer mode. On the other hand, in hourly time granularity, 57.42% cost will be reduced if manufacturers transform from island mode to prosumer without TOU tariffs mode. Also, 60.96% cost will be reduced if manufacturers transform from island mode to prosumer with TOU tariffs mode. Furthermore, in hourly time granularity, 8.31% cost will be reduced if manufacturers transform from prosumer without TOU tariffs mode to prosumer with TOU tariffs mode. The IM hourly model always incurs in the highest cost because of the high stochasticity in the hourly weather conditions and the impossibility to energy from main grid in adverse weather conditions or sell energy that it has to spill when the weather conditions are favorable but there is no capacity in the BS, it it was adopted and given that adopting BS is somehow expensive.

4.6.2 Energy cost comparison

From Table 4.12 and Figure 4.15 , it is evident that the prosumer models always outperform the island microgrid models regarding energy cost. For the daily time granularity, 46.98% energy cost will be reduced if manufacturers transform from island mode to prosumer mode.

Table 4.12: Energy cost comparison

Model type	Time granularity	Total cost ($)
Island microgrid	Daily	23,220,186
Prosumer without TOU	Daily	12,310,395
Island microgrid	Hourly	75,339,170
Prosumer without TOU	Hourly	18,840,457
Prosumer with TOU	Hourly	15,309,347

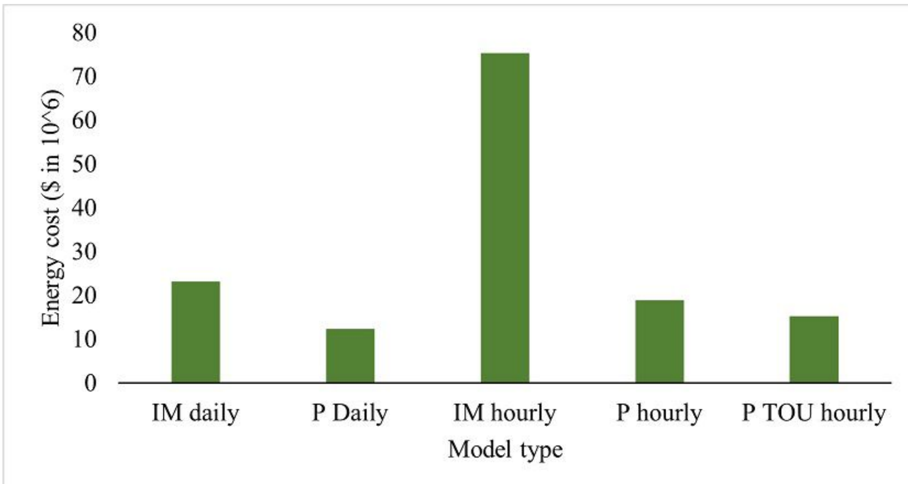

Figure 4.15: Energy cost comparison

However, for the hourly time granularity there is a drastic change when the island microgrid mode transforms into a prosumer mode. There is a 74.99% energy cost reduction if manufacturers transform from island mode to prosumer without TOU tariffs mode and a 79.68% cost reduction if manufacturers transform from island mode to prosumer with TOU tariffs mode. Furthermore, in the hourly time granularity, there is a 18.74% energy cost reduction if manufacturers transform from prosumer without TOU tariffs mode to prosumer with TOU tariffs mode. The high stochasticity in hourly weather conditions and the lack of an option to by energy from the main grid in adverse weather conditions make the Island microgrid hourly model the least attractive.

4.6.3 Total energy produced and bought

Table 4.13 presents the total energy produced and bought in the five model instances compared. Island microgrid with hourly time granularity has the highest energy production because of the highly stochastic hourly wind profile and weather conditions and the nonexistence of an option to buying energy from the main grid to cope with the energy demands from the hours with low capacity factors.

Table 4.13: Energy produced, bought and sold comparison

Model type	Time granularity	Produce (MWh)	Buy (MWh)	Sell or spill (MWh)
Island microgrid	Daily	378,238	0	136,760
Prosumer without TOU	Daily	409,466	12,379	187,788
Island microgrid	Hourly	931,760	0	689,500
Prosumer without TOU	Hourly	404,684	81,722	252,736
Prosumer with TOU	Hourly	331,611	90,222	188,173

To deal with the stochasticity of wind and solar generation, the island microgrid model prefers to produce more energy when there is a strong wind or sun and keep energy in battery systems for later usage. On the other hand, the prosumer model with TOU tariffs has the lowest energy production. This model finds an advantage in the option to buy more energy in off-peak hours to balance the energy demand of the facilities.

4.6.4 Microgrid sizing of San Francisco

Table 4.14 and Figure 4.16 present the microgrid sizing of San Francisco for all models developed in this thesis work. There is a significant difference in microgrid capacity adopted for the island microgrid with daily and hourly time granularity. Island microgrid daily mode does not install WT whereas the island microgrid hourly mode install 26.3MW WT. This is because in hourly time granularity PV

Table 4.14: Microgrid sizing of San Francisco

Model type	Time granularity	WT (MW)	PV (MW)	BS (MWh)
Island microgrid	Daily	0	35.9	12.3
Prosumer without TOU	Daily	1.9	14.7	0.5
Island microgrid	Hourly	26.3	41.3	57.3
Prosumer without TOU	Hourly	4.9	5.7	0
Prosumer with TOU	Hourly	2.9	6.6	0

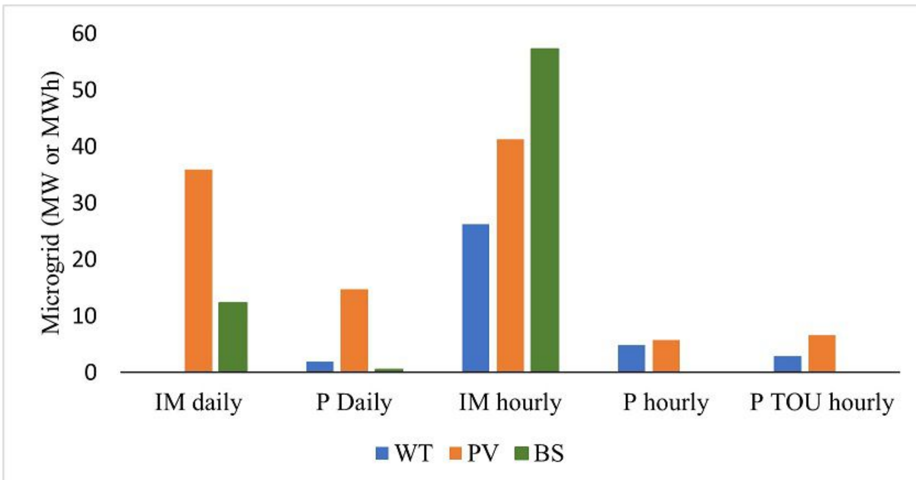

Figure 4.16: Microgrid sizing of San Francisco

does not generate electricity in night time as it is the real case. In daily time granularity, the model uses an average capacity factor calculated from the 24 hours weather data. Similarly, the prosumer hourly models decreased PV installation if compared to the one in daily time granularity. Another significant observation is that at the assumed BS cost (i.e. \$500,000/MWh) the hourly prosumer models do not install battery. Island microgrid hourly installs the highest amounts of all WT, PV and BS for the same reasons mentioned in the previous section, Section 4.6.3.

4.6.5 Microgrid sizing of Austin

Table 4.15 and Figure 4.17 present the microgrid sizing of Austin for all models developed in this thesis work. There is a significant difference in the BS capacity adopted in the island microgrid mode with daily vs. hourly time granularity.

Table 4.15: Microgrid sizing of Austin

Model type	Time granularity	WT (MW)	PV (MW)	BS (MWh)
Island microgrid	Daily	8.7	2.8	12.3
Prosumer without TOU	Daily	2.5	13.6	0.5
Island microgrid	Hourly	11.6	8.4	57.3
Prosumer without TOU	Hourly	5.2	5.8	0
Prosumer with TOU	Hourly	3.0	7.0	0

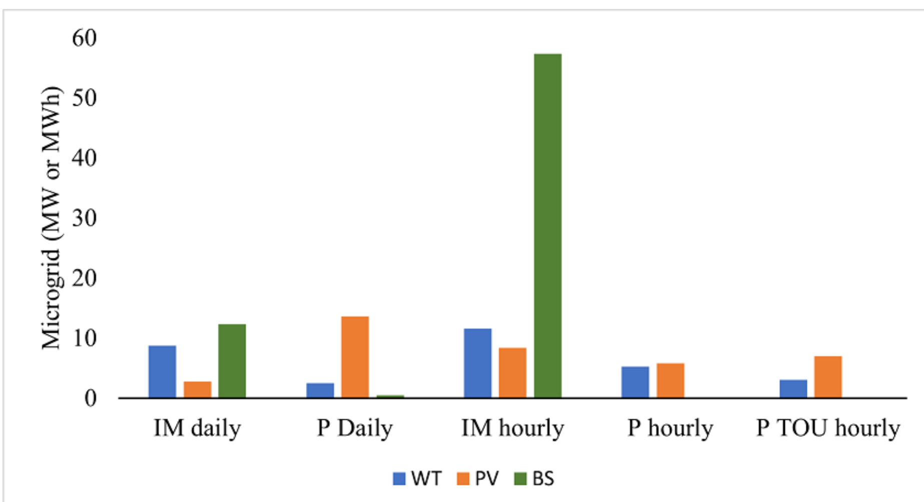

Figure 4.17: Microgrid sizing of Austin

Island microgrid daily mode installs BS 12.3MWh, but island microgrid hourly mode installs BS 57.3MWh. For the prosumer hourly models, a decrease of PV installation is observed if compared to the one in the daily time granularity. Another significant observation is that the hourly prosumer models' do not install battery. IM hourly installs the highest amounts of all WT and BS because of the reasons already mentioned in Section 4.6.3.

4.6.6 Microgrid sizing of Boston

Table 4.16 and 4.18 presents the microgrid sizing of Boston for all the models developed in this thesis work. It is observed a significant difference between the island models with daily and hourly time granularity models.

Table 4.16: Microgrid sizing of Boston

Model type	Time granularity	WT (MW)	PV (MW)	BS (MWh)
Island microgrid	Daily	8.3	0	12.3
Prosumer without TOU	Daily	6.2	4.1	0.5
Island microgrid	Hourly	18.0	71.7	57.3
Prosumer without TOU	Hourly	6.8	2.7	0
Prosumer with TOU	Hourly	4.9	3.6	0

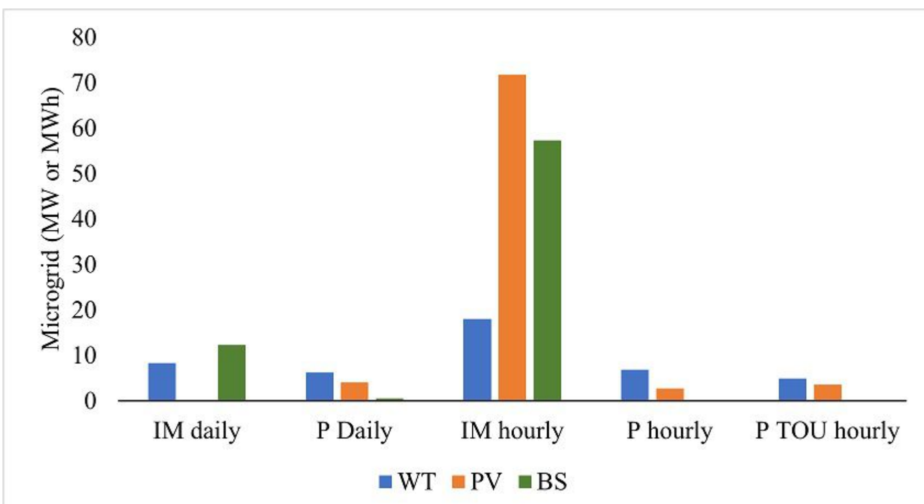

Figure 4.18: Microgrid sizing of Boston

Island microgrid daily mode does not install PV whereas the island microgrid hourly mode install 71.7MW PV. This is because in daily time granularity the average capacity factor is calculated from the 24 hours weather data. In some hours the solar PV capacity factor is 0 which makes the average daily solar PV capacity factor very low. On the contrary, in hourly time granularity for some hours the capacity factor is high enough to make the model end choosing a higher PV capacity. Similarly, in prosumer hourly models a decrease in PV installation is observed if compared to the PV installed in daily time granularity. It is because at night the PV does not generate electricity which makes prosumer model to buy energy from the main grid. Another significant observation is that the hourly prosumer models' do not install BS. Again, IM hourly installs the highest amounts of all WT, PV and BS because of the reasons mentioned in Section 4.6.3.

4.6.7 Microgrid sizing of Phoenix

Table 4.17 and Figure 4.19 present the microgrid sizing of Phoenix for all models developed in this thesis work. In the island models, there is a significant difference on the capacities adopted in the daily and hourly time granularity models.

Table 4.17: Microgrid sizing of Phoenix

Model type	Time granularity	WT (MW)	PV (MW)	BS (MWh)
Island microgrid	Daily	0	61.1	19.6
Prosumer without TOU	Daily	0	92.0	1.1
Island microgrid	Hourly	21.5	121.8	91.7
Prosumer without TOU	Hourly	0	80.5	0
Prosumer with TOU	Hourly	0	71.4	0

Island microgrid daily mode does not install WT whereas the island microgrid hourly mode install 21.5MW WT. In hourly time granularity, for some hours the solar PV capacity factor is 0. It makes the model to install WT to meet the energy

demand of the facilities. Similarly, in prosumer hourly models a decrease of PV installation is observed if compared to the one in the daily time granularity. It is because at night the PV does not generate electricity, which makes prosumer model to opt for buying energy from the main grid as the cehapest recourse action.
Another significant observation is that the hourly prosumer models' do not install BS.Again, IM hourly installs the highest amounts of all WT, PV and BS because of the reasons mentioned in 4.6.3.

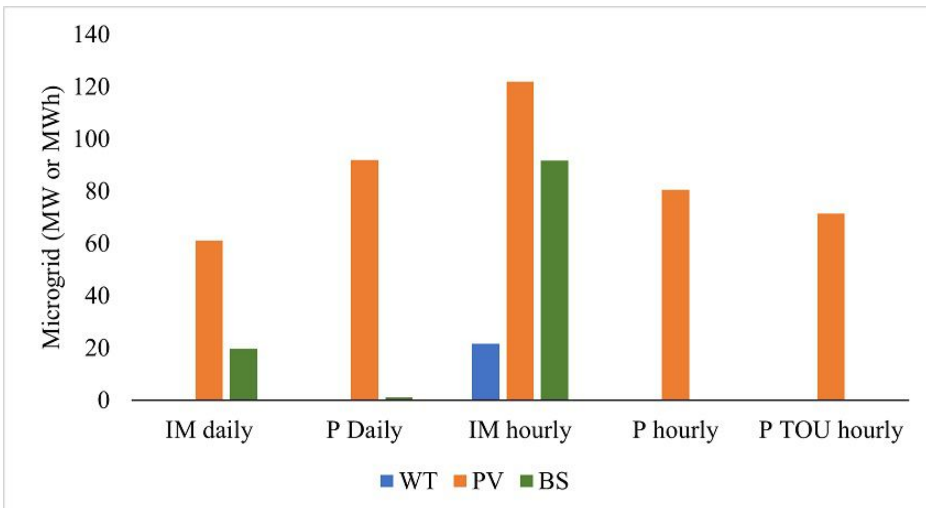

Figure 4.19: Microgrid sizing of Phoenix

4.6.8 Microgrid sizing of Dallas

Table 4.18 presents the microgrid scalability of Dallas of all the models developed in this thesis work. There is a significant difference in daily and hourly time granularity of island microgrid mode.
Island microgrid daily mode install 19.6MWh BS whereas the island microgrid hourly mode install 91.7MWh BS. This is because the hourly capacity factor is highly stochastic than the daily capacity factor.Furthermore, in hourly time granularity in some hours the solar PV capacity factor is 0 which makes the model to install WT to meet the energy demand of the facilities. Similarly, in prosumer

Table 4.18: Microgrid sizing of Dallas

Model type	Time granularity	WT (MW)	PV (MW)	BS (MWh)
Island microgrid	Daily	15.2	27.2	19.6
Prosumer without TOU	Daily	13.4	25.9	1.1
Island microgrid	Hourly	27.5	68.4	91.7
Prosumer without TOU	Hourly	22.4	9.5	0
Prosumer with TOU	Hourly	15.2	12.6	0

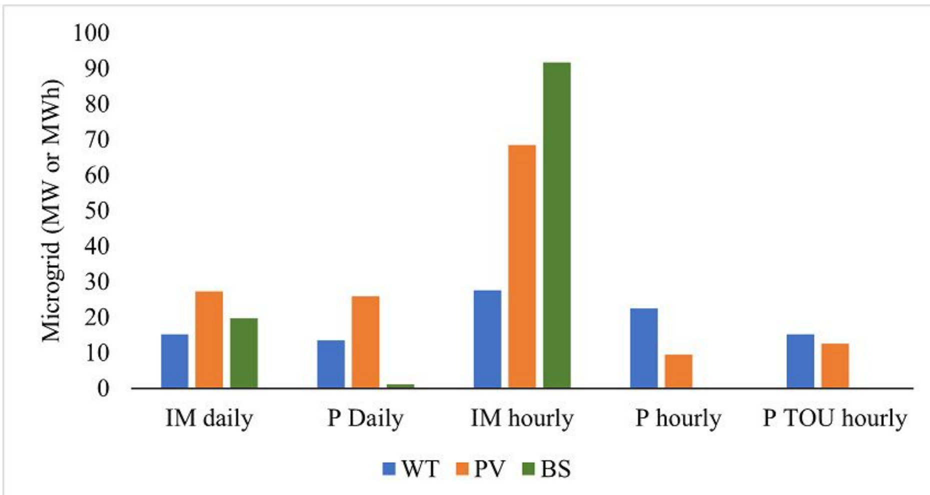

Figure 4.20: Microgrid sizing of Dallas

hourly models', decrease of PV installation is observed from the daily time granularity because in night the PV does not generate electricity which makes prosumer model to buy energy from the main grid or install more WT to meet the energy demand of the facilities. Another significant observation is that the hourly prosumer models' do not install BS. In Figure 4.20 is observed that Island model hourly time granularity installs the highest WT, PV, and BS. The resons for it were mentioned in Section 4.6.3 Also prosumer models install low WT and PV capacity if compared to island microgrid. This result is explained because of the energy buying option from the main grid in adverse weather conditions.

4.6.9 Microgrid sizing of New York

Table 4.19 presents the microgrid scalability of New York for all the models developed in this thesis work.

Table 4.19: Microgrid sizing of New York

Model type	Time granularity	WT (MW)	PV (MW)	BS (MWh)
Island microgrid	Daily	14.1	27.8	19.6
Prosumer without TOU	Daily	24.8	0	1.1
Island microgrid	Hourly	31.1	51.6	91.7
Prosumer without TOU	Hourly	24.4	1.7	0
Prosumer with TOU	Hourly	19.1	5.5	0

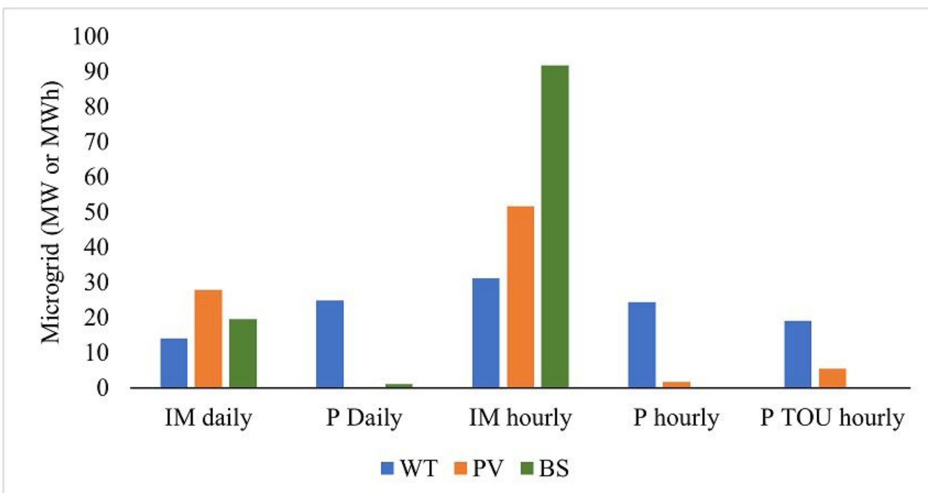

Figure 4.21: Microgrid sizing of New York

There is a significant difference in the capacities adopted in daily and hourly time granularity of island microgrid mode. The daily model installs 19.6MWh BS whereas the hourly mode install 91.7MWh BS. This is because the higher fluctuations in the hourly capacity factor while the daily capacity factor is an average value. Furthermore, in the hourly time granularity for some hours the solar PV capacity factor is 0. It makes the model to install WT to meet the energy demand of the facilities. Another significant observation is that the hourly prosumer models do not install BS. As in the previous subsection, Figure 4.21 shows that Island microgrid hourly model installs the highest WT, PV and BS compared to other models. The reasons for this behaviour were given in Section 4.6.3. Prosumer models install low capacity WT and PV compared to island microgrid because of the energy buying option from the main grid that result advantageous in adverse weather conditions.

4.6.10 LCOE comparison

The levelized cost of energy is defined as the cost of producing one MWh of energy. It is considered as the main indicator to decide if a renewable energy project is attractive or not compared to the conventional sources of energy.

Table 4.20: LCOE comparison

Model type	Time granularity	LCOE ($/MWh)
Island microgrid	Daily	61.4
Prosumer without TOU	Daily	29.2
Island microgrid	Hourly	80.9
Prosumer without TOU	Hourly	38.7
Prosumer with TOU	Hourly	36.3

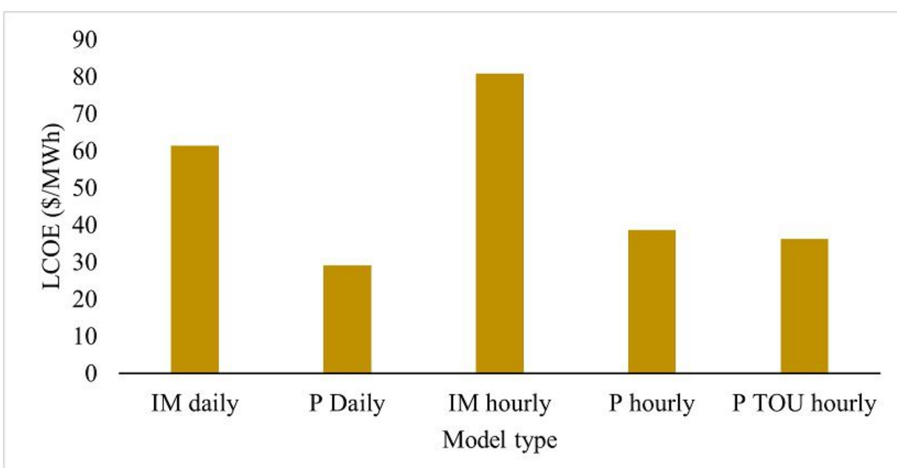

Figure 4.22: LCOE comparison

Since the range for the actual cost of traditional sources of energy is $50-$100 per MWh, the goal is to obtain LCOE within this range. The LCOE for island microgrid operation is calculated in this thesis work by using the following equation (Shea and Ramgolam, 2019). Table 4.20 and Figure 4.22 presents the LCOEs for all the models developed in this thesis work. The prosumer mode always give less LCOE than the island microgrid mode as the prosumer mode can make revenue from selling energy and also can buy energy from main grid when the low capacity factor is not cost effective for generating electricity from onsite microgrid. Encouragingly, all the LCOEs present in table 4.20 indicate that it is cheaper to operate facilities with onsite renewable microgrid installation rather than solely purchasing energy from main grid.

4.6.11 Computational time comparison

All the hourly models have a large number of decision variables and constraints. Model 3, Model 4, and Model 5 were run in one of the two Texas State University large memory nodes (1.5TB) available in the LEAP cluster (LEAP, 2021). The characteristics of the LEAP large memory nodes were provided in the previous chapter. It was also necessary to follow the procedure for dealing with insufficient memory to run the CPLEX solver in AMPL available in "AMPL software website" (AMPL, 2021) also detailed in the computational results section in the previous chapter. Table 4.21 summarizes the computational time for the hourly models presented in the previous chapter and in this one. The solve user time is the time the processor spends running the application code. The solve system time is defined as the time in CPU seconds that the operating system spends running operating system functions connected to the application (e.g., reading and writing files). The total solve time (i.e., solve user time plus solve system time), abbreviated as solve time in the last column of Table 4.21, seems a comprehensive way to appraise the models' computational time as seen from the definitions for these times. The solve time may seem large but because of LEAP uses multiple processors the actual clock time elapsed to run these models was about one-third the reported solve time. Cplex used a combination of the dual simplex and the barrier method. The dual simplex method was used to get a starting basic feasible solution in Phase I of the two-phase simplex method.

Table 4.21: Computational time comparison (CPU seconds)

Model type	Solve user time	Solve system time	Solve time
IM with BS	297,446	133	297,579
Prosumer without TOU	271,422	159	271,581
Prosumer with TOU	213,812	158	213,970

In this chapter the prosumer model with hourly time granularity was enhanced to consider TOU energy rate. Numerical experiments for the implemented base case and sensitivity analysis performed through a DOE show that it is feasible and cost-effective to decarbonize the manufacturing, warehousing, and transportation activities of a company (or supply chain) operating three factories and three warehouses. The DOE hypothesis was that five different factors: products demand distributions, probabilities for the scenarios in the two-stage stochastic model, PV installation cost, carbon incentives from PV installation, and battery cost could affect the model total expected cost. The DOE analysis showed that from these five factors only two were significantly affecting the total expected cost of the model. These factors were PV cost and carbon incentives. It is desirable that actual PV cost continues decreasing and that carbon incentives for adopting PV be kept and ideally increased to continue motivating more manufacturing companies to adopt microgrids coupled with PV systems. A difference found between the island model and the prosumer models under hourly time granularity is that BS adoption is highly relevant for the island model but irrelevant for the prosumer models since they ended preferring to purchase energy from the main grid. The value of solving the two-stage stochastic APP prosumer models with and without TOU under hourly time granularity to satisfy energy constraint was assessed and it is practically relevant since it is near one million dollars per year for both models. Once again this chapter showed the advantages of energy prosumer microgrid operation over island one with respect to total expected cost and LCOE.

5. CONCLUSIONS AND FUTURE WORK

This thesis work implemented island and energy prosumer based two-stage stochastic models for the attainment of cost-effective aggregate production planning plans for manufacturing companies and supply chains. The models are relevant to industries adopting microgrid consisting of solar photovoltaic, wind turbines, and battery storage systems and interested on optimizing production, machine, and work force levels. The goal of this thesis is to decarbonize the manufacturing, transportation, and warehouse operations under uncertain product demand, machine hour capacity, labor hour capacity and renewable energy supply. In the stochastic models developed, the first-stage decisions are the sitting and sizing of the renewable generation technologies, the capacity of the battery systems, amount of product to produce, hours of labor to keep, hire or layoff, and regular, overtime, and idle machine hours to use for the entire planning horizon. Second-stage recourse actions include storing product in inventory, subcontracting or backorder it, buying energy, selling renewable energy to the main grid, and using BS to respond to variations in wind profile and weather conditions.

Three sets of realistic climate data were collected from weather underground for San Francisco, Austin, Boston, Phoenix, Dallas and New York to fed the models. The data sets are statistically analyzed and used to calculate hourly capacity factors that reflect the variability of climate conditions over a one-year planning horizon. The main research questions answered in this thesis were: (1) Is it possible to decarbonize the manufacturing, transportation and warehousing operations of a manufacturing company with RE integration? (2) Is it possible to integrate RE into manufacturing and warehouse operations with affordable levelized cost of energy (LCOE)? (3) what are the costs when the energy constraints are satisfied under hourly and daily time granularity? and (4) what is the cost advantage a manufacturing facility gets if enrolling in a time of use (TOU) energy tariff plan?

Numerical experiments show that the integration of renewable energy into the manufacturing facilities and warehouses is feasible and it would significantly reduce the use of fossil fuels and the emission of harmful gases into the atmosphere. The proposed two-stage aggregate production planning model potentially accelerates the manufacturers plans to transition toward eco-friendly operations. Three managerial insights are derived. First, under current and future installation prices and carbon incentive levels for the renewables, onsite renewable microgrid penetrated with WT and PV promises to attain zero-carbon industrial operations. Second, energy prosumer under time-of-use (TOU) tariff is a more attractive option than energy prosumer without TOU and island microgrid operations, given cost affordability and system reliance are the company objectives. Third, onsite renewable microgrid is capable of meeting the hourly energy demand under stochastic wind profile and weather conditions with an affordable levelized cost of energy. When the microgrid operation is transformed from daily granularity to hourly granularity, a drastic cost change is observed in island microgrid where the annual cost goes up by approximately 112%. On the other hand, only 18.2% increase is observed in the annual cost for prosumer microgrid. Another interesting finding is that under time-of-use tariff, PV installation goes up because it is more cost-effective than buying electricity in daytime or peak hours. However, the wind installation decreases because of the lower electricity buying cost in night or off-peak hours.

In this thesis, experimental analysis was performed on five instances to test the feasibility of adopting renewable microgrid in manufacturing facilities. One of the goal of this thesis was: (1) Is it possible to achieve net-zero carbon in the manufacturing operations with RE integration? From Table 4.13 we can conclude that the Island microgrid always achieves a net-zero carbon manufacturing environment. The prosumer models (i.e., both daily and hourly time granularity with and without TOU) always sell more RE than the amount of conventional energy they buy from the main grid. Hence, we can conclude that prosumer models also achieve net-zero carbon manufacturing environment in the cities studied in this thesis work.

A further numerical analysis was performed by changing the buying cost of energy from \$130/MWh to \$105/MWh in the prosumer model without TOU and hourly granularity in the energy balance constraints. The objective was to see the relative changes in total cost, energy cost, microgrid sizing and LCOE values. It was hypothesized that the prosumer model without TOU using the buying energy cost of \$105/MWh would always give a lower total cost. The results show that, by reducing the buying cost of energy from \$130/MWh to \$105/MWh the total cost reduces approximately 4.6%, energy cost reduces approximately 11.3%, and the sizing of RE microgrid is also reduced in each city. These results occur because now the prosumer model without TOU buys approximately 10% more energy (i.e. 89,715 MWh) from the main grid. But still the prosumer model without TOU with buying energy cost of \$105/MWh cannot outperform the prosumer hourly TOU model (\$140/MWh on-peak; \$70/MWh off-peak) in terms of total expected cost, energy cost and LCOE. The prosumer TOU model has approximately 3.9% lower total cost, 8.4% lower energy cost and lower LCOE (i.e., \$36.29/MWH for TOU model vs. \$39.09/MWh for the prosumer model without TOU and \$105/MWh buying energy cost). The prosumer TOU model installs more PV compared to the prosumer without TOU at \$105/MWh buying energy cost. On the contrary, the prosumer TOU model installs less WT because of the lower buying energy cost in off-peak hours.

In this thesis, the product demand data was generated synthetically from pre-defined discrete uniform and triangular distributions. This research work could be extended to forecast the demand of the products using traditional and artificial intelligence forecasting methods and real historical data. In addition, it would be relevant to derive the single probability distribution for the scenarios assumed in the model based on the individual probability distributions for the different random elements that define a scenario. Another future work to be considered is implementing mirrors with the microgrid system (Budiyanto and Fadliondi, 2017) that would maximize the heat and generate more energy from solar PV. Application of decomposition algorithms for solving this type of large-scale stochastic optimization problem could open the doors to solve even larger model instances or improve the computational efficiency of the current model instances. Finally the inclusion of other realistic aspects to the model, such as budget limitations and additional renewable technologies is a way to enhance the models presented in this thesis work.

APPENDIX SECTION

APPENDIX A: Notation used in the computation of solar PV generation

Parameters and variables used to compute solar PV generation

Notation	Factor	Unit	Explanation
W_t	Weather condition	N/A	Random variable between 0 and 1
A	PV size	m^2	PV module area
η	PV efficiency	%	Typically between 15-25%
d	Date	N/A	d$\in \{1, 2, ..., 365\}$
ω	Solar hour	rad	Related to the local clock hour
T_0	PV temperature	°C	PV operating temperature
ϕ	Latitude	rad	Depends on geographic location
α	Surface azimuth angle	rad	$\alpha = 0$, if facing south
β	PV tilt angle	rad	Between PV and ground
t	Local time	hour	t$\in \{1, 2, ..., 24\}$
γ	Sun zenith angle	rad	Angle between sun ray and the normal to the ground
θ	PV incident angle	rad	Angle between sun ray and the normal to PV surface
ω_{rise}	Sunrise hour	hour	Perceived by the PV
ω_{set}	Sunset hour	hour	Perceived by the PV
δ	Declination angle	rad	Depending on the date
T	Total number of generation hours	N/A	Depends on the sunrise and sunset hour. In the equator, it is (8760/2)= 4380 h
P_{PV}^{Max}	Rated capacity of a PV system	W	Maximum output power of the PV panel considered

APPENDIX A: Parameters and variables in solar PV generation

Values of W_t under different weather conditions

Scenario	Condition	Value of W_t
1	Clear sky	1.00
2	Scattered cloud	0.70
3	Partially cloudy	0.50
4	Mostly cloudy	0.30
5	Overcast	0.20
6	Light Rain	0.10
7	Rain	0.10
8	Heavy Rain	0.10
9	Haze	0.10
10	Widespread Dust	0.10
11	Patches of Fog	0.10
12	Fog	0.10
13	Light Thunderstorms and Rain	0.10
14	Thunderstorms	0.10
15	Thunderstorms and Rain	0.10
16	Heavy Thunderstorms and Rain	0.10
17	Light Drizzle	0.10
18	Mist	0.10
19	Snow	0.00
20	Unknown	0.00

APPENDIX B: Values for the product demand

Values for product demand if it follows discrete uniform distribution

Factory	Period	Product A low	Product A high	Product B low	Product B high	Unit
San Francisco	1	504	656	764	892	item/period
	2	509	694	753	889	item/period
	3	520	707	751	870	item/period
	4	531	731	735	866	item/period
	5	549	735	730	859	item/period
	6	573	738	729	853	item/period
	7	582	741	726	832	item/period
	8	583	760	706	810	item/period
	9	594	776	689	796	item/period
	10	605	793	670	787	item/period
	11	629	795	622	782	item/period
	12	653	799	603	766	item/period
Austin	1	455	514	751	795	item/period
	2	460	515	742	791	item/period
	3	461	515	737	789	item/period
	4	462	528	732	779	item/period
	5	463	530	731	777	item/period
	6	484	532	725	777	item/period
	7	488	534	720	775	item/period
	8	490	535	719	772	item/period
	9	503	544	714	771	item/period
	10	512	547	714	761	item/period
	11	513	548	712	754	item/period
	12	514	548	710	752	item/period

APPENDIX B: Values for product demand

Values for product demand if it follows discrete uniform distribution continuation

Factory	Period	Product low	A high	Product low	B high	Unit
Boston	1	557	649	766	842	item/period
	2	560	657	748	827	item/period
	3	566	659	740	821	item/period
	4	580	666	716	820	item/period
	5	584	694	689	814	item/period
	6	594	696	688	803	item/period
	7	608	722	686	796	item/period
	8	629	740	680	792	item/period
	9	631	741	673	780	item/period
	10	635	745	672	779	item/period
	11	640	747	669	775	item/period
	12	643	749	665	773	item/period

APPENDIX B: Values for product demand

Values for product demand of San Francisco factory if it follows triangular distribution

Period	Product low	A high	Product low	B high	Unit	Comment
1	549	732	842	878	item/period	mode +10% than the mean of base case
2	581	735	820	876	item/period	
3	592	741	816	875	item/period	
4	597	753	801	874	item/period	
5	603	755	790	874	item/period	
6	636	756	777	868	item/period	
7	668	761	744	863	item/period	
8	680	769	708	863	item/period	
9	691	769	703	861	item/period	
10	706	769	697	851	item/period	
11	709	772	685	846	item/period	
12	731	774	651	844	item/period	
1	531	688	787	857	item/period	mode -10% than the mean of base case
2	552	692	754	853	item/period	
3	559	703	749	850	item/period	
4	562	723	732	849	item/period	
5	566	726	721	848	item/period	
6	587	727	711	836	item/period	
7	610	736	688	828	item/period	
8	620	748	666	827	item/period	
9	631	748	663	824	item/period	
10	648	750	660	803	item/period	
11	653	753	652	793	item/period	
12	686	757	632	789	item/period	

Values for product demand if it follows triangular distribution (-7% mean)

Factory	Period	Product low	A high	Product low	B high	Unit
San Francisco	1	534	759	635	860	item/period
	2	557	755	658	856	item/period
	3	565	752	666	853	item/period
	4	569	751	670	852	item/period
	5	572	751	674	851	item/period
	6	596	739	698	840	item/period
	7	619	731	721	832	item/period
	8	629	730	731	831	item/period
	9	640	727	742	828	item/period
	10	656	708	758	809	item/period
	11	660	698	762	799	item/period
	12	691	694	793	795	item/period
Austin	1	459	535	699	791	item/period
	2	465	534	702	789	item/period
	3	467	532	704	787	item/period
	4	468	532	705	787	item/period
	5	469	532	706	787	item/period
	6	475	527	714	781	item/period
	7	483	525	724	777	item/period
	8	487	524	729	777	item/period
	9	491	523	734	775	item/period
	10	497	516	741	766	item/period
	11	499	512	743	761	item/period
	12	510	511	758	759	item/period

APPENDIX B: Values for product demand

Values for product demand if it follows triangular distribution (-7% mean) continuation

Factory	Period	Product low	A high	Product low	B high	Unit
Boston	1	570	721	669	820	item/period
	2	584	718	681	817	item/period
	3	588	716	685	815	item/period
	4	591	715	687	814	item/period
	5	593	715	689	814	item/period
	6	607	707	702	805	item/period
	7	622	701	717	799	item/period
	8	629	700	725	799	item/period
	9	637	698	733	796	item/period
	10	648	685	744	782	item/period
	11	651	677	748	775	item/period
	12	673	675	771	772	item/period

APPENDIX B: Values for product demand

Values for product demand if it follows triangular distribution (+7% mean)

Factory	Period	Product low	A high	Product low	B high	Unit
San Francisco	1	547	771	649	874	item/period
	2	577	768	681	872	item/period
	3	588	766	692	870	item/period
	4	593	765	698	869	item/period
	5	598	765	703	869	item/period
	6	630	756	737	861	item/period
	7	660	750	768	856	item/period
	8	672	750	781	856	item/period
	9	682	748	792	854	item/period
	10	696	734	806	841	item/period
	11	700	727	810	835	item/period
	12	722	724	831	833	item/period
Austin	1	468	545	716	805	item/period
	2	480	545	730	804	item/period
	3	484	545	735	804	item/period
	4	486	545	737	804	item/period
	5	488	545	739	804	item/period
	6	501	543	754	802	item/period
	7	513	542	767	801	item/period
	8	517	542	772	801	item/period
	9	521	542	777	801	item/period
	10	527	539	783	797	item/period
	11	528	537	785	795	item/period
	12	536	536	794	793	item/period

APPENDIX B: Values for product demand

Values for product demand if it follows triangular distribution (+7% mean) continuation

Factory	Period	Product low	A high	Product low	B high	Unit
Boston	1	583	733	683	834	item/period
	2	604	731	705	832	item/period
	3	612	730	713	831	item/period
	4	615	729	716	830	item/period
	5	619	729	720	830	item/period
	6	641	724	743	825	item/period
	7	662	721	764	822	item/period
	8	671	721	772	822	item/period
	9	678	719	780	821	item/period
	10	688	711	790	813	item/period
	11	690	707	792	809	item/period
	12	704	705	806	807	item/period

APPENDIX B: Machine hours for the different factories

Machine hour capacity in San Francisco and Austin

Factory	Period	Low	Medium	High	Unit
San Francisco	1	150,633	152,856	155,997	hour/period
	2	150,972	153,353	156,221	hour/period
	3	151,071	153,815	156,840	hour/period
	4	151,233	153,856	157,049	hour/period
	5	151,621	155,137	157,569	hour/period
	6	151,751	155,153	157,585	hour/period
	7	151,809	155,287	157,766	hour/period
	8	151,898	155,300	158,250	hour/period
	9	152,088	155,577	158,395	hour/period
	10	152,277	155,650	158,421	hour/period
	11	152,713	155,667	158,996	hour/period
	12	152,798	155,715	159,258	hour/period
Austin	1	150,011	150,264	150,483	hour/period
	2	150,018	150,285	150,515	hour/period
	3	150,079	150,287	150,520	hour/period
	4	150,091	150,300	150,562	hour/period
	5	150,113	150,329	150,597	hour/period
	6	150,126	150,348	150,612	hour/period
	7	150,129	150,353	150,667	hour/period
	8	150,139	150,400	150,835	hour/period
	9	150,182	150,406	150,874	hour/period
	10	150,217	150,440	150,913	hour/period
	11	150,220	150,443	150,917	hour/period
	12	150,235	150,450	150,977	hour/period

APPENDIX B: Machine hours for the different factories

Machine hour capacity in Boston

Factory	Period	Low	Medium	High	Unit
Boston	1	151,046	153,722	156,276	hour/period
	2	151,567	153,848	156,468	hour/period
	3	151,859	154,173	156,820	hour/period
	4	151,917	154,370	157,397	hour/period
	5	151,940	154,551	157,404	hour/period
	6	151,983	154,911	157,488	hour/period
	7	152,143	155,370	157,947	hour/period
	8	152,406	155,485	158,928	hour/period
	9	152,439	155,541	159,102	hour/period
	10	152,467	155,643	159,388	hour/period
	11	152,474	155,778	159,845	hour/period
	12	153,685	155,781	160,421	hour/period

APPENDIX B: Labor hours for the different factories

Labor hour capacity in San Francisco and Austin

Factory	Period	Low	Medium	High	Unit
San Francisco	1	46,004	46,121	46,314	hour/period
	2	46,011	46,140	46,325	hour/period
	3	46,015	46,141	46,326	hour/period
	4	46,043	46,147	46,400	hour/period
	5	46,054	46,156	46,408	hour/period
	6	46,058	46,166	46,424	hour/period
	7	46,063	46,191	46,448	hour/period
	8	46,064	46,215	46,453	hour/period
	9	46,068	46,244	46,472	hour/period
	10	46,079	46,264	46,488	hour/period
	11	46,096	46,265	46,489	hour/period
	12	46,102	46,307	46,492	hour/period
Austin	1	46,104	46,274	46,465	hour/period
	2	46,105	46,280	46,467	hour/period
	3	46,113	46,317	46,489	hour/period
	4	46,129	46,333	46,497	hour/period
	5	46,151	46,339	46,501	hour/period
	6	46,154	46,371	46,513	hour/period
	7	46,165	46,377	46,518	hour/period
	8	46,198	46,385	46,555	hour/period
	9	46,213	46,386	46,556	hour/period
	10	46,230	46,387	46,558	hour/period
	11	46,253	46,401	46,570	hour/period
	12	46,273	46,423	46,587	hour/period

APPENDIX B: Labor hours for the different factories

Labor hour capacity in Boston

Factory	Period	Low	Medium	High	Unit
Boston	1	46,201	46,379	46,560	hour/period
	2	46,220	46,420	46,588	hour/period
	3	46,227	46,435	46,590	hour/period
	4	46,227	46,450	46,602	hour/period
	5	46,266	46,483	46,613	hour/period
	6	46,276	46,487	46,615	hour/period
	7	46,289	46,508	46,635	hour/period
	8	46,300	46,521	46,652	hour/period
	9	46,320	46,523	46,667	hour/period
	10	46,336	46,524	46,682	hour/period
	11	46,339	46,540	46,696	hour/period
	12	46,346	46,551	46,696	hour/period

APPENDIX B: Model input parameters

Production input parameter values

Items	Notation	A	B	Unit
Materials cost	c_{it}^{x}	66	68	\$/item/period
Inventory holding cost	c_{it}^{y}	5	5	\$/item/period
Backorder cost	c_{it}^{b}	200	230	\$/item/period
Transportation cost	c_{it}^{w}	26	26	\$/item/period
Subcontracting cost	c_{it}^{q}	720	730	\$/item/period
Defective items cost	c_{it}^{m}	66	68	\$/item/period
Recycle items cost	c_{it}^{r}	352	352	\$/item/period
Factory energy consumption	e_{i}^{x}	0.8	0.9	MWh/item
Warehouse energy consumption	e_{i}^{f}	0.01	0.01	MWh/item
Production allowable defect	ν	1	1	%
Allowable recycle percentage	η	1	1	%
Initial inventory	y_{in0}	0	0	item
Initial backorder	b_{ik0}	0	0	item
Maximum allowable defect	β	2	2	%
Unit machine hour	a_i	100	100	hour/item
Unit labor hour	u_i	16	16	hour/item

APPENDIX B: Model input parameters

Other input parameter values

Parameter	Notation	Value	Unit
Labor hour cost	c_t^l	23	\$/hour
Labor hiring and layoff hour cost	c_t^h, c_t^f	38, 14	\$/hour
Energy sell and buy	u^-, u^+	30, 130	\$/MWh
Energy buy considering TOU	u_h^+	70, 140	\$/MWh
Warehouse capacity	WH_t^{max}	2,000	item
Initial machine hour	w_{k0}	152,714	hour
Initial labor hour	l_{k0}	23,000	hour
Allowable labor hour variation	α	20	%/period
Battery cost for single fty & Wh	a_b	520,000	\$/MWh
Battery cost for other models	a_b	500,000	\$/MWh
WT and PV cost	a_{g1}	1.5M, 1.0M	\$/MW
Capital recovery factor WT and PV	ϕ_g	0.0858	N/A
Capital recovery factor BSS	ϕ_b	0.1424	N/A
O&M cost of WT and PV	b_{g1},b_{g2}	8, 4	\$/MWh
Carbon incentive for WT and PV	c_g	0, 25	\$/MWh
Energy intensity rate	q_v	0.000000119	MWh/kg/km
Distance between fty and wh	d_{11},d_{22},d_{33}	435,195,215	km
No of trips	β	1	trip/day
Vehicle self weight	m_v	2,630	kg
WT and PV generation hours	λ_{gj}	24, 12	hour/day
Fty and wh electricity load	L_k, L_n	2, 7	MW
Battery capacity	B_k^{max}, B_n^{max}	1,300	MWh
WT and PV capacity	P_{kg}^{max}, P_{ng}^{max}	150	MW
Daily operating hours of facilities	δ, ξ	24	hour/day

Levels for the factors in the DOE for the prosumer model with daily granularity

Level	Probability distribution for scenarios			Distribution for product demand		PV cost	Carbon incentive
	L	M	H	A	B		
1	0.2037	0.5926	0.2037	U [500, 800]	U [600, 900]	1M	$30
2	0.7995	0.1088	0.0917	Tri [500, 657, 800]	Tri [600, 770, 900]	0.75M	$25
3	0.0917	0.1088	0.7995	Tri [500, 723, 800]	Tri [600, 847, 900]	0.5M	$15
4	N/A	N/A	N/A	Tri [500, 591, 800]	Tri [600, 693, 900]	N/A	N/A

Levels for the factors in the DOE for prosumer model with hourly granularity and TOU

	Probability dist. scenarios		Distribution for product demands				
Level	L	H	A	B	PV cost	Carbon	BS cost
1	0.7995	0.0917=M	Tri [mode +7% mean]	Tri [mode +7% mean]	$1M	$30	$0.5M
2	0.0917=M	0.7995	Tri [mode -7% mean]	Tri [mode -7% mean]	$0.75M	$20	$0.3M
3	N/A	N/A	N/A	N/A	$0.50M	$10	$0.15M

San Francisco WT capacity factor of year 2012

Day	CF	Day	CF	Day	CF	Day	CF	Day	CF
1	0.055	36	0.018	71	0.316	106	0.685	141	0.639
2	0.054	37	0.038	72	0.480	107	0.427	142	0.790
3	0.055	38	0.311	73	1.000	108	0.415	143	0.655
4	0.030	39	0.033	74	0.906	109	0.567	144	0.904
5	0.211	40	0.062	75	0.233	110	0.843	145	0.977
6	0.470	41	0.083	76	0.169	111	0.605	146	0.982
7	0.196	42	0.286	77	0.316	112	0.677	147	0.838
8	0.351	43	0.604	78	0.724	113	0.544	148	0.650
9	0.063	44	0.322	79	0.560	114	0.375	149	0.640
10	0.038	45	0.736	80	0.901	115	0.340	150	0.630
11	0.035	46	0.294	81	0.112	116	0.655	151	0.711
12	0.027	47	0.777	82	0.141	117	0.205	152	0.637
13	0.034	48	0.322	83	0.224	118	0.331	153	0.925
14	0.025	49	0.290	84	0.563	119	0.851	154	0.793
15	0.219	50	0.707	85	0.272	120	0.641	155	0.465
16	0.558	51	0.753	86	0.297	121	0.760	156	0.753
17	0.057	52	0.255	87	0.064	122	0.957	157	0.880
18	0.084	53	0.182	88	0.367	123	0.494	158	0.833
19	0.056	54	0.126	89	0.524	124	0.404	159	0.915
20	0.199	55	0.303	90	0.717	125	0.819	160	0.951
22	1.000	57	0.201	92	0.519	127	0.450	162	0.539
23	0.479	58	0.799	93	0.458	128	0.583	163	0.621
24	0.475	59	0.349	94	0.583	129	0.502	164	0.671
25	0.951	60	0.603	95	0.746	130	0.665	165	0.716
26	0.437	61	0.453	96	0.686	131	0.427	166	0.664
27	0.081	62	0.179	97	0.474	132	0.380	167	0.660
28	0.239	63	0.182	98	0.318	133	0.506	168	0.500
29	0.498	64	0.369	99	0.339	134	0.298	169	0.543
30	0.024	65	0.922	100	0.400	135	0.306	170	0.351
31	0.067	66	0.879	101	0.153	136	0.721	171	0.440
32	0.234	67	0.188	102	0.453	137	0.621	172	0.473
33	0.051	68	0.230	103	0.729	138	0.652	173	0.743
34	0.220	69	0.479	104	0.395	139	0.679	174	0.307
35	0.021	70	0.508	105	0.899	140	0.582	175	0.395

San Francisco WT capacity factor of year 2012 continuation

Day	CF	Day	CF	Day	CF	Day	CF	Day	CF
176	0.515	211	0.453	246	0.349	281	0.359	316	0.172
177	0.649	212	0.474	247	0.390	282	0.281	317	0.128
178	0.647	213	0.495	248	0.573	283	0.216	318	0.169
179	0.595	214	0.431	249	0.363	284	0.322	319	0.120
180	0.555	215	0.487	250	0.330	285	0.392	320	0.239
181	0.640	216	0.357	251	0.489	286	0.184	321	0.204
182	0.229	217	0.460	252	0.906	287	0.177	322	0.384
183	0.471	218	0.309	253	0.674	288	0.299	323	0.397
184	0.743	219	0.558	254	0.367	289	0.390	324	0.092
185	0.489	220	0.828	255	0.373	290	0.141	325	0.245
186	0.321	221	0.651	256	0.302	291	0.575	326	0.656
187	0.767	222	0.584	257	0.539	292	0.691	327	0.393
188	0.642	223	0.735	258	0.725	293	0.133	328	0.182
189	0.564	224	0.505	259	0.765	294	0.208	329	0.166
190	0.770	225	0.625	260	0.679	295	0.380	330	0.214
191	0.768	226	0.677	261	0.558	296	0.426	331	0.250
192	0.507	227	0.616	262	0.374	297	0.676	332	0.151
193	0.617	228	0.561	263	0.512	298	0.495	333	0.142
195	0.697	230	0.601	265	0.841	300	0.217	335	0.376
196	0.484	231	0.767	266	0.578	301	0.178	336	0.111
197	0.361	232	0.584	267	0.389	302	0.239	337	0.409
198	0.537	233	0.706	268	0.355	303	0.254	338	0.130
199	0.400	234	0.612	269	0.378	304	0.192	339	0.154
200	0.467	235	0.510	270	0.318	305	0.137	340	0.040
201	0.525	236	0.472	271	0.340	306	0.191	341	0.111
202	0.753	237	0.412	272	0.360	307	0.222	342	0.114
203	0.632	238	0.324	273	0.332	308	0.283	343	0.290
204	0.638	239	0.402	274	0.326	309	0.189	344	0.271
205	0.522	240	0.704	275	0.251	310	0.193	345	0.073
206	0.171	241	0.484	276	0.249	311	0.414	346	0.053
207	0.209	242	0.475	277	0.055	312	0.568	347	0.038
208	0.310	243	0.437	278	0.369	313	0.375	348	0.230
209	0.370	244	0.385	279	0.292	314	0.359	349	0.312
210	0.410	245	0.355	280	0.346	315	0.426	350	0.470

Experimental cases in the sensitivity analysis in Chapter 4

SI.	PV cost	Carbon incentive	BS cost	Product demand	Scen. Probability distribution
1	1 M	30	0.5 M	Tri [+7% mean]	(0.80, 0.11, 0.09)
2	1 M	30	0.5 M	Tri [+7% mean]	(0.09, 0.11, 0.80)
3	1 M	30	0.5 M	Tri [-7% mean]	(0.80, 0.11, 0.09)
4	1 M	30	0.5 M	Tri [-7% mean]	(0.09, 0.11, 0.80)
5	1 M	30	0.3 M	Tri [+7% mean]	(0.80, 0.11, 0.09)
6	1 M	30	0.3 M	Tri [+7% mean]	(0.09, 0.11, 0.80)
7	1 M	30	0.3 M	Tri [-7% mean]	(0.80, 0.11, 0.09)
8	1 M	30	0.3 M	Tri [-7% mean]	(0.09, 0.11, 0.80)
9	1 M	30	0.15 M	Tri [+7% mean]	(0.80, 0.11, 0.09)
10	1 M	30	0.15 M	Tri [+7% mean]	(0.09, 0.11, 0.80)
11	1 M	30	0.15 M	Tri [-7% mean]	(0.80, 0.11, 0.09)
12	1 M	30	0.15 M	Tri [-7% mean]	(0.09, 0.11, 0.80)
13	1 M	20	0.5 M	Tri [+7% mean]	(0.80, 0.11, 0.09)
14	1 M	20	0.5 M	Tri [+7% mean]	(0.09, 0.11, 0.80)
15	1 M	20	0.5 M	Tri [-7% mean]	(0.80, 0.11, 0.09)
16	1 M	20	0.5 M	Tri [-7% mean]	(0.09, 0.11, 0.80)
17	1 M	20	0.3 M	Tri [+7% mean]	(0.80, 0.11, 0.09)
18	1 M	20	0.3 M	Tri [+7% mean]	(0.09, 0.11, 0.80)
19	1 M	20	0.3 M	Tri [-7% mean]	(0.80, 0.11, 0.09)
21	1 M	20	0.15 M	Tri [+7% mean]	(0.80, 0.11, 0.09)
22	1 M	20	0.15 M	Tri [+7% mean]	(0.09, 0.11, 0.80)
23	1 M	20	0.15 M	Tri [-7% mean]	(0.80, 0.11, 0.09)
25	1 M	10	0.5 M	Tri [+7% mean]	(0.80, 0.11, 0.09)
26	1 M	10	0.5 M	Tri [+7% mean]	(0.09, 0.11, 0.80)
27	1 M	10	0.5 M	Tri [-7% mean]	(0.80, 0.11, 0.09)
29	1 M	10	0.3 M	Tri [+7% mean]	(0.80, 0.11, 0.09)
30	1 M	10	0.3 M	Tri [+7% mean]	(0.09, 0.11, 0.80)
31	1 M	10	0.3 M	Tri [-7% mean]	(0.80, 0.11, 0.09)
32	1 M	10	0.3 M	Tri [-7% mean]	(0.09, 0.11, 0.80)
33	1 M	10	0.15 M	Tri [+7% mean]	(0.80, 0.11, 0.09)
34	1 M	10	0.15 M	Tri [+7% mean]	(0.09, 0.11, 0.80)
35	1 M	10	0.15 M	Tri [-7% mean]	(0.80, 0.11, 0.09)
36	1 M	10	0.15 M	Tri [-7% mean]	(0.09, 0.11, 0.80)

Experimental cases in the sensitivity analysis in Chapter 4 continuation

SI.	PV cost	Carbon incentive	BS cost	Product demand	Scen. Probability distribution
37	0.75 M	30	0.5 M	Tri [+7% mean]	(0.80, 0.11, 0.09)
38	0.75 M	30	0.5 M	Tri [+7% mean]	(0.09, 0.11, 0.80)
39	0.75 M	30	0.5 M	Tri [-7% mean]	(0.80, 0.11, 0.09)
40	0.75 M	30	0.5 M	Tri [-7% mean]	(0.09, 0.11, 0.80)
41	0.75 M	30	0.3 M	Tri [+7% mean]	(0.80, 0.11, 0.09)
42	0.75 M	30	0.3 M	Tri [+7% mean]	(0.09, 0.11, 0.80)
43	0.75 M	30	0.3 M	Tri [-7% mean]	(0.80, 0.11, 0.09)
44	0.75 M	30	0.3 M	Tri [-7% mean]	(0.09, 0.11, 0.80)
45	0.75 M	30	0.15 M	Tri [+7% mean]	(0.80, 0.11, 0.09)
46	0.75 M	30	0.15 M	Tri [+7% mean]	(0.09, 0.11, 0.80)
47	0.75 M	30	0.15 M	Tri [-7% mean]	(0.80, 0.11, 0.09)
49	0.75 M	20	0.5 M	Tri [+7% mean]	(0.80, 0.11, 0.09)
50	0.75 M	20	0.5 M	Tri [+7% mean]	(0.09, 0.11, 0.80)
51	0.75 M	20	0.5 M	Tri [-7% mean]	(0.80, 0.11, 0.09)
52	0.75 M	20	0.5 M	Tri [-7% mean]	(0.09, 0.11, 0.80)
53	0.75 M	20	0.3 M	Tri [+7% mean]	(0.80, 0.11, 0.09)
54	0.75 M	20	0.3 M	Tri [+7% mean]	(0.09, 0.11, 0.80)
56	0.75 M	20	0.3 M	Tri [-7% mean]	(0.09, 0.11, 0.80)
57	0.75 M	20	0.15 M	Tri [+7% mean]	(0.80, 0.11, 0.09)
58	0.75 M	20	0.15 M	Tri [+7% mean]	(0.09, 0.11, 0.80)
59	0.75 M	20	0.15 M	Tri [-7% mean]	(0.80, 0.11, 0.09)
60	0.75 M	20	0.15 M	Tri [-7% mean]	(0.09, 0.11, 0.80)
61	0.75 M	10	0.5 M	Tri [+7% mean]	(0.80, 0.11, 0.09)
63	0.75 M	10	0.5 M	Tri [-7% mean]	(0.80, 0.11, 0.09)
64	0.75 M	10	0.5 M	Tri [-7% mean]	(0.09, 0.11, 0.80)
65	0.75 M	10	0.3 M	Tri [+7% mean]	(0.80, 0.11, 0.09)
66	0.75 M	10	0.3 M	Tri [+7% mean]	(0.09, 0.11, 0.80)
67	0.75 M	10	0.3 M	Tri [-7% mean]	(0.80, 0.11, 0.09)
68	0.75 M	10	0.3 M	Tri [-7% mean]	(0.09, 0.11, 0.80)
69	0.75 M	10	0.15 M	Tri [+7% mean]	(0.80, 0.11, 0.09)
70	0.75 M	10	0.15 M	Tri [+7% mean]	(0.09, 0.11, 0.80)
71	0.75 M	10	0.15 M	Tri [-7% mean]	(0.80, 0.11, 0.09)
72	0.75 M	10	0.15 M	Tri [-7% mean]	(0.09, 0.11, 0.80)

Experimental cases in the sensitivity analysis in Chapter 4 continuation

SI.	PV cost	Carbon incentive	BS cost	Product demand	Scen. Probability distribution
73	0.50 M	30	0.5 M	Tri [+7% mean]	(0.80, 0.11, 0.09)
74	0.50 M	30	0.5 M	Tri [+7% mean]	(0.09, 0.11, 0.80)
75	0.50 M	30	0.5 M	Tri [-7% mean]	(0.80, 0.11, 0.09)
76	0.50 M	30	0.5 M	Tri [-7% mean]	(0.09, 0.11, 0.80)
77	0.50 M	30	0.3 M	Tri [+7% mean]	(0.80, 0.11, 0.09)
78	0.50 M	30	0.3 M	Tri [+7% mean]	(0.09, 0.11, 0.80)
79	0.50 M	30	0.3 M	Tri [-7% mean]	(0.80, 0.11, 0.09)
80	0.50 M	30	0.3 M	Tri [-7% mean]	(0.09, 0.11, 0.80)
81	0.50 M	30	0.15 M	Tri [+7% mean]	(0.80, 0.11, 0.09)
82	0.50 M	30	0.15 M	Tri [+7% mean]	(0.09, 0.11, 0.80)
83	0.50 M	30	0.15 M	Tri [-7% mean]	(0.80, 0.11, 0.09)
85	0.50 M	20	0.5 M	Tri [+7% mean]	(0.80, 0.11, 0.09)
86	0.50 M	20	0.5 M	Tri [+7% mean]	(0.09, 0.11, 0.80)
87	0.50 M	20	0.5 M	Tri [-7% mean]	(0.80, 0.11, 0.09)
88	0.50 M	20	0.5 M	Tri [-7% mean]	(0.09, 0.11, 0.80)
89	0.50 M	20	0.3 M	Tri [+7% mean]	(0.80, 0.11, 0.09)
90	0.50 M	20	0.3 M	Tri [+7% mean]	(0.09, 0.11, 0.80)
91	0.50 M	20	0.3 M	Tri [-7% mean]	(0.80, 0.11, 0.09)
93	0.50 M	20	0.15 M	Tri [+7% mean]	(0.80, 0.11, 0.09)
94	0.50 M	20	0.15 M	Tri [+7% mean]	(0.09, 0.11, 0.80)
95	0.50 M	20	0.15 M	Tri [-7% mean]	(0.80, 0.11, 0.09)
96	0.50 M	20	0.15 M	Tri [-7% mean]	(0.09, 0.11, 0.80)
98	0.50 M	10	0.5 M	Tri [+7% mean]	(0.09, 0.11, 0.80)
99	0.50 M	10	0.5 M	Tri [-7% mean]	(0.80, 0.11, 0.09)
100	0.50 M	10	0.5 M	Tri [-7% mean]	(0.09, 0.11, 0.80)
101	0.50 M	10	0.3 M	Tri [+7% mean]	(0.80, 0.11, 0.09)
102	0.50 M	10	0.3 M	Tri [+7% mean]	(0.09, 0.11, 0.80)
103	0.50 M	10	0.3 M	Tri [-7% mean]	(0.80, 0.11, 0.09)
104	0.50 M	10	0.3 M	Tri [-7% mean]	(0.09, 0.11, 0.80)
105	0.50 M	10	0.15 M	Tri [+7% mean]	(0.80, 0.11, 0.09)
106	0.50 M	10	0.15 M	Tri [+7% mean]	(0.09, 0.11, 0.80)
107	0.50 M	10	0.15 M	Tri [-7% mean]	(0.80, 0.11, 0.09)
108	0.50 M	10	0.15 M	Tri [-7% mean]	(0.09, 0.11, 0.80)

REFERENCES

Aliev, R. A., Fazlollahi, B., Guirimov, B., and Aliev, R. R. (2007). Fuzzy-genetic approach to aggregate production–distribution planning in supply chain management. *Information Sciences*, 177(20):4241–4255.

AMPL (2021). What should i do if i suspect that there is insufficient memory for my ampl session? https://ampl.com/faqs/what-should-i-do-if-i-suspect-that-there-is-insufficient-memory-for-my-ampl-session/.

Anderson, K., Diorio, N., Butt, Robert, S., and Cutler, Dylan, S. (2017). Resilient renewable energy microgrids. https://www.osti.gov/biblio/1409493.

Apple (2018). Apple now globally powered by 100 percent renewable energy. https://www.apple.com/newsroom/2018/04/apple-now-globally-powered-by-100-percent-renewable-energy/.

Azar, A. G., Nazaripouya, H., Khaki, B., Chu, C.-C., Gadh, R., and Jacobsen, R. H. (2018). A non-cooperative framework for coordinating a neighborhood of distributed prosumers. *IEEE Transactions on Industrial Informatics*, 15(5):2523–2534.

Bakir, M. A. and Byrne, M. D. (1998). Stochastic linear optimisation of an mpmp production planning model. *International Journal of Production Economics*, 55(1):87–96.

Ball, P. D., Evans, S., Levers, A., and Ellison, D. (2009). Zero carbon manufacturing facility towards integrating material, energy, and waste process flows. *Proceedings of the Institution of Mechanical Engineers, Part B: Journal of Engineering Manufacture*, 223(9):1085–1096.

Bañuelos-Ruedas, F., Camacho, C. Á., and Rios-Marcuello, S. (2011). Methodologies used in the extrapolation of wind speed data at different heights and its impact in the wind energy resource assessment in a region. *Wind Farm-Technical Regulations, Potential Estimation and Siting Assessment*, pages 97–114.

Birge, J. R. (1995). Models and model value in stochastic programming. *Annals of Operations Research*, 59(1):1–18.

Birge, J. R. and Louveaux, F. (2011). *Introduction to stochastic programming*. Springer Science & Business Media.

Blackadar, A. K. and Tennekes, H. (1968). Asymptotic similarity in neutral barotropic planetary boundary layers. *Journal of the Atmospheric Sciences*, 25(6):1015–1020.

Budiyanto, B. and Fadliondi, F. (2017). The improvement of solar cell output power using cooling and reflection from mirror. *International Journal of Power Electronics and Drive Systems*, 8(3):1320.

Carlton (2018). World energy consumption by fuel type and sector. https://grandsolarminimum.com/2018/11/19/world-energy-consumption/.

Chakrabortty, R. K., Hasin, M. A. A., Sarker, R. A., and Essam, D. L. (2015). A possibilistic environment based particle swarm optimization for aggregate production planning. *Computers & Industrial Engineering*, 88:366–377.

Chaturvedi, N. D. and Bandyopadhyay, S. (2015). Targeting aggregate production planning for an energy supply chain. *Industrial & Engineering Chemistry Research*, 54(27):6941–6949.

Che, A., Zeng, Y., and Lyu, K. (2016). An efficient greedy insertion heuristic for energy-conscious single machine scheduling problem under time-of-use electricity tariffs. *Journal of Cleaner Production*, 129:565–577.

Che, A., Zhang, S., and Wu, X. (2017). Energy-conscious unrelated parallel machine scheduling under time-of-use electricity tariffs. *Journal of Cleaner Production*, 156:688–697.

Cheraghalikhani, A., Khoshalhan, F., and Mokhtari, H. (2019). Aggregate production planning: A literature review and future research directions. *International Journal of Industrial Engineering Computations*, 10(2):309–330.

Choi, Y.-C. and Xirouchakis, P. (2015). A holistic production planning approach in a reconfigurable manufacturing system with energy consumption and environmental effects. *International Journal of Computer Integrated Manufacturing*, 28(4):379–394.

Cui, S., Wang, Y.-W., Xiao, J.-W., and Liu, N. (2018). A two-stage robust energy sharing management for prosumer microgrid. *IEEE Transactions on Industrial Informatics*, 15(5):2741–2752.

Ding, J.-Y., Song, S., Zhang, R., Chiong, R., and Wu, C. (2015). Parallel machine scheduling under time-of-use electricity prices: New models and optimization approaches. *IEEE Transactions on Automation Science and Engineering*, 13(2):1138–1154.

Djordjevic, I., Petrovic, D., and Stojic, G. (2019). A fuzzy linear programming model for aggregated production planning (app) in the automotive industry. *Computers in Industry*, 110:48–63.

EIA (2021). Average price of electricity to ultimate customers by end-use sector. https://www.eia.gov/electricity/monthly/epm$_{t}able_{g}rapher.php?t = epmt_{56a}$.

Escudero, L. F., Garín, A., Merino, M., and Pérez, G. (2007). The value of the stochastic solution in multistage problems. *Top*, 15(1):48–64.

Fang, K., Uhan, N. A., Zhao, F., and Sutherland, J. W. (2016). Scheduling on a single machine under time-of-use electricity tariffs. *Annals of Operations Research*, 238(1-2):199–227.

Forde, M. (2019). Nike opens new distribution center running on 100% renewable energy. https://www.supplychaindive.com/news/nike-distribution-center-100-renewable-energy/563497/.

Fourer, R., Gay, D. M., and Kernighan, B. W. (1990). A modeling language for mathematical programming. *Management Science*, 36(5):519–554.

Geisz, J. F., France, R. M., Schulte, K. L., Steiner, M. A., Norman, A. G., Guthrey, H. L., Young, M. R., Song, T., and Moriarty, T. (2020). Six-junction iii–v solar cells with 47.1% conversion efficiency under 143 suns concentration. *Nature Energy*, 5(4):326–335.

Gholamian, N., Mahdavi, I., and Tavakkoli-Moghaddam, R. (2016). Multi-objective multi-product multi-site aggregate production planning in a supply chain under uncertainty: fuzzy multi-objective optimisation. *International Journal of Computer Integrated Manufacturing*, 29(2):149–165.

Golari, M., Fan, N., and Jin, T. (2017). Multistage stochastic optimization for production-inventory planning with intermittent renewable energy. *Production and Operations Management*, 26(3):409–425.

Golpîra, H., Khan, S. A. R., and Zhang, Y. (2018). Robust smart energy efficient production planning for a general job-shop manufacturing system under combined demand and supply uncertainty in the presence of grid-connected microgrid. *Journal of cleaner production*, 202:649–665.

Gupta, V. and Grossmann, I. E. (2011). Solution strategies for multistage stochastic programming with endogenous uncertainties. *Computers & Chemical Engineering*, 35(11):2235–2247.

Honda (2019). Honda secures auto industry′s largest renewable energy purchase, resulting in 60% reduction in co2 emissions from its north american manufacturing operations. https://www.greencarcongress.com/2019/09/20190924-honda.html.

Hottel, H. C. (1976). A simple model for estimating the transmittance of direct solar radiation through clear atmospheres. *Solar energy*, 18(2):129–134.

Hussain, I., Ali, S., Khan, B., Ullah, Z., Mehmood, C., Jawad, M., Farid, U., and Haider, A. (2019). Stochastic wind energy management model within smart grid framework: a joint bi-directional service level agreement (sla) between smart grid and wind energy district prosumers. *Renewable energy*, 134:1017–1033.

Iria, J., Soares, F., and Matos, M. (2018). Optimal supply and demand bidding strategy for an aggregator of small prosumers. *Applied energy*, 213:658–669.

Jin, T., Golari, M., and Fan, N. (2015). Multi-period production-inventory decision under integration of renewable energy sources. In *IISE Annual Conference. Proceedings*, page 753. Institute of Industrial and Systems Engineers (IISE).

John (2017). Intel goes 100% renewable to power 360-acre leixlip campus. https://irishtechnews.ie/intel-goes-100-renewable-to-power-360-acre-leixlip-campus/.

Kaldjian, E. and Barua, P. (2019). The us underwent a quiet clean energy revolution last year. https://www.wri.org/blog/2019/01/us-underwent-quiet-clean-energy-revolution-last-year.

Lai, Y.-J. and Hwang, C.-L. (1992). A new approach to some possibilistic linear programming problems. *Fuzzy sets and systems*, 49(2):121–133.

Lave, M. and Kleissl, J. (2011). Optimum fixed orientations and benefits of tracking for capturing solar radiation in the continental united states. *Renewable Energy*, 36(3):1145–1152.

LEAP (2021). Leap-high performance computing cluster. https://doit.txstate.edu/rc/leap.html.

Leung, S. C., Wu, Y., and Lai, K. (2006). A stochastic programming approach for multi-site aggregate production planning. *Journal of the Operational Research Society*, 57(2):123–132.

Liang, J., Wang, Y., Zhang, Z.-H., and Sun, Y. (2019). Energy efficient production planning and scheduling problem with processing technology selection. *Computers & Industrial Engineering*, 132:260–270.

Modarres, M. and Izadpanahi, E. (2016). Aggregate production planning by focusing on energy saving: A robust optimization approach. *Journal of Cleaner Production*, 133:1074–1085.

Montgomery, D. C. (2017). *Design and analysis of experiments*. John wiley & sons.

Nam, S.-j. and Logendran, R. (1992). Aggregate production planning - a survey of models and methodologies. *European Journal of Operational Research*, 61(3):255–272.

Northwester (2020). Northwester 2 offshore wind farm delivers energy to the belgian grid. https://www.renewableenergymagazine.com/wind/northwester-2-offshore-wind-farm-delivers-energy-20200114.

Nour, A., Galal, N. M., and El-Kilany, K. S. (2017). Energy-based aggregate production planning for porcelain tableware manufacturer in egypt. In *Proceedings of the International Conference on Industrial Engineering and Operations Management, Rabat, Morocco*.

NREL (2021). Documenting a decade of cost declines for pv systems. https://www.nrel.gov/news/program/2021/documenting-a-decade-of-cost-declines-for-pv-systems.html.

Pham, A., Jin, T., Novoa, C., and Qin, J. (2019). A multi-site production and microgrid planning model for net-zero energy operations. *International Journal of Production Economics*, 218:260–274.

Radford, R. (2017). How important is the internal supply chain? https://www.allthingssupplychain.com/how-important-is-the-internal-supply-chain/.

Rardin, R. L. (1998). *Optimization in operations research*, volume 166. Prentice Hall Upper Saddle River, NJ.

Roberts, D. (2018). Utilities have a problem: the public wants 100% renewable energy, and quick. https://www.vox.com/energy-and-environment/2018/9/14/17853884/utilities-renewable-energy-100-percent-public-opinion.

Shea, R. P. and Ramgolam, Y. K. (2019). Applied levelized cost of electricity for energy technologies in a small island developing state: A case study in mauritius. *Renewable energy*, 132:1415–1424.

Stehly, T., Beiter, P., and Duffy, P. (2019). National renewable energy laboratory. https://www.nrel.gov/docs/fy21osti/78471.pdf.

Su, Q., Yang, W., and Liu, Y. (2017). Optimization of carbon emission considering production planning at enterprise level. *Journal of Cleaner Production*, 162:635–645.

Taboada, H., Xiong, Z., Jin, T., and Jimenez, J. (2012). Exploring a solar photovoltaic-based energy solution for green manufacturing industry. In *2012 IEEE International Conference on Automation Science and Engineering (CASE)*, pages 40–45. IEEE.

Tao, C., Shanxu, D., and Changsong, C. (2010). Forecasting power output for grid-connected photovoltaic power system without using solar radiation measurement. In *The 2nd International Symposium on Power Electronics for Distributed Generation Systems*, pages 773–777. IEEE.

Tesla (2019). Inside tesla′s 100% renewable design for the gigafactory. https://www.fastcompany.com/90334858/inside-teslas-100-renewable-design-for-the-gigafactory.

Thiringer, T. and Linders, J. (1993). Control by variable rotor speed of a fixed-pitch wind turbine operating in a wide speed range. *IEEE Transactions on Energy Conversion*, 8(3):520–526.

Tran, T. T. and Smith, A. D. (2019). Stochastic optimization for integration of renewable energy technologies in district energy systems for cost-effective use. *Energies*, 12(3):533.

Van Der Stelt, S., AlSkaif, T., and van Sark, W. (2018). Techno-economic analysis of household and community energy storage for residential prosumers with smart appliances. *Applied Energy*, 209:266–276.

Vestas (2020). Vestas to become carbon-neutral by 2030. https://www.renewableenergymagazine.com/wind/vestas-to-become-carbonneutral-by-2030-20200106.

Villarreal, S., Jimenez, J. A., Jin, T., and Cabrera-Rios, M. (2012). Designing a sustainable and distributed generation system for semiconductor wafer fabs. *IEEE Transactions on Automation Science and Engineering*, 10(1):16–26.

Walmart (2020). Getting to 100% renewable: Walmart′s approach. https://cdn.corporate.walmart.com/eb/80/4c32210b44ccbae634ddedd18a27/walmarts-approach-to-renewable-energy.pdf.

Wang, Y. and Li, L. (2013). Time-of-use based electricity demand response for sustainable manufacturing systems. *Energy*, 63:233–244.

WeatherUnderground (2019). Weather underground. (n.d.) local weather forecast, news and conditions. https://www.wunderground.com/.

WINDExchange (2021). Production tax credit and investment tax credit for wind. https://windexchange.energy.gov/projects/tax-credits.

Yu, J., Ryu, J.-H., and Lee, I.-b. (2019). A stochastic optimization approach to the design and operation planning of a hybrid renewable energy system. *Applied energy*, 247:212–220.

Zhang, H., Zhao, F., Fang, K., and Sutherland, J. W. (2014). Energy-conscious flow shop scheduling under time-of-use electricity tariffs. *CIRP Annals*, 63(1):37–40.

Zhao, H., Ierapetritou, M. G., and Rong, G. (2016). Production planning optimization of an ethylene plant considering process operation and energy utilization. *Computers & Chemical Engineering*, 87:1–12.